Reservoir Characterization of the Clinton Sandstone in Eastern Ohio Utilizing 3D Seismic Interpretation and Well Log Analysis

---

A Thesis Presented to

the Faculty of the Department of Earth and Atmospheric Sciences

University of Houston

In Partial Fulfillment

of the Requirements for the Degree

Master of Science

By

Dylan Klaus Wiemer

May 2018

Reservoir Characterization of the Clinton Sandstone in Eastern Ohio Utilizing 3D Seismic Interpretation and Well Log Analysis

_____

Dylan Klaus Wiemer

APPROVED:

Dr. Hua-Wei Zhou

Dr. William Keller

Dr. Johnny Wu

Dr. Heather Bedle

Dean, College of Natural Sciences and Mathematics

ACKNOWLEDGEMENTS

I would like to thank my grandfather, Dr. Klaus C. Wiemer foremost for making my graduate education possible as well as instilling a passion in me for seeking higher education. While I struggled with mathematics at a young age, you helped push me to enjoy it and eventually pursue a mathematically dense degree choice. I will always cherish the times we spent together whether it be conversing or fishing. Dad, thanks for all of the encouragement and for believing in me over all of these years, it's been a long road to get here and I wouldn't have gotten here without your guidance. Next I would like to thank my family for their unconditional support for me throughout life and encouraging my pursuits. Sammy, thank you for being there and for your positive encouragement throughout this endeavor. In addition I would like to thank Dr. William Keller for giving me shot as a Geophysicist. My three month internship turned into a three year experience that helped me grow professionally and personally. Additional thanks to everyone at EnerVest who assisted me with this research and for making my time there positive and memorable. Thank you to James Ayers for answering my countless questions and for contributing to my geologic understanding of this region. Thank you to Jorge Peinado for showing me the nuances and intricacies of seismic inversion. Last but not least, thank you to TGS for allowing me to use this seismic data for my thesis research.

Reservoir Characterization of the Clinton Sandstone in Eastern Ohio Utilizing 3D Seismic Interpretation and Well Log Analysis

---

An Abstract of a Thesis

Presented to

the Faculty of the Department of Earth and Atmospheric Sciences

University of Houston

In Partial Fulfillment

of the Requirements for the Degree

Master of Science

By

Dylan Klaus Wiemer

May 2018

ABSTRACT

The Clinton Sandstone is a tight, laterally discontinuous sandstone that was deposited in the Early Silurian in both deltaic and shallow marine environments. This interval is well known in the western Appalachian Basin as the reservoir rock for several large as well as historic oil and gas fields. In eastern Ohio exists the East Canton Oil Field (ECOF) which is primarily controlled by stratigraphic trapping and is estimated to have contained 1.5 billion barrels of oil in place. The presence of a thick regional carbonate above the Clinton Sandstone and advances in directional drilling make it an ideal candidate for horizontal drilling and completion. Located over the southeastern extent of the north south trending ECOF is a 400 square mile 3D survey of which a 40 square mile cutout will be used in this study. Within the 3D survey study area, are 3 wells that contain dipole sonic and bulk density log curves. At the base of the Clinton Sand exists an AVO anomaly seen in the log data by a large increase in shear wave velocity and a large decrease in Poisson's ratio. Using the available logs and seismic data, a pre stack inversion was generated for both compressional impedance, shear impedance and Poisson's ratio. Variations in seismic response of the Clinton Sandstone are closely related to porosity variability within the reservoir interval. Inverting for Poisson's Ratio has shown to be a useful tool for tight sand exploration in the Appalachian Basin as its relationship to clean sand is utilized to better understand and map reservoir variability within the ECOF boundaries as well as outside.

CONTENTS

Chapter 1: Appalachian Basin Geologic History

1.1 Depositional & Orogenic History

During the Precambrian, eastern Ohio was part of the Grenville Province. This province is composed of Middle to Upper Proterozoic metamorphic rocks that also contain igneous intrusions (Wickstrom et al., 2005). This province was part of eastern Laurentia and ranges in age from 1.35 to 0.95 Ga. and was a product of widespread Mesoproterozoic metamorphism that ranged from Labrador to the Llano Uplift of East Texas (Ettensohn, 2008). During the Grenville Orogeny, the Grenville Provence was thrusted over Precambrian strata. This event created a large mountain belt which was subsequently eroded during Late Precambrian exposure which in turn created a large regional unconformity (Wickstrom et al., 2005). The western limit of the province is represented by the north-south trending Grenville Front. This front represents the western most boundary of the Appalachian Basin (Figure 1.1.1) (Ettensohn, 2008).

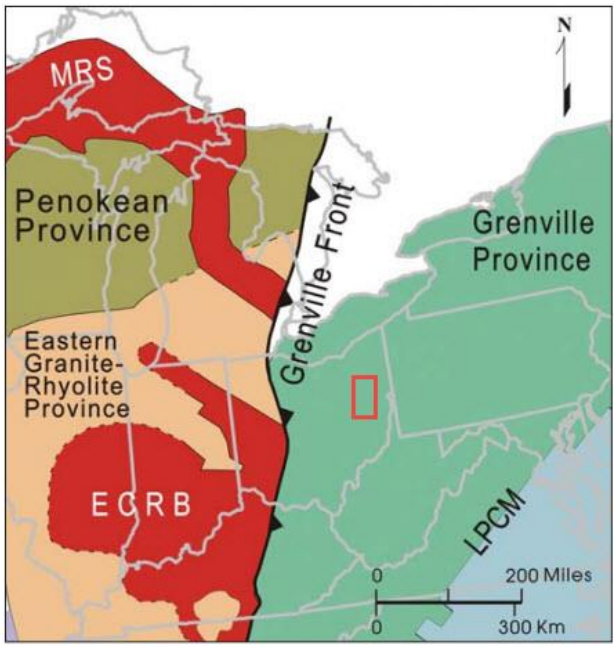

Figure 1.1.1: Tectonic provinces during the Precambrian illustrating the western extent of the Appalachian Basin. Study area highlighted (Ettensohn, 2008).

During the Late Precambrian and Early Cambrian, eastern Ohio was part of Laurentia which was positioned around the equator. It was during this time that Laurentia rifted away from its adjacent plate creating the Iapetus Ocean and establishing a passive continental margin. The large mountain belt composed of Grenville Province rock continued to be eroded as sea level rose (Figure 1.1.2A) (Wickstrom et al., 2005).The combination of relief and tectonic setting allowed for clastic deposition to dominate the Early Cambrian. Clastic sediments derived from the exposed Grenville rock were deposited from the northwest along the Appalachian margin in coastal plain environments (Ettensohn, 2008). This is represented in the Mt. Simon Sandstone which was deposited on top of the Precambrian Unconformity. This shaley, arkosic sandstone was deposited in a wide range of environments which include, marine, fluvial and estuarine (Wickstrom et al., 2005).

Sedimentary deposition was primarily controlled by sea level changes during the Middle and Late Cambrian as can be seen by the shale-carbonate cycles. Deposited above the Mt. Simons Sandstone is the Rome Formation. This formation is composed of shales, sandstones and dolomites and represents a regression period followed by submergence. This submergence is represented by the Consauga Formation. This formation is composed of prodelta muds and is intertongued with shallow open-marine dolostones. Submergence continued into the Late Cambrian as the passive seaward margin grew which established increasing carbonate deposition and restricted clastic deposition to shore areas. In addition to sea level rise, the northward shift of Laurentia further moved the continent further towards the equator. This moved the Appalachian Basin area into an arid environment which is favorable for carbonate deposition. This depositional environment allowed for large scale carbonate deposition throughout the Appalachian Basin as well as the Eastern/Central United States and is often referred to as the "Great American Bank" (Figure 1.1.2B) (Ettensohn, 2008).

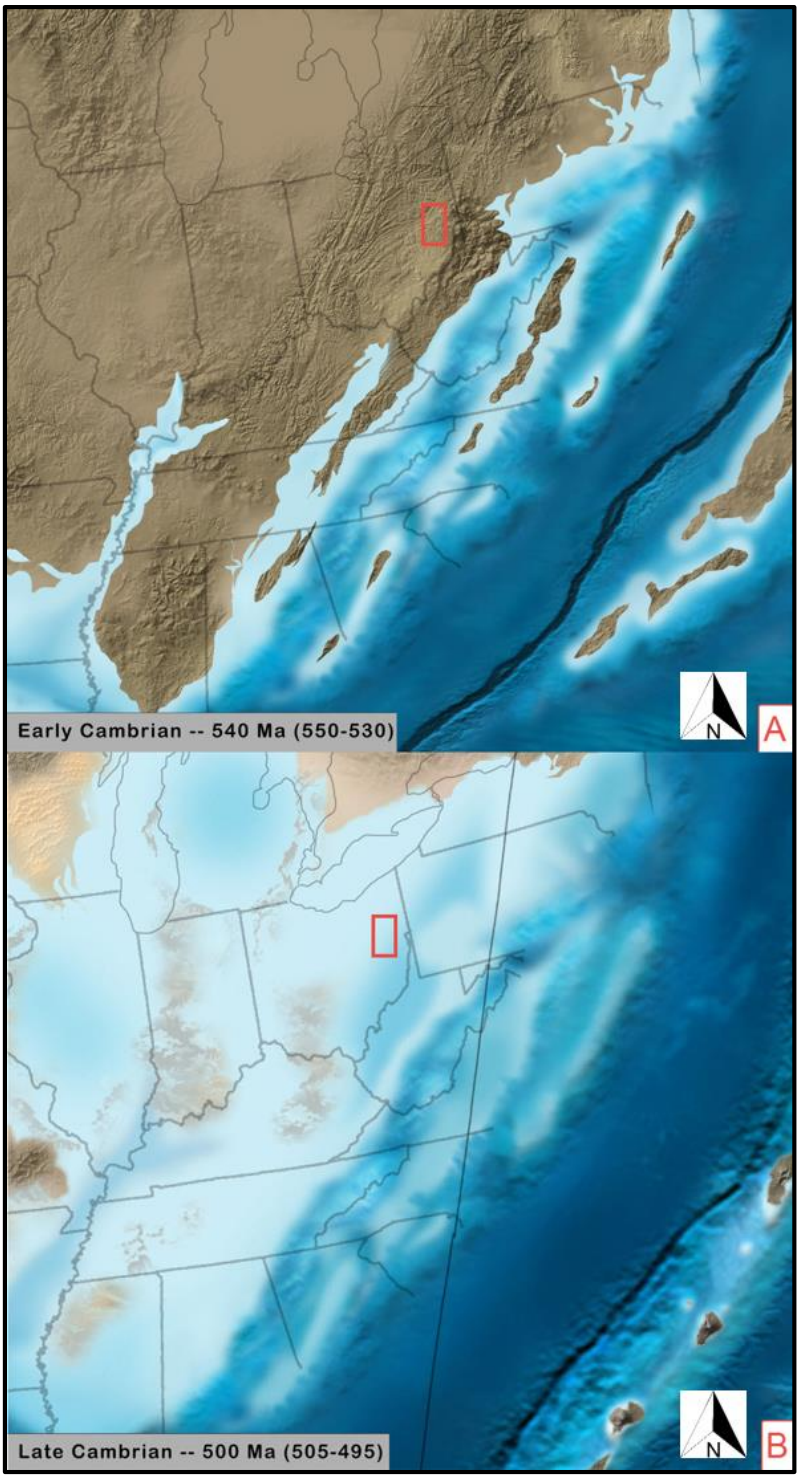

Figure 1.1.2 The Paleogeography during the Early Cambrian. (A) The Eastern United States following the Laurentia rifting and the now established Iapetus Ocean. In (B) an increase in sea level allowed for widespread carbonate deposition throughout the region. Study area is highlighted. (Blakey, 2007).

During this time, the Copper Ridge Dolomite was deposited. The Copper Ridge is a sandy dolostone that contains interbedded sandstones as well as argillaceous limestones (Wickstrom et al., 2005). Due to the depositional setting of the time, the Copper Ridge is thick in nature and is part of the "Great American Bank" deposition which ranges in thickness from 160-3000 ft (Ettensohn, 2008). Above the Copper Ridge Dolomite is the Rose Run Sandstone which has gradational contact with the Copper Ridge. The Rose Run is compositionally mature and was sourced from the Precambrian shield (Grenville Province Rock) from which it was transported onto the carbonate platform and reworked. Deposition occurred concurrently with Copper Ridge Dolomite and was deposited into a shallow subtidal marine environment. The depositional environment is exhibited by its lithology which is predominantly quartz arenites to subarkoses with interbedded lenses of dolostone with low angle cross-beds (Wickstrom et al., 2005). Towards the end of the Cambrian, sandstone deposition ceased while carbonate deposition continued (Riley, 1994).

Carbonate dominated deposition continued in the Early Ordovician can be seen by the Beekmantown Group. This group is made up of quartz sandstones and clean dolomites and was deposited into a shallow subtidal to peritidal environment. The sandstone intervals present in the Beekmantown Group represent local periods of relatively low sea level as the study area during the Early Ordovician was still in a tectonically passive environment (Figure 1.1.3) (Dykstra et al., 1995).

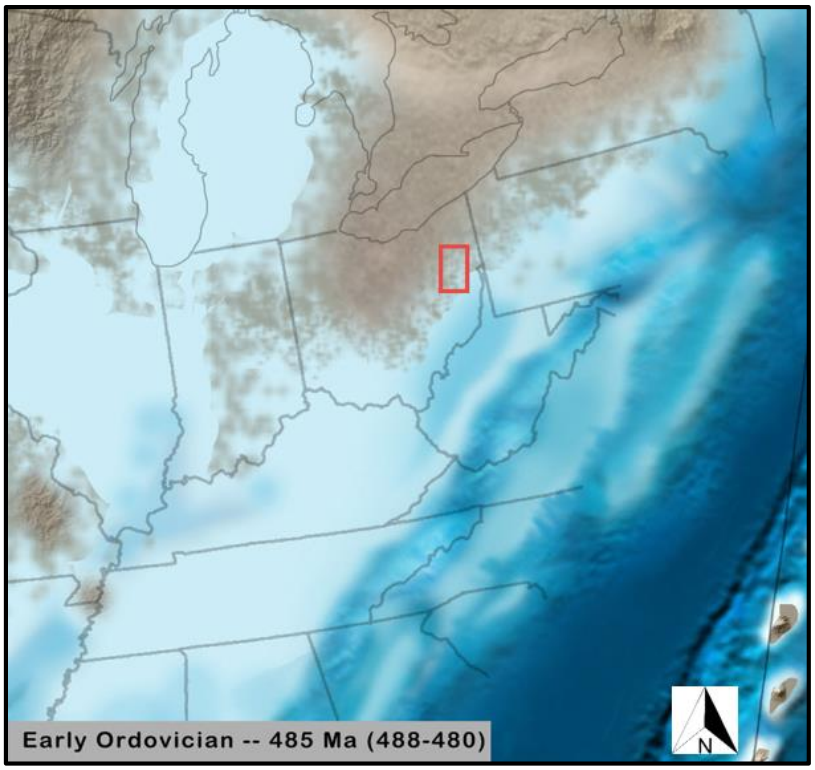

Figure 1.1.3 Paleogeography during the Early Ordovician. Study area highlighted (Blakey, 2007).

During the Early Ordovician to Middle Ordovician, the Taconic Orogeny began which involved the southern and central parts of Laurentia colliding with an offshore island arc shifting the Appalachian region from a passive to convergent margin and creating the Appalachian Foreland Basin (Figure 1.1.4). This event closed the Iapetus Ocean and uplifted/eroded the Appalachian shelf which can be represented by the Knox Unconformity located at the top of the Beekmantown Group (Ettensohn, 2008). The Knox Unconformity (aka the Owl Creek Unconformity throughout North America) represents 30 ma of erosion in places due to the prolonged exposure of Middle Ordovician to Upper Cambrian strata (Wickstrom et al., 2005). In addition, the Taconic Orogeny marks a sedimentary differentiation between eastern and central Laurentia, from widespread carbonate deposition resulting in the Great American Bank to deep shallow clastics (Ettensohn, 2008). This change in deposition style becomes expressed in the Late Ordovician.

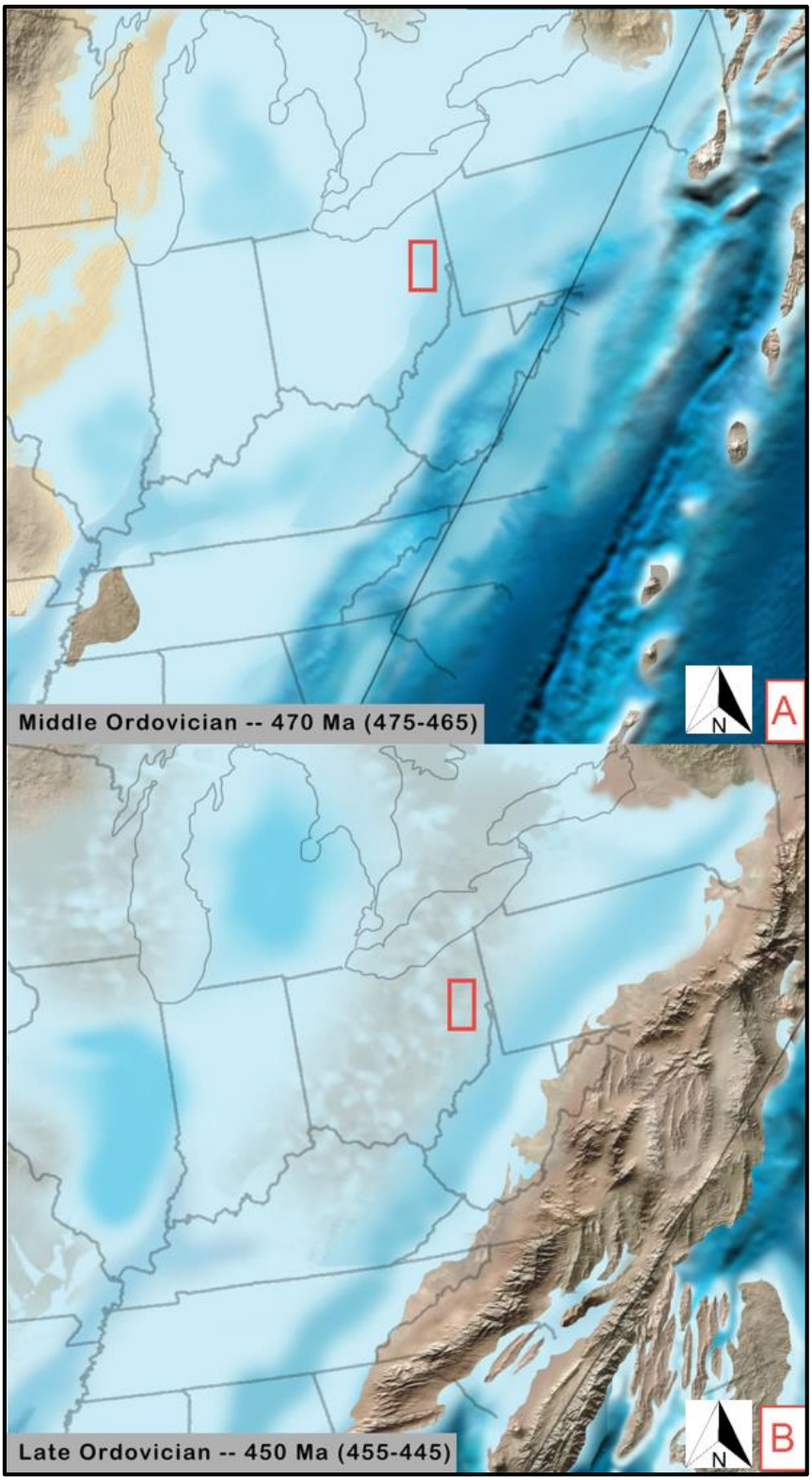

Figure 1.1.4 Paleogeography during the Middle (A) and Late Ordovician (B). Study area highlighted (Blakey, 2007).

Following the Knox Unconformity, Middle Ordovician deposition was dominated by carbonates, carbonate/shale intervals, carbonate mudstones, and bioclastic grainstones. Figure 1.1.5 shows a generalized depositional model for this time period. Overlying the Knox Unconformity is the Wells Creek Formation. This thin formation was deposited in a shallow sea and is composed of silty to sandy, fine grained dolostone with interbedded limestones (Wickstrom et al., 2005). Directly above the Wells Creek lies the Black River Group. This group is made up of muddy, fine grained shallow marine carbonates and was deposited in in both shallow subtidal and tidal flat environments (Smith, 2006) (Wickstrom et al., 2005). Above the Black River Group is the Trenton Limestone. This limestone represents an extensive marine transgression and represents the maximum subsidence for the Ordovician time period. This increased subsidence allowed for high energy, carbonate platforms to develop (Figure 1.14A). The Trenton was deposited in a high energy environment and consists of clean carbonates with grainstone-packstone textures (Patchen et al., 2005).

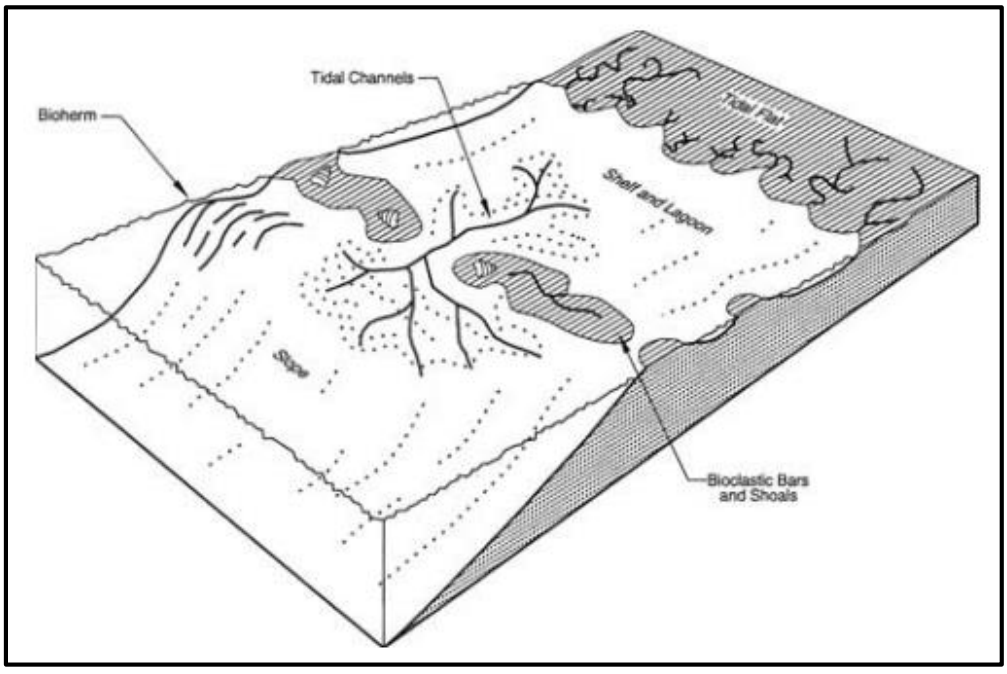

Figure 1.1.5 General model of depositional environments during the Middle and Upper Ordovician periods (Wickstrom et al., 2005).

The transgression that allowed for the deposition of the Trenton Limestone also resulted in the development of an anoxic, deep interplatform sub-basin in response to the continued compression from the ongoing Taconic Orogeny. The large inpouring of organics and restricted circulation within the sub-basin allowed for the deposition of the Utica/Point Pleasant in the Late Ordovician (Wickstrom et al., 2005) (Figure 1.1.6). The depositional environment during the Trenton/Point Pleasant time was storm dominated and experienced frequent algal blooms which influenced the lithological and organic characteristics of the Point Pleasant Formation (Patchen et al., 2015). The contact between the Point Pleasant and the Trenton Limestone is sharp in Eastern Ohio and can be visualized clearly in both seismic and log resolutions. The Point Pleasant Formation was deposited simultaneously with the Trenton Limestone with the Trenton being thickest along the platform and thinning as it approaches the sub-basin wherein the shale content increases with the deposition of the Point Pleasant (Patchen et al., 2005). This organic rich (TOC ranging from 4-5% in lower portion) formation is made up of interbedded limestones and black shales with the limestone and shale occurring in equal amounts along with minimal amounts of clay. In addition to this, storm beds are present indicating periods of high-energy sedimentary influx which was most likely transported off of the Trenton platform. The top of the Point Pleasant Formation is marked by a disconformity and is followed by the Utica Shale. This shale is made up of dark fissile shale with interbedded calcareous shale. When compared to the underlying Point Pleasant, the Utica has higher clay content (as seen in Gamma Ray logs), less calcite and less TOC (up to 3.5%). In addition, the Utica Shale contains few storm beds but is highly laminated (Patchen et al., 2015).

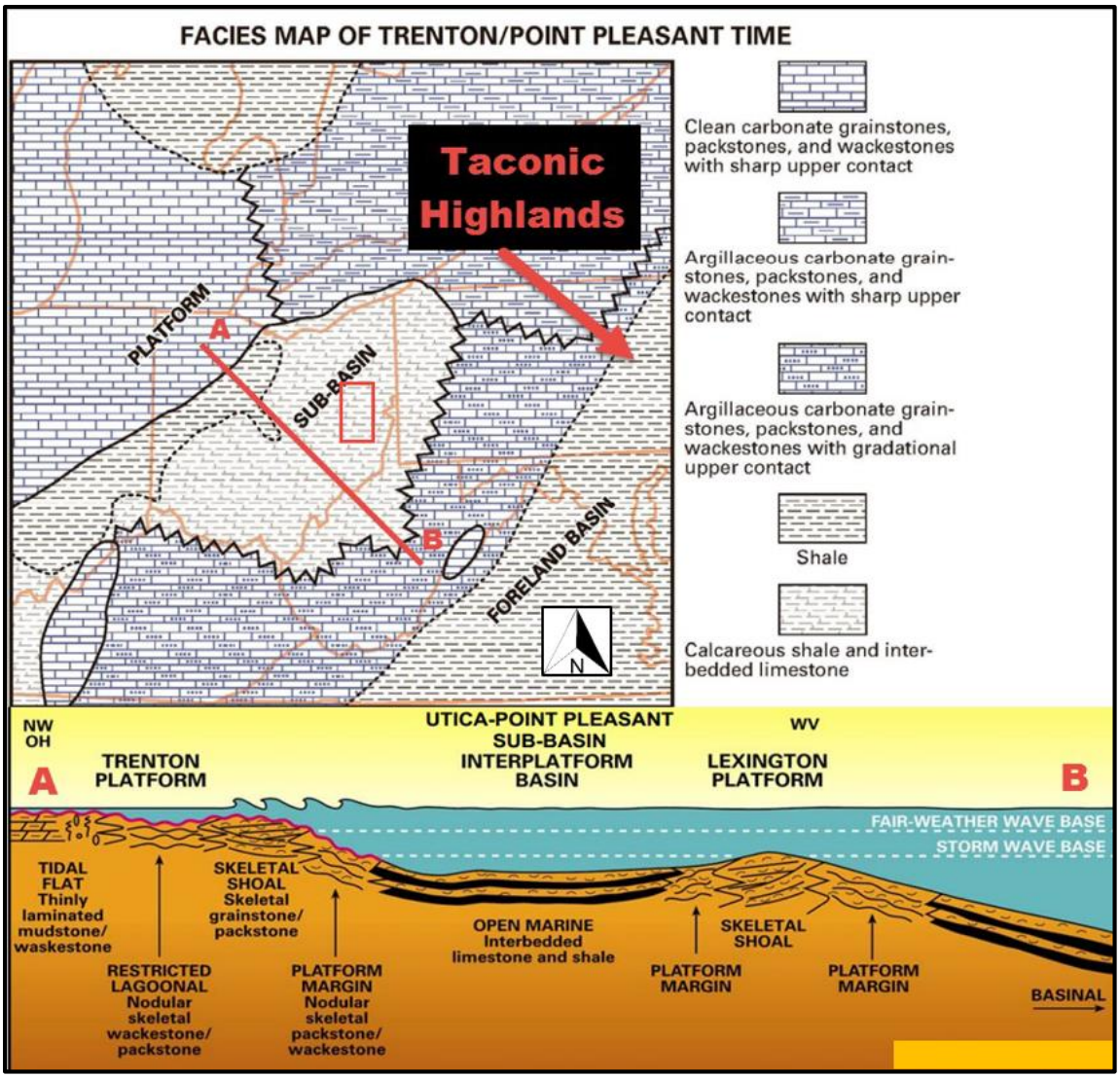

Figure 1.1.6 Facies during Trenton/Point Pleasant time along with a generalized cross section view. Red arrow points towards Taconic Highlands. Modified from Wickstrom et al (2012) and Patchen, 2005.

As the Late Ordovician continued, the Taconic Highlands and foreland basin continued to move towards Eastern Ohio as seen in Figure 1.1.4 B. The remainder of the Ordovician was dominated by thick, regionally extensive shales with less organic content and decreased carbonate deposition as the Late Ordovician continued. This change from carbonate rich shales in the Middle Ordovician to carbonate poor shales represents an increase in subsidence in both the Utica/Point Pleasant sub-basin and Trenton platform (Patchen et al., 2005). Deposited above the Utica Shale is a thick shale sequence known as the Reedsville Formation. This thick unit was

deposited in a shallow marine environment and is predominantly composed of gray shales with sandstone as well as minor amounts of limestone (Thompson, 1999) (Wickstrom et al., 2005). The final unit to be deposited in the Late Ordovician following the Reedsville is the Queenston Formation. This marginal-marine unit was deposited on the foreland of the Taconic orogenic belt on what was known as the Queenston delta and is distinguished by its red coloring (Ettensohn, 2008) (Wickstrom et al., 2005).

The Ordovician-Silurian transition is marked by an unconformity known as the Cherokee Unconformity. This erosional surface was most likely caused by tectonics and represents the final tectophase of the Taconic Orogeny (Ettensohn, 2008). During the Early Silurian, clastic material was eroded from the Taconic highlands which were made up of plutonic igneous rocks formed by island arc orogenic events. Eroded sediments were transported in both southeast-northwest (perpendicular to the shoreline) and northeast-southwest (parallel to the shoreline) directions. The depositional setting in eastern Ohio during the Early Silurian was made up of a shelf/longshore-bar/tidal-flat/delta environment (Figure 1.1.7). Deposited on top of the Queenston Shale is the Cabot Head Shale. This unit is made up of shelf muds and transitional silty sands (Wickstrom et al., 2005). Deposition of the Cabot Head Shale represents the extent of the Appalachian foreland basin (Ettensohn, 2008).

Following the deposition of the Cabot Head Shale is the Clinton Sandstone. The Clinton Sandstone is made up clastics from the eroding foreland highlands and plutonic igneous rocks of the island arc orogens located in the eastern portion of the Appalachian Basin (Carter et al., 2010). The Clinton interval is made up of interbedded sandstones, siltstones, shales, and small amounts of carbonate. The sandstones present consist of medium to very fine grained, quartzose sandstone, subangular to rounded grains, variable sorting, and discontinuous interbedded shales. Due to the variability in color of the Clinton sands, drillers' names have been used in Eastern

Ohio to distinguish the various sand bodies within the Clinton interval. Using these drillers' terms the Clinton interval can be divided into the Clinton White, Clinton Red, and Clinton Stray from oldest to youngest.

As illustrated in Figure 1.1.7, the Clinton Sandstone was deposited in a marine, shoreline-deltaic environment. According to literature the Clinton Sandstone is represented by several deltaic lobes within the ECOF that are oriented east to west and contains multiple regressive and transgressive cycles which are represented by thin interbedded shale intervals. Due to the active depositional environment in the Early Silurian, thickness variations are present in the Clinton. The Clinton interval is thinnest in the west which is predominantly an offshore marine/inter-channel environment while it thickens to the east in the deltaic/ tidal channel environment.

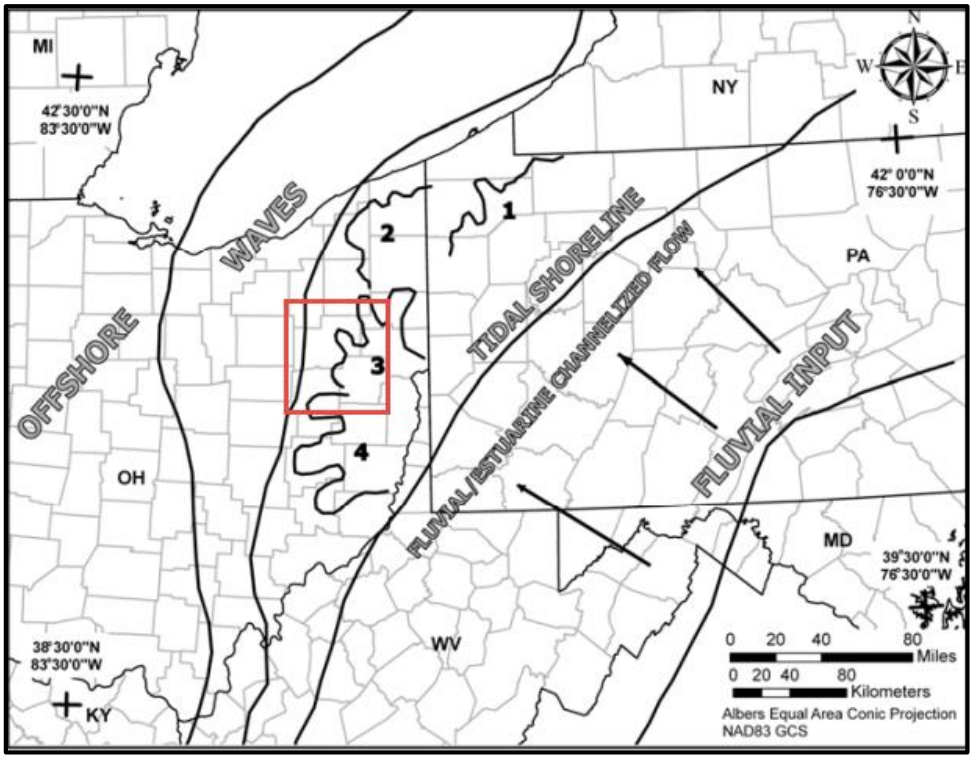

Figure 1.1.7 Paleoenvironment during the time of Clinton deposition in the Early Silurian. The various numbering represent the 4 different shoreline facies present: (1) tidal flat/creek and lagoonal; (2) braided fluvial channels; (3) littoral setting; (4) offshore bars (Carter et al., 2010). Red box highlights study area.

Bounding the top of the Clinton interval is the Upper Cabot Head Shale. The boundary between these units is marked by a fining up sequence. Lying above the Cabot Head Shale is the Packer Shell. This clean limestone formation is more formally known as the Dayton Formation (Riley et al., 2009). The boundary between the Upper Cabot Head Shale and the Packer Shell is marked by an unconformity related to a pre-Acadian Orogeny metamorphic event. This event occurring in the early to middle Silurian allowed for unconformity development caused by a rise in sea level. Following this unconformity sea level rose allowing for the Packer Shell to be deposited in a shallow water carbonate ramp (Ettensohn, 2008).

1.2 Petroleum Geology of the East Canton Oil Field

The East Canton Oil Field (ECOF) is a north-south trending oil field located in eastern Ohio. The field was first discovered in the in 1953 while active drilling and development did not begin until 1966. This field contains primarily oil but also contains large amounts of gas. The estimated reserves are 380 bcfg of gas and 1.5 billion barrels of oil (McCormac et al., 1995). As a disclaimer, all maps shown in this manuscript will not contain latitude and longitude information due to the proprietary nature of the data.

Source

The source rock for the ECOF/Clinton has been of much debate. Within the literature, two hypotheses exist. One being that the Lower Silurian Cabot Head Shale is the hydrocarbon source while the other is that the Ordovician black shales (Utica/Point Pleasant) is the source. It is suggested by Knight (1969) that the Lower Cabot Head Shale is the source due to its depositional environment and stratigraphic position below the Clinton interval. While the Lower Cabot Head would be an intuitive source rock given its stratigraphy and small migration path, geochemical analysis has shown that this shale lacks enough total organic carbon (TOC) to be a hydrocarbon source according to Cole et al. (1987).

In addition to lacking TOC, the Cabot Head is most likely too thin to produce economic amounts of oil and gas. The geochemical analysis discussed in Cole et al., 1987 suggests that the most likely source rocks for the Clinton Sandstone are the Ordovician black shales. Oil found in the Clinton Sandstones of Ohio are geochemically similar to those found in Ordovician reservoirs (McCormac et al., 1995) (Ryder et al., 2003).

Migration

With the Point Pleasant/Utica shales being the most likely source rock, 1000-2000 ft. of vertical migration occurred to reach the Clinton Sandstone reservoir rocks in eastern Ohio. The Clinton Sand reservoirs can best be described by both basin-center gas and hybrid-conventional oil and gas accumulations. What defines this distinction is a regional barrier (up to 10 miles wide) of water saturated rock occurring within the low permeability zones of the Clinton interval. This water block lies just west and adjacent of the ECOF (Figure 1.2.1). While a water contact is suggested to exist in the western portions of the field by Ryder., 2003, water data does not suggest its existence.

Ryder 2003 puts the hydrocarbon generation occurring during the Middle Devonian and migration occurring at the latest during the Upper Permian. Figure 1.2.2 best illustrates the three stages of hydrocarbon migration/generation for the Clinton Sands. (A) Oil and gas from the Point Pleasant/Utica source rock vertically migrates through basement controlled fracture networks into Clinton Sand reservoirs during the late Paleozoic. Very little migration occurs in the Tuscarora Sandstone facies of the Clinton due to a lack of permeability. (B) Peak subsidence occurs during the latest Paleozoic/early Mesozoic. During this time, gas generation occurred causing over pressuring and the movement of water updip. This in turn created both the basin-center gas and hybrid conventional oil and gas accumulations found in eastern Ohio. In addition, oil that was not converted to gas but increased in maturity. (C) During the late Mesozoic, uplift and erosion of the

Appalachian Basin occurred which altered the Clinton Sand reservoirs. This basin scale uplift event caused the Clinton Sand reservoirs to become under pressured. This subsequently caused gas loss due to accelerated migration through fracture networks and an increase in pore space. This gas loss also caused the down dip retreat of the basin-center gas allowing for water to fill the updip pore space. Supplementary, this decrease in size of the Clinton Sand accumulations allowed for updip recharge with meteoric water as well as brine water most likely sourced from Silurian evaporate deposits (Ryder et al.,2003).

Structure & Trap

In general, the ECOF is located in the east-southeast dipping monocline that characterizes the western margins of the Appalachian Basin. Within proximity to the ECOF are several north-northwest striking faults that align with structural highs along the Packer Shell (top of reservoir) In addition, the Akron-Suffield fault trends to the northwest along the northern margin of the ECOF and can be seen in Figure 1.2.3 just north of the ECOF boundaries (Riley et al.,2009). While literature describes ECOF hydrocarbon entrapment being primarily stratigraphic, residual structure mapping illustrates potential structural controls. The residual structure map taken from formation top depths at the base of the Packer Shell correlates well with the ECOF boundaries. When production and structure are considered, higher gas to oil ratios (GOR) are found along the structural highs while lower ratios are seen in the structural lows (Figure 1.2.4). While further investigation is needed to further determine structural controls for the ECOF, the primary trapping mechanism is stratigraphic. Based on the marine and fluvial deltaic depositional environment, up dip thinning and pinchouts of the Clinton Sand provide the hydrocarbon entrapment while the Upper Cabot Head Shale (gradational contact with Clinton) and Packer Shell provide a seal to limit hydrocarbon movement.

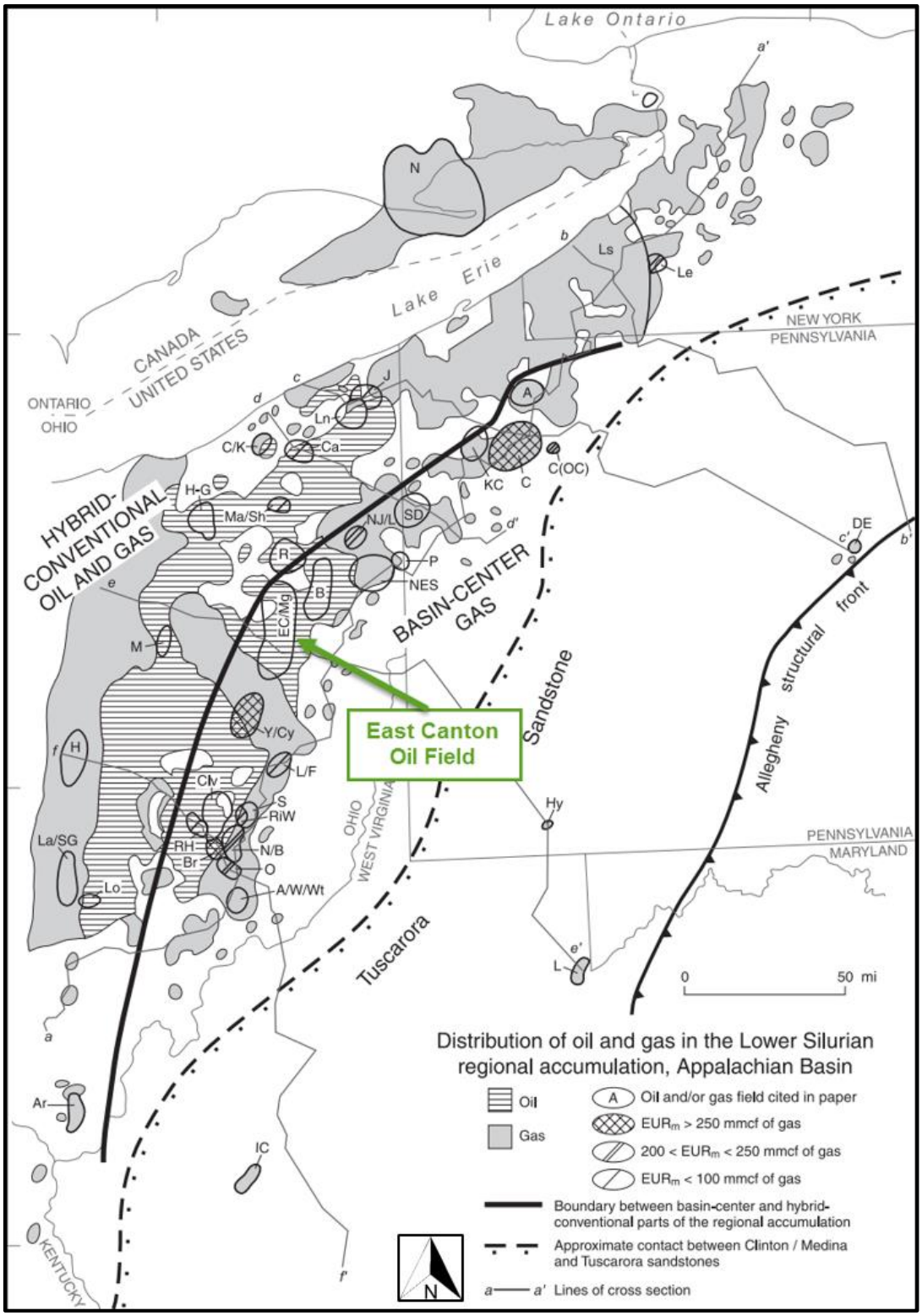

Figure 1.2.1 Map of the types of hydrocarbon accumulations within the Clinton Sandstone. Modified figure by (Ryder et al., 2003).

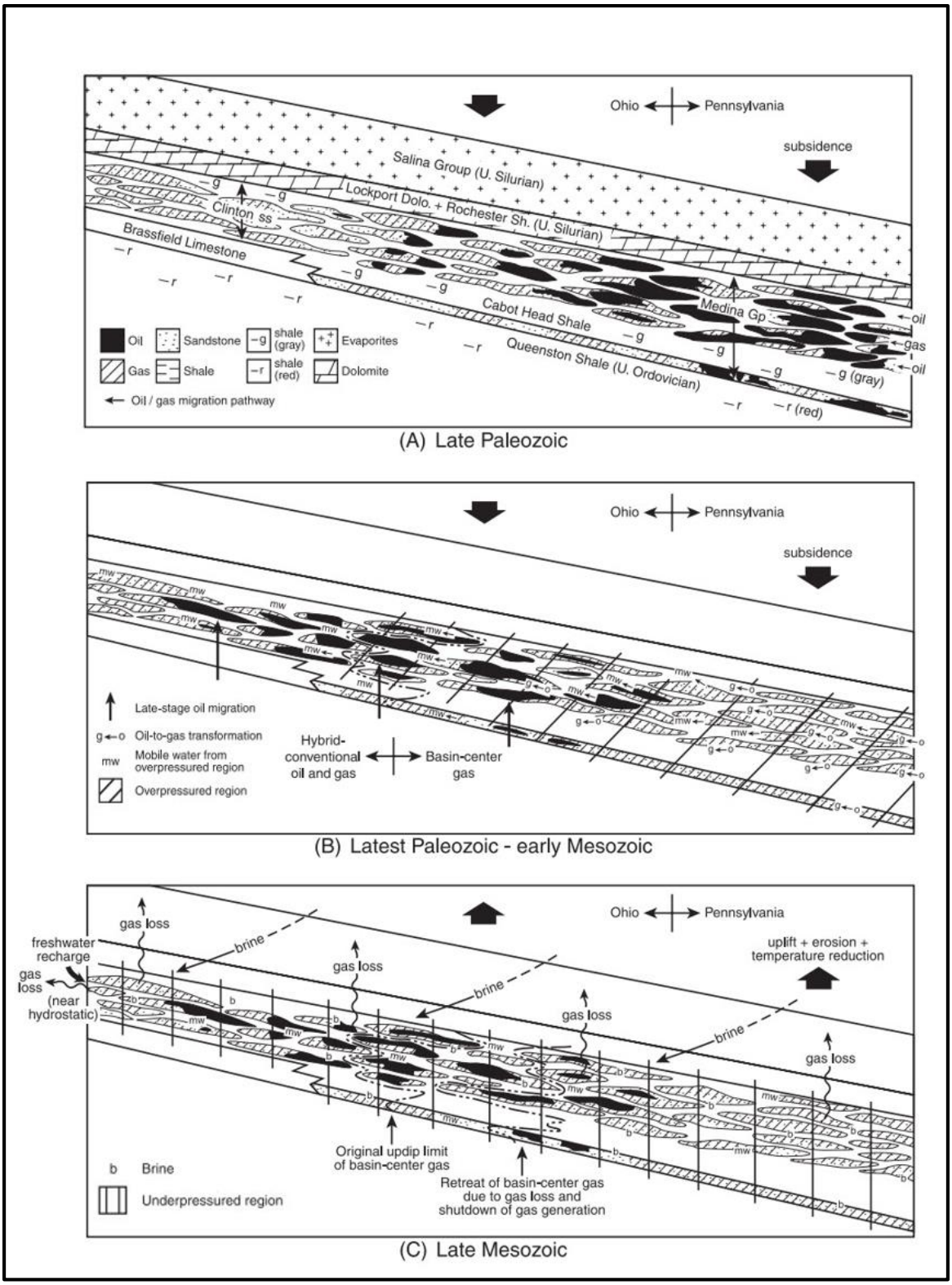

Figure 1.2.2 Model showing the hydrocarbon migration and timing for the Clinton Sand reservoirs (Ryder et al., 2003).

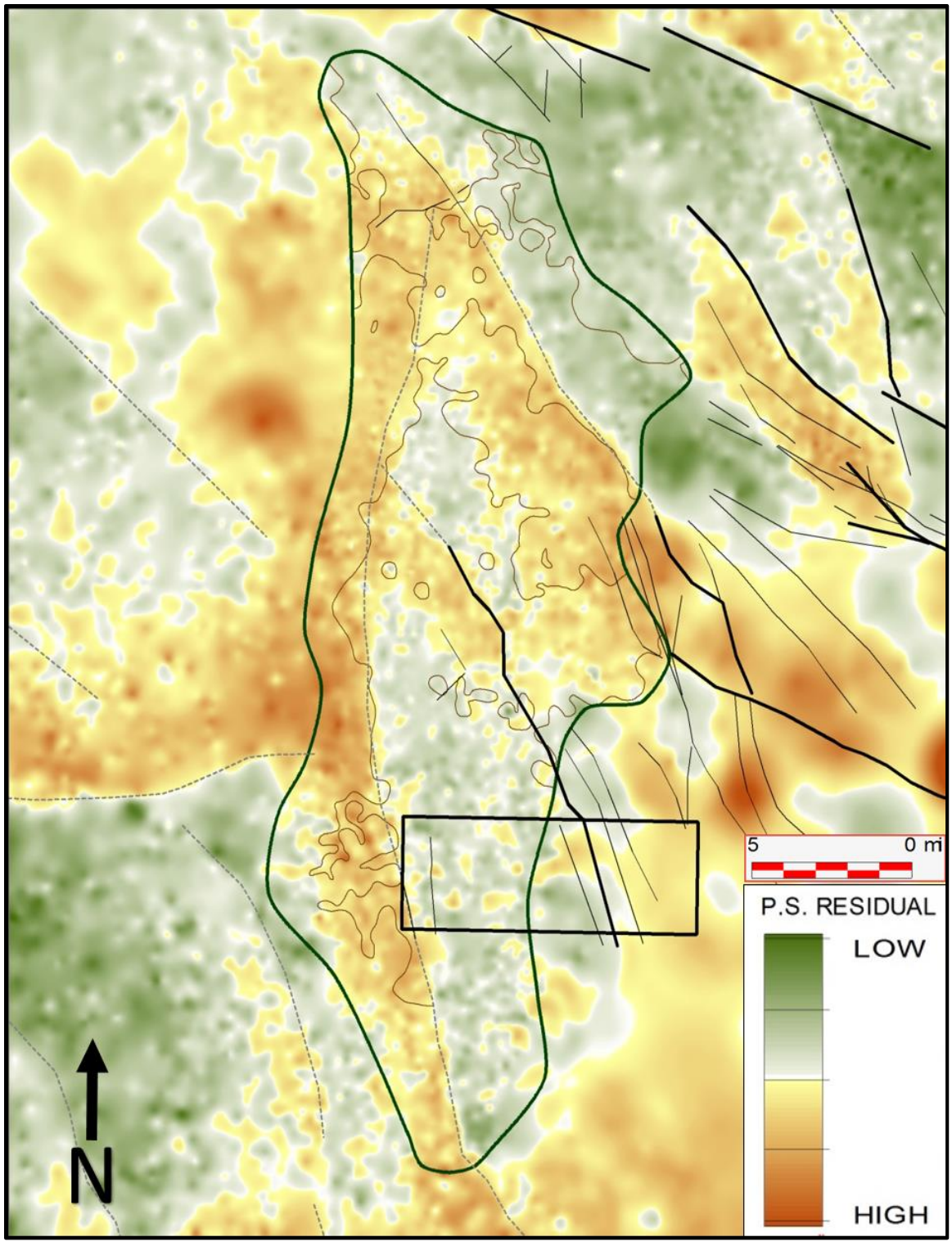

Figure 1.2.3 Residual structure map created from the top of the Packer Shell highlighting potential structural controls on the ECOF. Rectangle represents seismic outline, solid black lines represent mapped faults while dashed lines represent interpreted faults from the residual mapping.

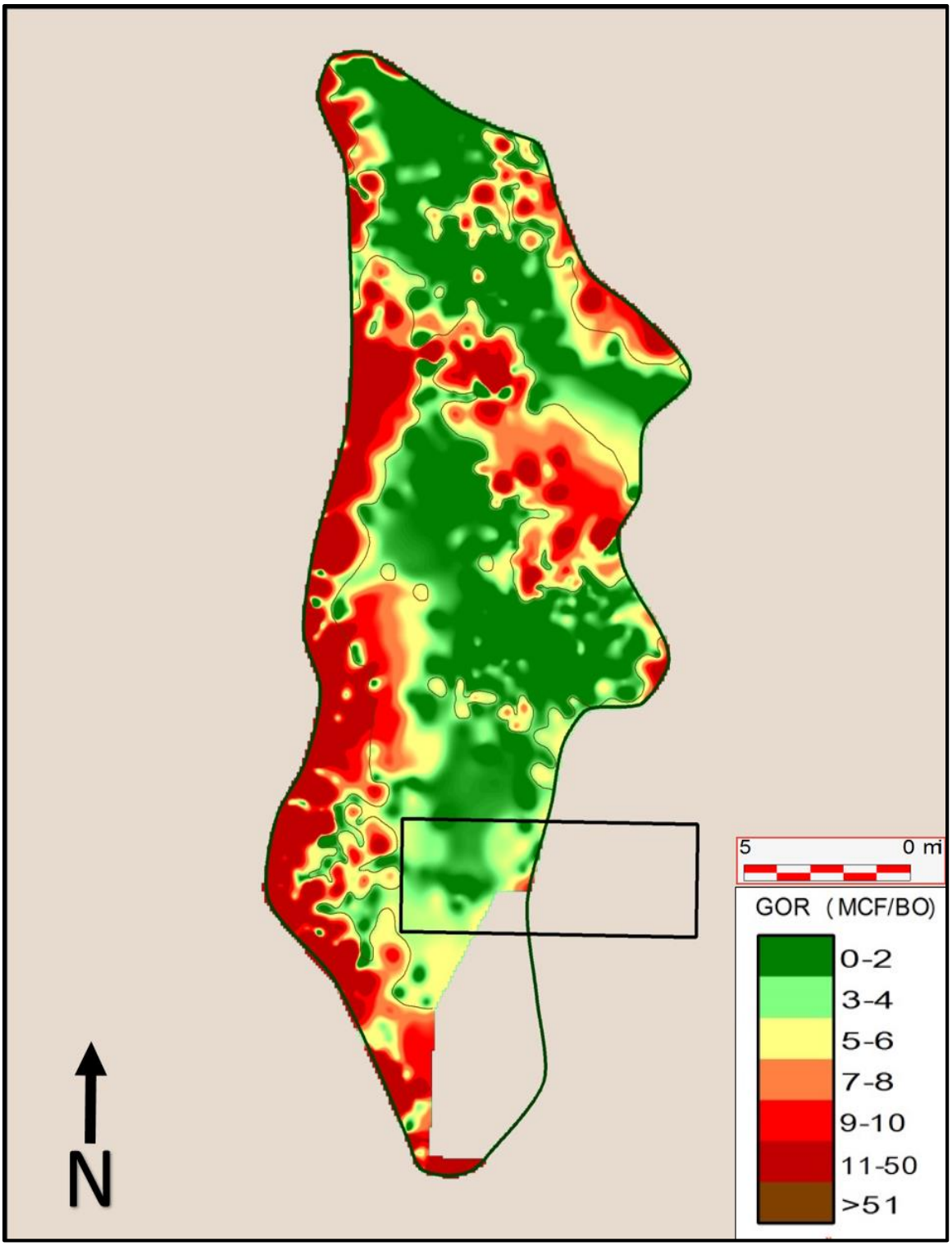

Figure 1.2.4 GOR (metric cubic foot (MCF)/ barrel of oil (BO)) map of the ECOF displaying largest 1 year production. Rectangle represents 3D seismic outline.

Reservoir Traits

The Clinton Sandstone can be described as a tight sandstone reservoir due to its low permeability and its heterogeneous nature that makes correlating individual sand bodies complex. Figure 1.2.5 shows a type log for the ECOF. Track 1 shows gamma ray, track 2 shows bulk density with lithological symbols overlain, track 3 shows density porosity (red) and neutron porosity (blue) while track 4 shows p-wave (red) and s-wave (blue) sonic logs. The Clinton interval can be divided into the Clinton Stray, Red, and White (Figure 1.2.5). Note: in later figures the Clinton Stray is also referred to as the Clinton Sand to mark the top of the interval. The Clinton White represents a coarsening up sequence and was deposited in a marine shore face and deltaic environment. The Clinton White is distinctive by its "blocky" GR log signature. Bounding the Red and White is marine shale which represents a maximum flooding surface. Deposited on top of this surface is the Clinton Red. This sandstone body represents the final transgression within the Clinton interval. Finally, the Clinton Red grades into the Clinton Stray. This sequence fines upward into the Upper Cabot Head Shale and can be described as a dirty sandstone based on its varying amounts of clay content. Within the Clinton interval, the Clinton White, and Red are the most important reservoir rocks. These units contain up to 90% of the original oil in place (OOIP) within the ECOF and can have a combined thickness of upwards of 60 ft (Riley et al., 2009). Well log responses indicate that these rocks have the highest reservoir quality within the Clinton interval with the Clinton White being the primary horizontal drilling target.

The heterogeneity of the Clinton reservoirs is controlled by many factors including grain size, clay content, cementation, and thickness. These, along with the complex depositional environments and digenetic processes, have created variations in porosity and permeability within the ECOF (McCormac et al., 1995). Average matrix permeability ranges between 0.10-0.16 md

while porosity ranges from 4-11% (Riley et al., 2009). Silica cement is found regionally within the Clinton Sandstone while carbonate cement occurs in localized areas. Due to the presence of silica cementation, primary porosities are not present leaving secondary porosity in the Clinton Sandstone. The types of secondary porosity that are present include intergranular and moldic with the moldic porosity contributing the most to the reservoir quality. Intergranular porosity is present from partial dissolution of primary calcite cement when present while the moldic porosity is related to the dissolution of feldspars grains. This moldic porosity developed in part due to fluids travelling in fractures/faults. It has been noted that porosity holds a greater influence on production than clean sandstone thickness (McCormac et al., 1995).

Water saturation is relatively high within the ECOF. Within the target interval (Clinton Red & White), water saturation ranges from 13-42% (Riley et al., 2009). Due to a lack of increasing water production rates, it can thus be inferred that a water drive is absent from the ECOF. The primary drive mechanism within the field is through solution gas thus making the ECOF an ideal candidate for multi-stage horizontal hydraulic fracturing (McCormac et al., 1995).

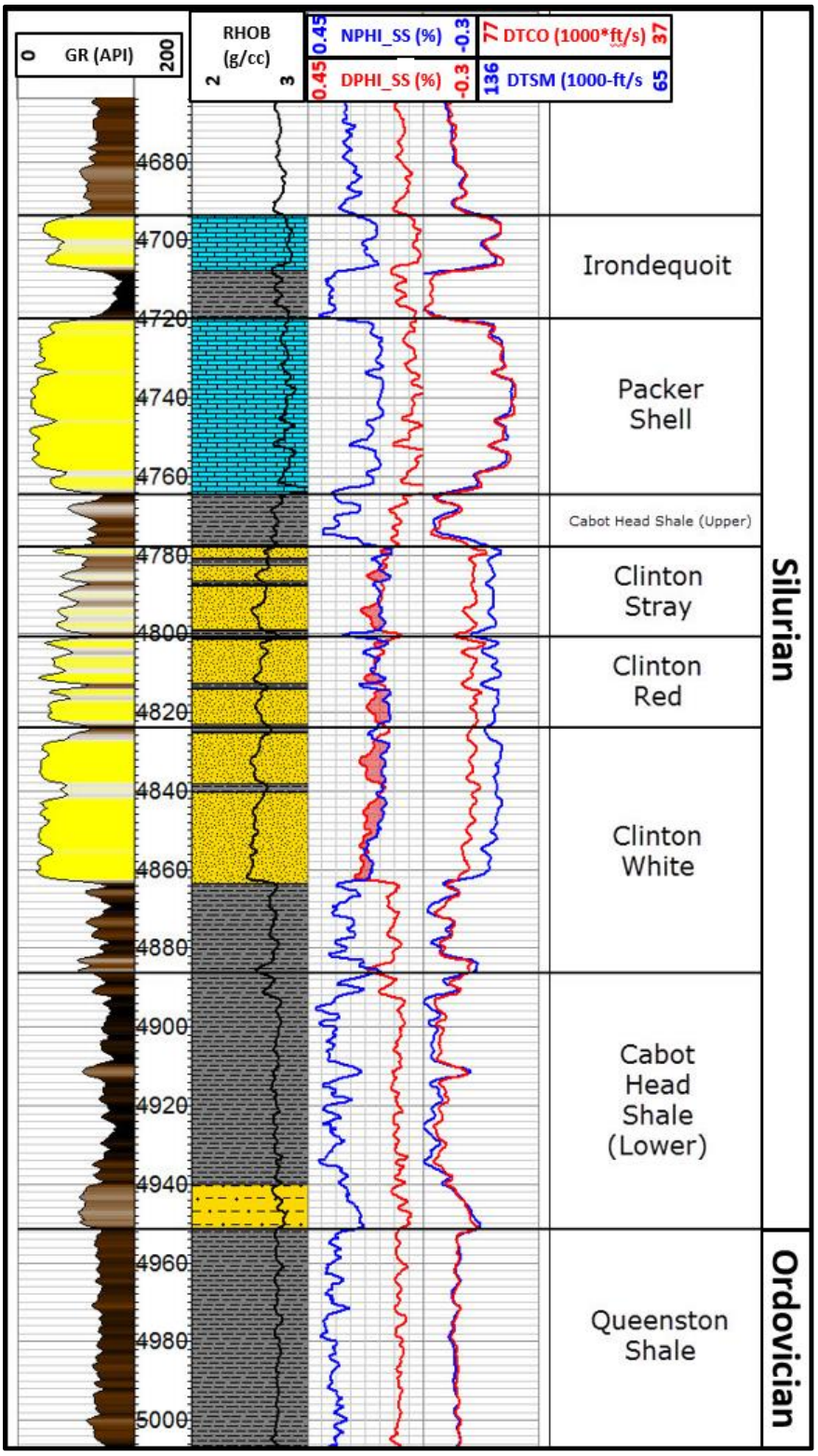

Figure 1.2.5 Type log for the ECOF showing, typical gamma ray, density, density porosity, neutron porosity, compressional wave and, shear wave log curve responses.

Chapter 2: Data

2.1 Firestone 3D Seismic Data

The Firestone 3D is a 406 sq mile 3D seismic volume owned by Tomlinson Geophysical Services (TGS) and overlies the eastern portions of the ECOF. Of this, a 40 sq mile cutout will be used for this study. This survey was acquired by TGS in 2011 using a combination of dynamite and vibroseis with a record length of 5000 ms The Geophone array used 6, 10 Hz phones at 25 ft of spacing. 2.2 lbs charges were used with 30 ft shot holes. 3 vibroseis were used with 80 ft of spacing with sweep lengths were 12 sec with a frequency range of 6-120 Hz For the acquisition parameters, a shot line interval of 1320 ft, shot point interval (diagonal) of 245.9 ft, receiver line interval of 880 ft, and a receiver interval of 220 ft was used. CMP bin size is 110 x 100.

The volume selected the pre-stack seismic inversion is a 5D post stack time migrated (PSTM) volume. This volume was originally processed in 2014 with the following processing flow outlined in Figure 2.1.1.

Step #	Processing Technique
1	Reformat SEG-D
2	Minimum Phase Conversion (Vib Records)
3	Geometry Assignment
4	Trace Edits
5	Phase Mathcing
6	Refraction Statics (Datum=1400 ft, Vw=2500 ft/s, Vr=12000 ft/s)
7	Gain Recovery
8	Surface Consistent Scaling
9	Surface Consistent Deconvolution (200-2000 ms@200 ft,400-2100 ms@2000 ft,600-2200 ms@4500 ft,800-2200 ms@7000 ft,1200-2200 ms@10000 ft,80 ms OPER,0.1 % PW)
10	Surface Consistent Scaling
11	Noise Attenuation (Hi Amp. SUP Linear Noise Atten)
12	CDP Sort
13	Velocity Analysis: 1 Mile x 1 Mile
14	1st Pass Residual Statics (400-2000 ms,+/-36 ms)
15	Velocity Analysis: 1/2 Mile x 1/2 Mile
16	2nd Pass Residual Statics (400-2000 ms,+/-12 ms)
17	Surface Consistent Scaling
18	Surface Consistent Statics & Phase Correction
19	NMO (Normal Moveout)
20	Trim Statics (400-1500 ms,+/-6 ms)
21	5D Interpolation
22	NMO Removal
23	PSTM Velocity Analysis
24	Kirchhoff Pre-Stack Time Migration (45 deg.) with ETA

Figure 2.1.1 Processing sequence for 5D PSTM volume

In order for reliable inversion results to be obtained, the 5D PSTM volume underwent conditioning in order to provide reliable results. The conditioning involves the following work flow applied pre-stack data; Automatic Velocity Picking (AVEL) + Elastic Dilatancy Anisotropy (EDA), Radon and RAC. AVEL+ EDA involves correcting for and achieving high-density velocities. Radon is then applied to remove multiples by forcing events that were originally

hyperbolic to become more parabolic. This approach is effective and preferable in that it preserves amplitude and phase characteristics important for amplitude inversion (Yilmaz, 2001). Finally, RAC (Relative Amplitude Correction) is applied to the volume. In this, amplitudes are balanced and equalized in the offset, space, and time domains. Figure 2.1.2 provides a visual as to how the workflow affects the stacked seismic data. Following the AVEL EDA, Figure 2.1.2 B shows the removal of potentially harmful multiples below the Clinton White event while the RAC in Figure 2.1.2 C shows more balanced and equalized seismic amplitudes. Figure 2.1.3 shows comparable conditioning results in the gathers. Note the AVO anomaly present in the Clinton White that goes from a low-impedance trough in the near offsets and becomes a large peak in the far offsets and is preserved throughout the gather conditioning.

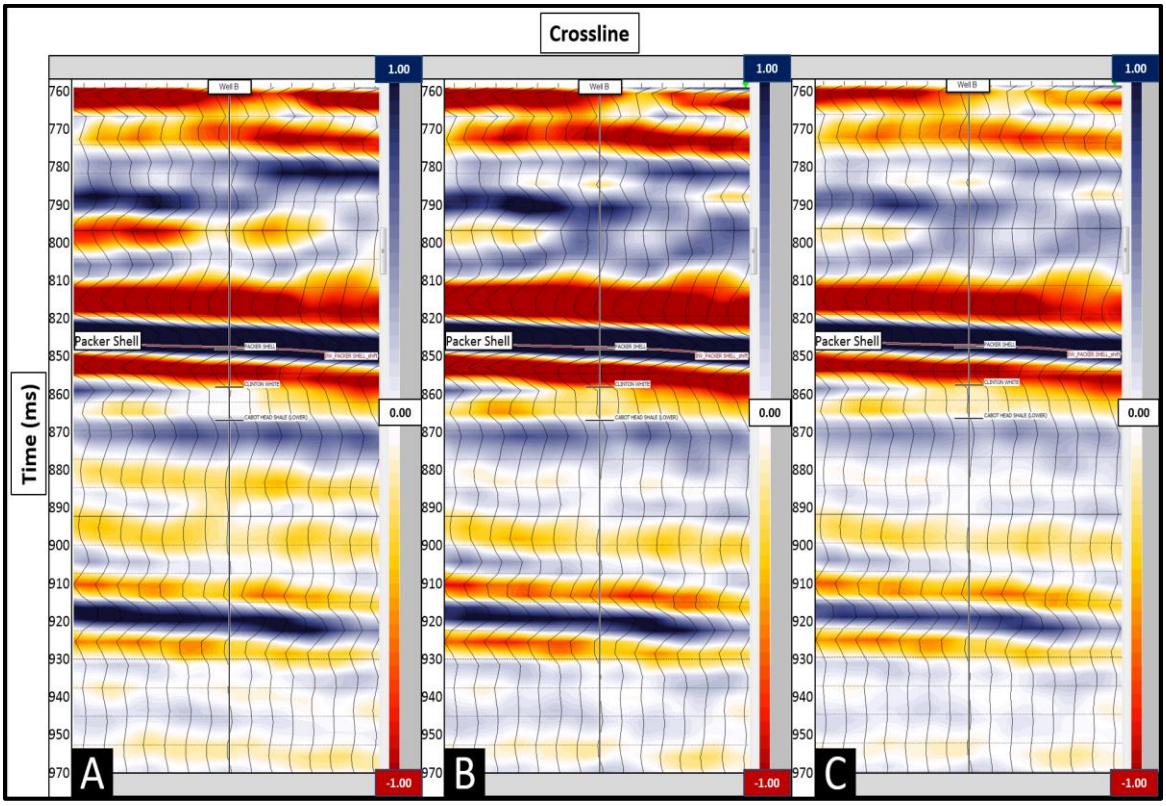

Figure 2.1.2 Seismic cross section of the stacked data at well B showing the conditioning workflow over the area of interest. The y axis is in time ranging from 760-970 ms while the x axis represents crossline. The Clinton White can be seen as a trough above the Lower Cabot Head Shale formation top. (A) AVEL EDA applied with a 30 deg normal move out correction. (B) Radon applied. (C) RAC applied (volume used for synthetic ties).

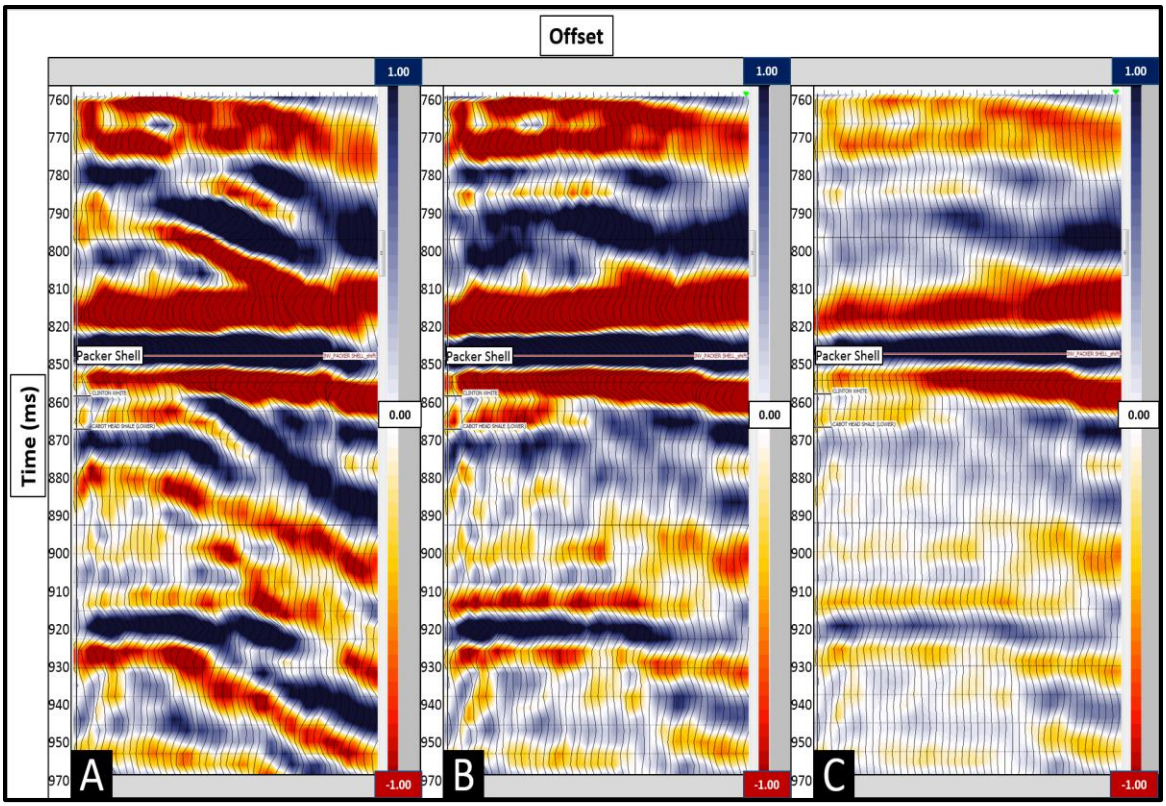

Figure 2.1.3 Seismic gathers cross section at well B showing the conditioning workflow over the area of interest. The y axis is in time ranging from 760-970 ms while the x axis represents offset. The Clinton White can be seen as a trough above the Lower Cabot Head Shale formation top. (A) AVEL EDA applied. (B) Radon applied. (C) RAC applied (inversion input)

2.2 Well Log Data

Within the 3D are three wells that will be defined as wells A, B, and C. These wells contain gamma ray (GR), caliper, resistivity, density correction (DRHO), density (RHOB), density porosity (DPHI), neutron porosity (NPHI), p-wave velocity (DT), and s-wave velocity (DTS) log curves over the entire range of Paleozoic strata in Eastern Ohio (Figure 2.2.1). Due to well A not containing measured DTS, DTS was predicted from DTC through a linear regression method that utilizes relationships found in the GR, NPHI, and RHOB curves by formation and lithology. All of the log curves used for the pre-stack inversion underwent petrophysical evaluation and editing in order to be consistent with the regional geology.

Including the inversion wells, 1856 wells were available for geologic mapping. All of which contain measured log data from the Packer Shell to the Lower Cabot Head Shale. Of this,

1856 wells contain GR logs while 450 of those contain GR, DPHI, and NPHI logs over the target interval (Figure 2.2.1).

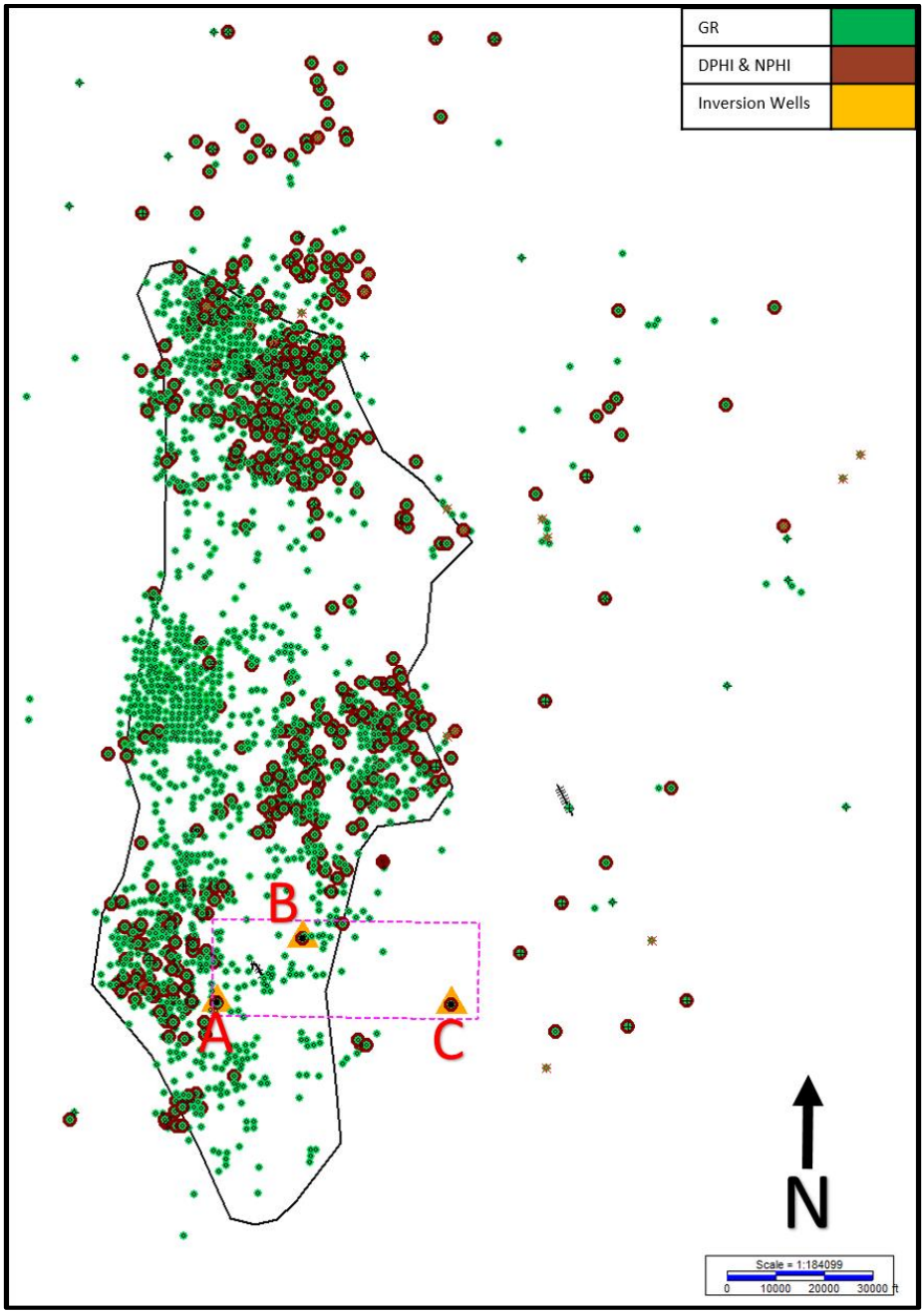

Figure 2.2.1 Map of the study area in showing well and seismic data available in the vicinity of the ECOF. The pink dashed outline represents the Firestone 3D seismic outline while the solid black outline marks the ECOF. Wells with GR are in green, wells with DPHI/NPHI are in brown while wells used in the inversion are represented by golden triangles. Of the inversion wells from west to east are wells A, B, and C.

Chapter 3: Methods

3.1 Historical Geologic Mapping

In order to better visualize and understand the reservoir geometry and depositional environment for the Clinton interval, net sandstone maps were created using 1856 GR logs available within the ECOF boundaries and the surrounding area. Formation tops were picked using the type log in Figure 1.2.5. The technique as outlined in (Knight, 1969) and applied in (Riley et al., 2009) involves using GR deflections from a shale base line of 200 API to map areas of clean sand. Clean "pay" sand for the Clinton and will be defined as having an API of 70 or less (65 percent deflection from shale base line) in this study. In order to understand the geologic changes within the Clinton interval, three net sandstone maps were generated for the Clinton interval, Clinton White, and Clinton Red. While (Knight, 1969) and (Riley et al., 2009) use 50 API as a cutoff, a cutoff of 70 API was used in order to show more of the geomorphic features and to aid in reservoir visualization. Figure 3.1.1 shows the difference in the GR cutoffs. This technique is useful in interpreting the depositional environment and identifying potential reservoir quality rock.

Of the 1856 wells that contain GR logs, 450 contain DPHI and NPHI logs. As seen in Figure 1.2.4, the Clinton Sand shows crossover between the DPHI and NPHI logs indicating the presence of gas and reservoir quality porosity. When gas is present in the pore space, the density porosity curve will read higher while the NPHI curve will decrease (Dewan, 1983). DPHI and NPHI logs using a Sandstone reference matrix were used to identify crossover. Net pay maps were created for the Clinton Interval, Clinton White, and the Clinton Red in which pay is defined as having crossover and having an API less than 70. While no use of pay flag mapping can be found in the literature, it is used to integrate geological and seismic mapping. Figure 3.1.2 shows the log curve cutoffs used to define pay.

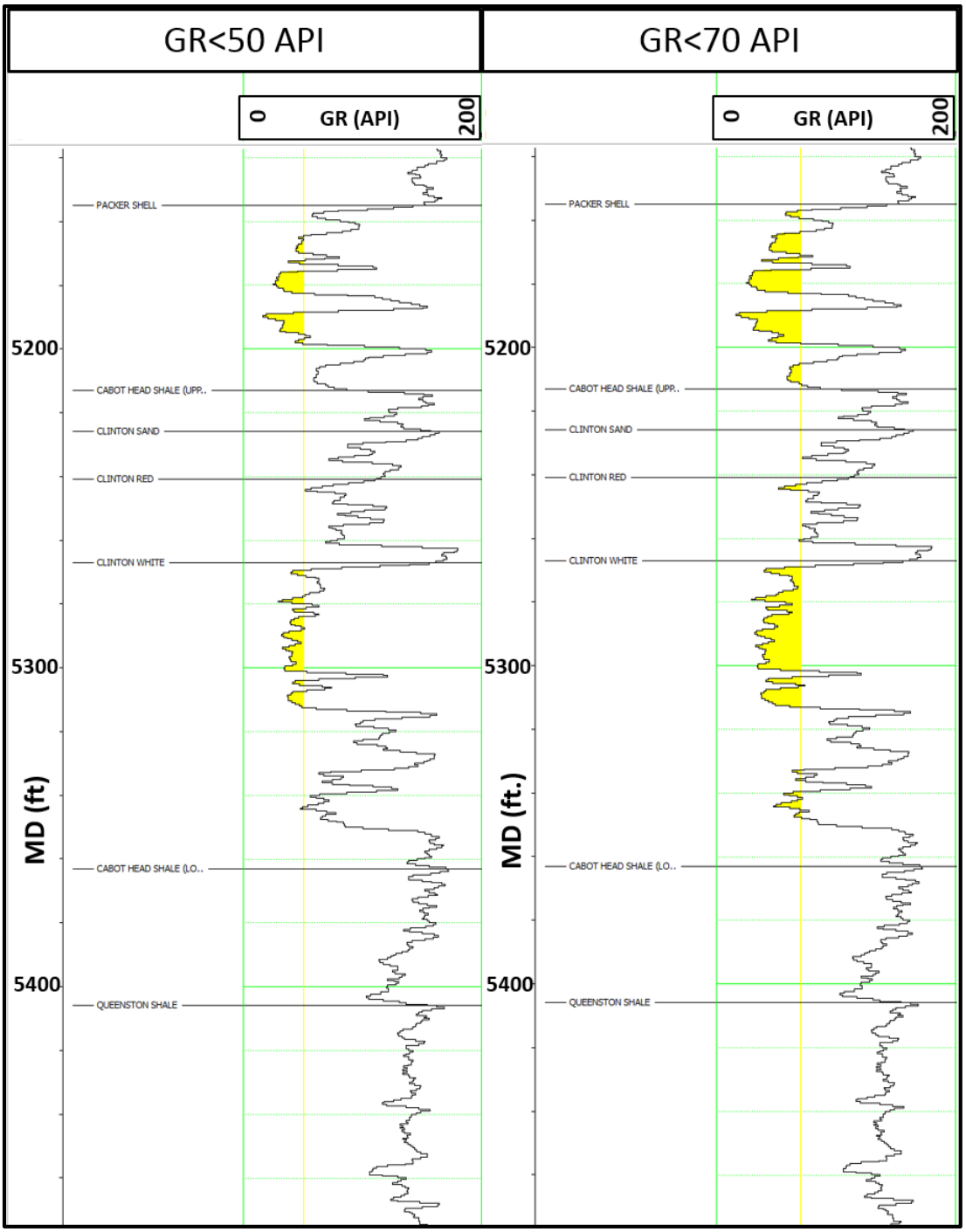

Figure 3.1.1 GR log at well B comparing the 50 API cutoff used by (Knight, 1969) and (Riley et al., 2009) and the 70 API cutoff used in this study. Cutoff ranges are defined by yellow coloring. Since horizontal completions allow for more rock to be accessed and permeability to be created, 70 API was chosen to define potential hydraulic fracturing targets.

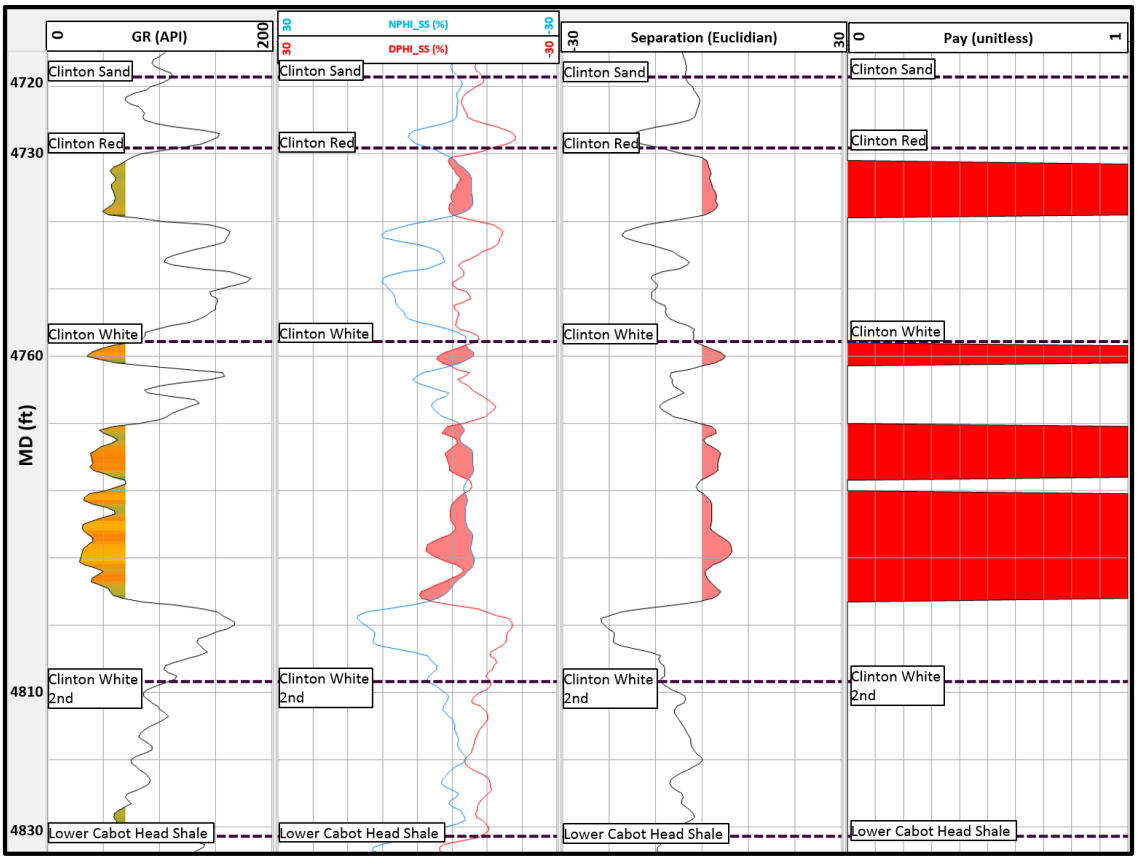

Figure 3.1.2 Log curve cutoffs used for geologic mapping of the Clinton interval. GR is colored to show 70 API or less, DHPI/NPHI crossover is colored red and separation is colored 0 or greater representing crossover. Separation is defined as DPHI-NPHI and is used to QC the crossover. A sand interval that meets this criteria it is flagged as pay.

3.2 Pre-Stack Inversion

Due to the thin discontinuous nature of the Clinton reservoir, pre-stack inversion was elected in order to visualize the varying reservoirs. From this compressional wave impedance, shear wave impedance and Vp/Vs volumes were created using Hampson-Russell software with the following methodology outlined in Figure 3.2.1.

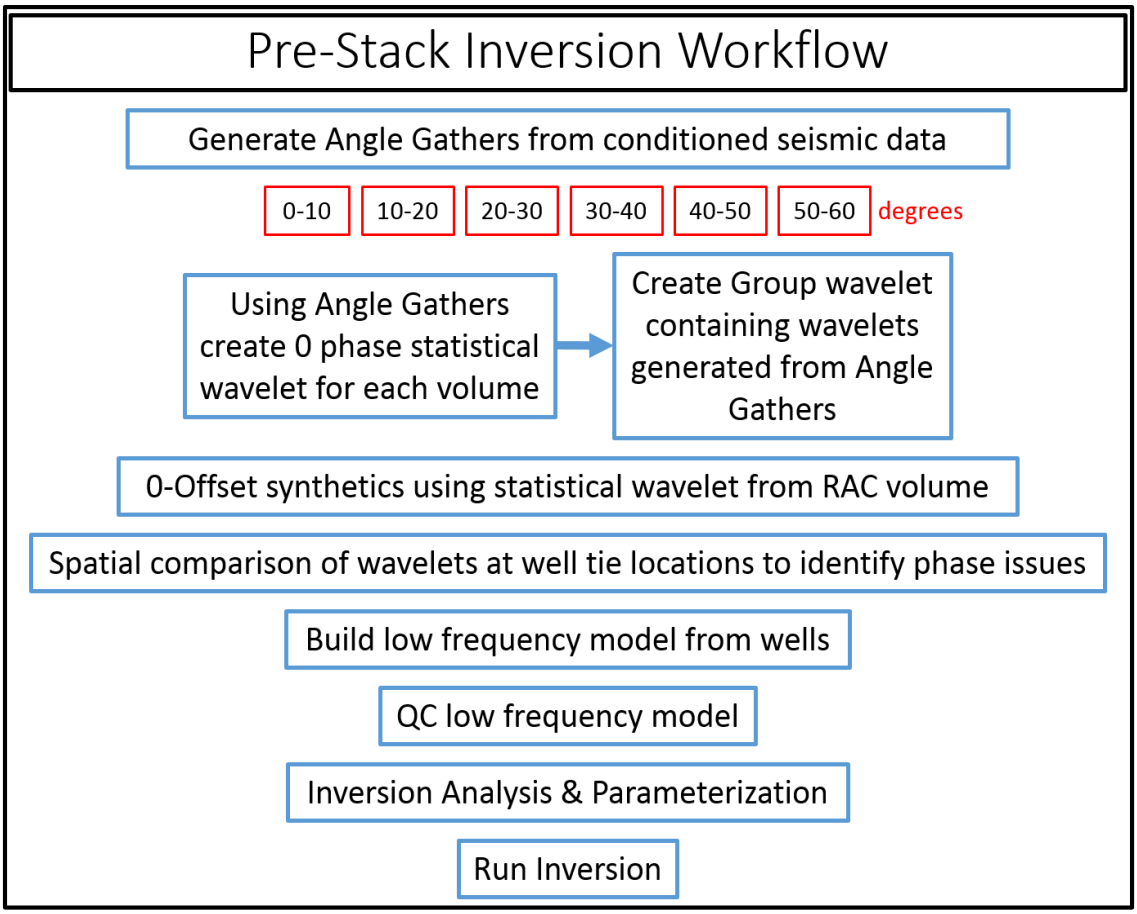

Figure 3.2.1 Outline of Pre-Stack Inversion workflow

Six angle gather volumes were created from the pre-stack volume with ranges of 0-10, 10-20, 20-30, 30-40, 40-50 and 50-60 degrees. From each angle group volume, a constant phase statistical wavelet from 300-1300 ms was generated. 300-1300 ms was chosen since it encompasses several key, strong regional reflectors such as the Onondaga Limestone (Devonian), Packer Shell (Silurian, Clinton Sand caprock), and the Trenton Limestone (Ordovician). With a wavelet generated from each angle gather, the subsequent wavelets were combined into an angle-dependent group wavelet. As seen in Figure 3.2.2, the lower angle groups have higher frequencies while the higher angle groups have lower frequencies.

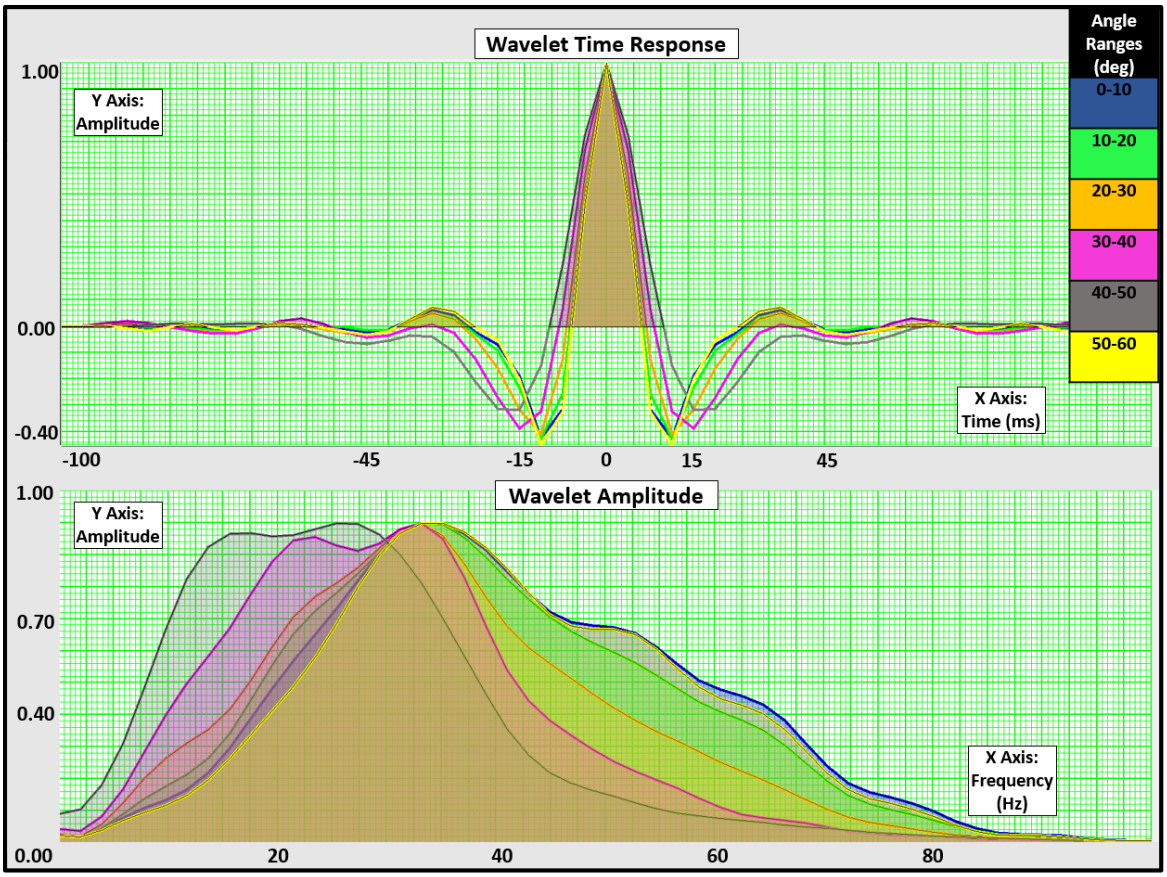

Figure 3.2.2 0 phase 0-60 degree statistical group wavelet used for pre-stack inversion

In order to establish a time depth relationship between the wells used in the inversion and the seismic volume, 0-offset synthetics were generated at each well location using a 300-1300 ms statistical wavelet. Three synthetics were created with an average suggested phase rotation of -37.88 degrees. From this, the volume was rotated +45 degrees in order for the seismic events to be coherent with previously interpreted geology by allowing peaks and troughs to remain as such. Synthetic ties were then done using the Final2_DECADE_Stack_Phas+45 volume. Figures 3.2.3, 3.2.4, and 3.2.5 show the synthetics for wells A, B, and C. Tie points for the synthetics include the Onondaga Limestone, Packer Shell, Utica Shale and the Trenton Limestone due to their prominent reflectivity and consistency within the study area. Using the three tied wells, a low-frequency model was built using the P-wave, S-wave and Density logs. A two way travel time window of 0-3500 ms was used along with a frequency

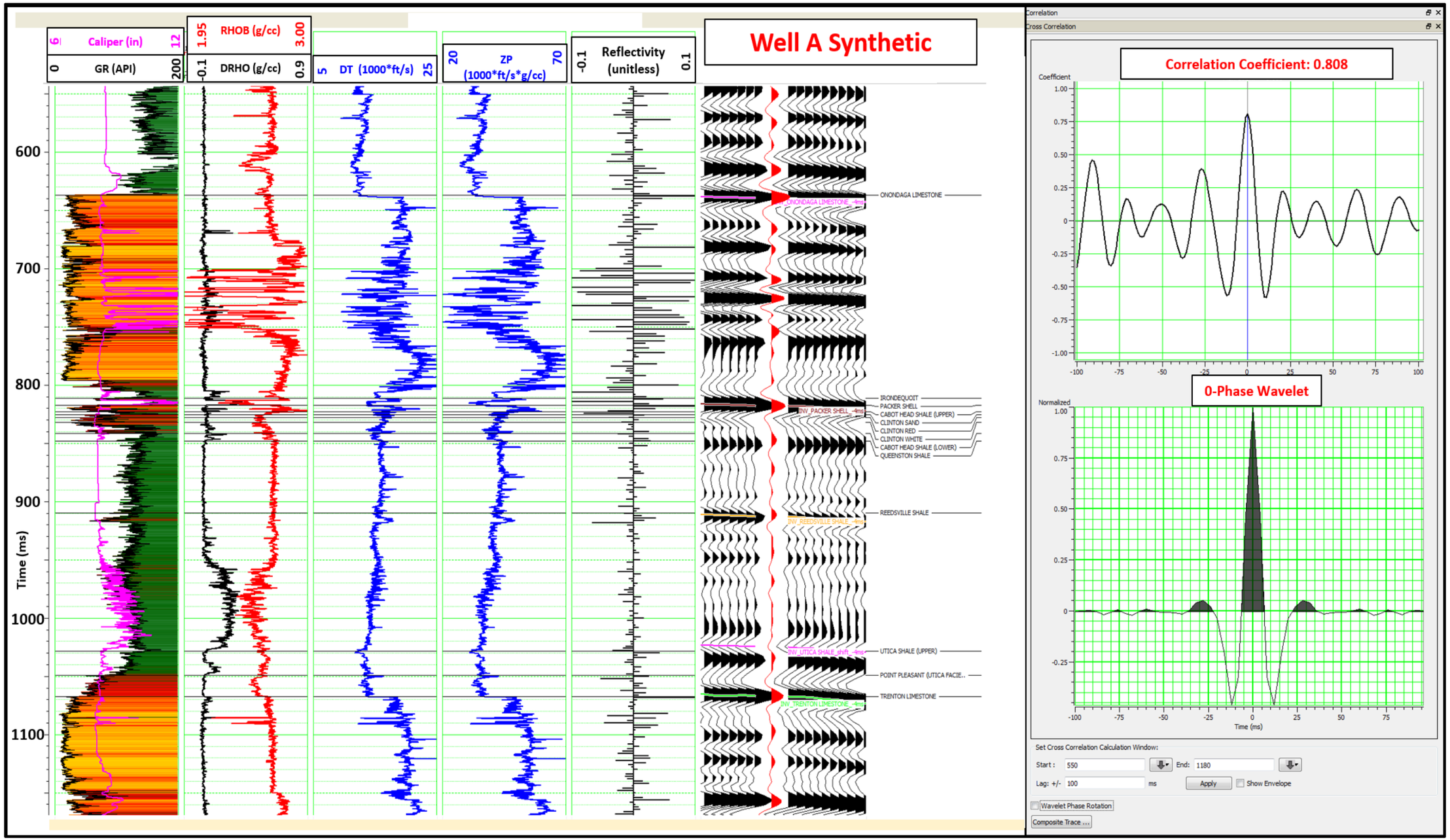

Figure 3.2.3 Synthetic at well A showing a 0.808 correlation coefficient.

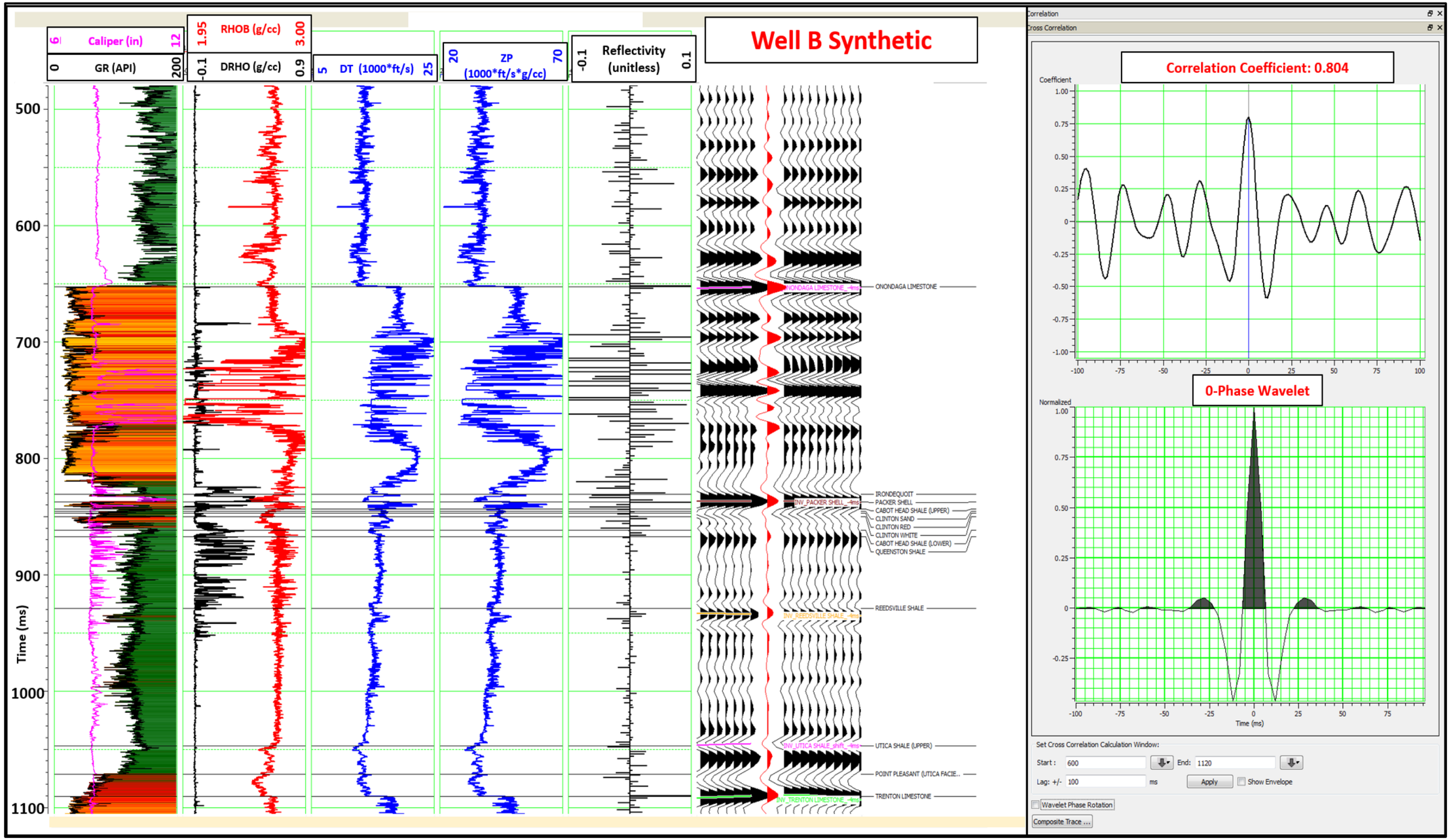

Figure 3.2.4 Synthetic at well B showing a 0.804 correlation coefficient.

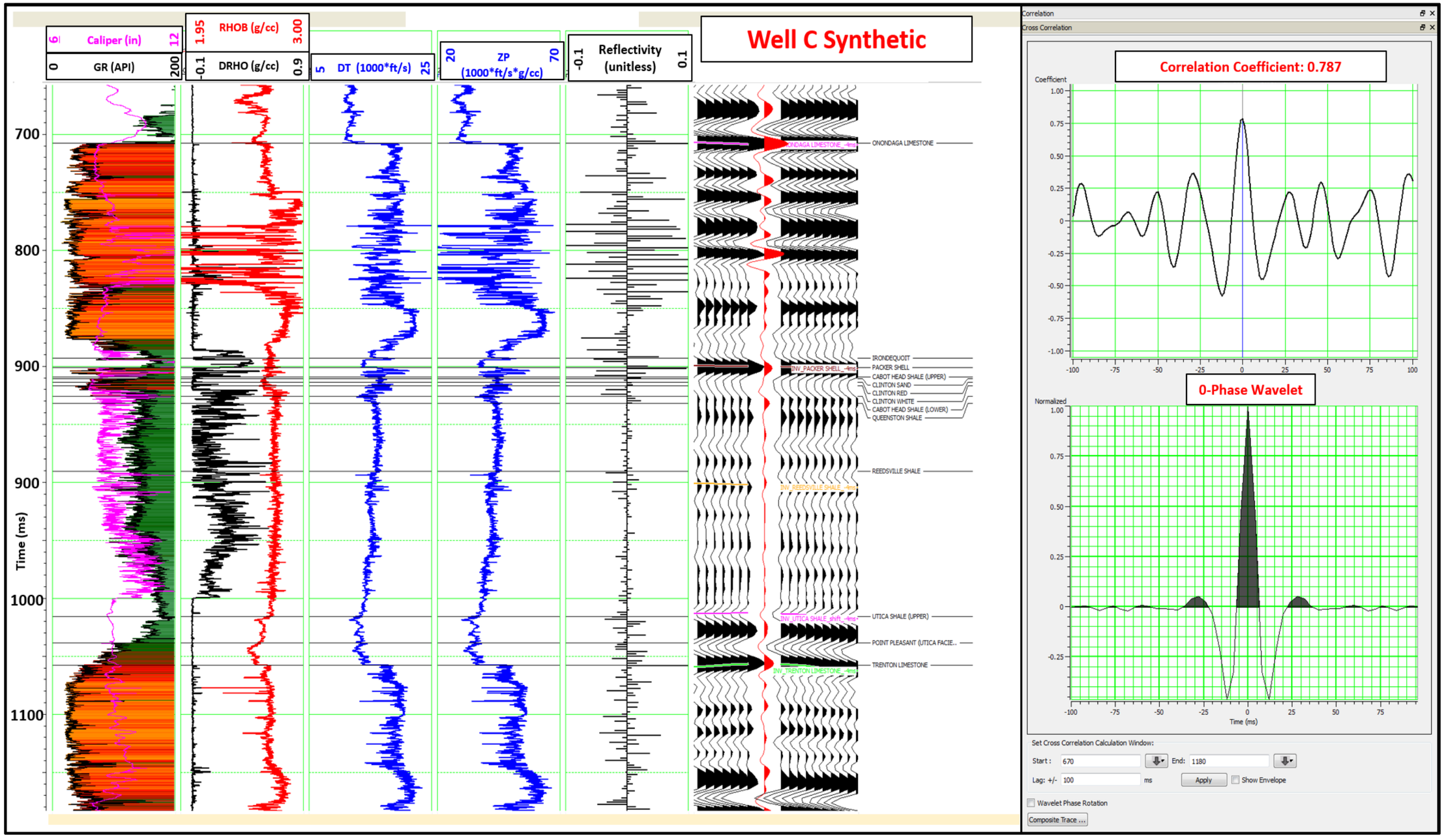

Figure 3.2.5 Synthetic at well C showing a 0.787 correlation coefficient.

range of [0, 0, 10, 32] Hz This frequency range was determined by analyzing the Firestone seismic frequency content and finding a peak frequency of 35 Hz (Figure 3.2.2). Kriging was used to interpolate from well to well using a spherical variogram structure while the Onondaga Limestone, Packer Shell, and Trenton Limestone horizons were used to guide the model.

In order to quality control (QC) the low-frequency model, a 3D visualization of the model was generated for P-impedance (Zp) and S-impedance (Zs) on the Onondaga Limestone, Packer Shell and Trenton Limestone horizons in order to identify and validate any large changes in impedance within the model (Figure 3.2.6 and 3.2.7). From viewing the figures, no "bulls eyeing" can be seen in the model indicating a consistent impedance profile. Further QC was done through a cross section view of the low-frequency model as seen by Figure 3.2.8. In addition to this, the P-wave, S-wave and Density logs were filtered to [0, 0, 10, 32] Hz to see how well the model represents the geology. This also allows for the caliper, density correction, and badhole flag log curves to be used in the QC assessment.

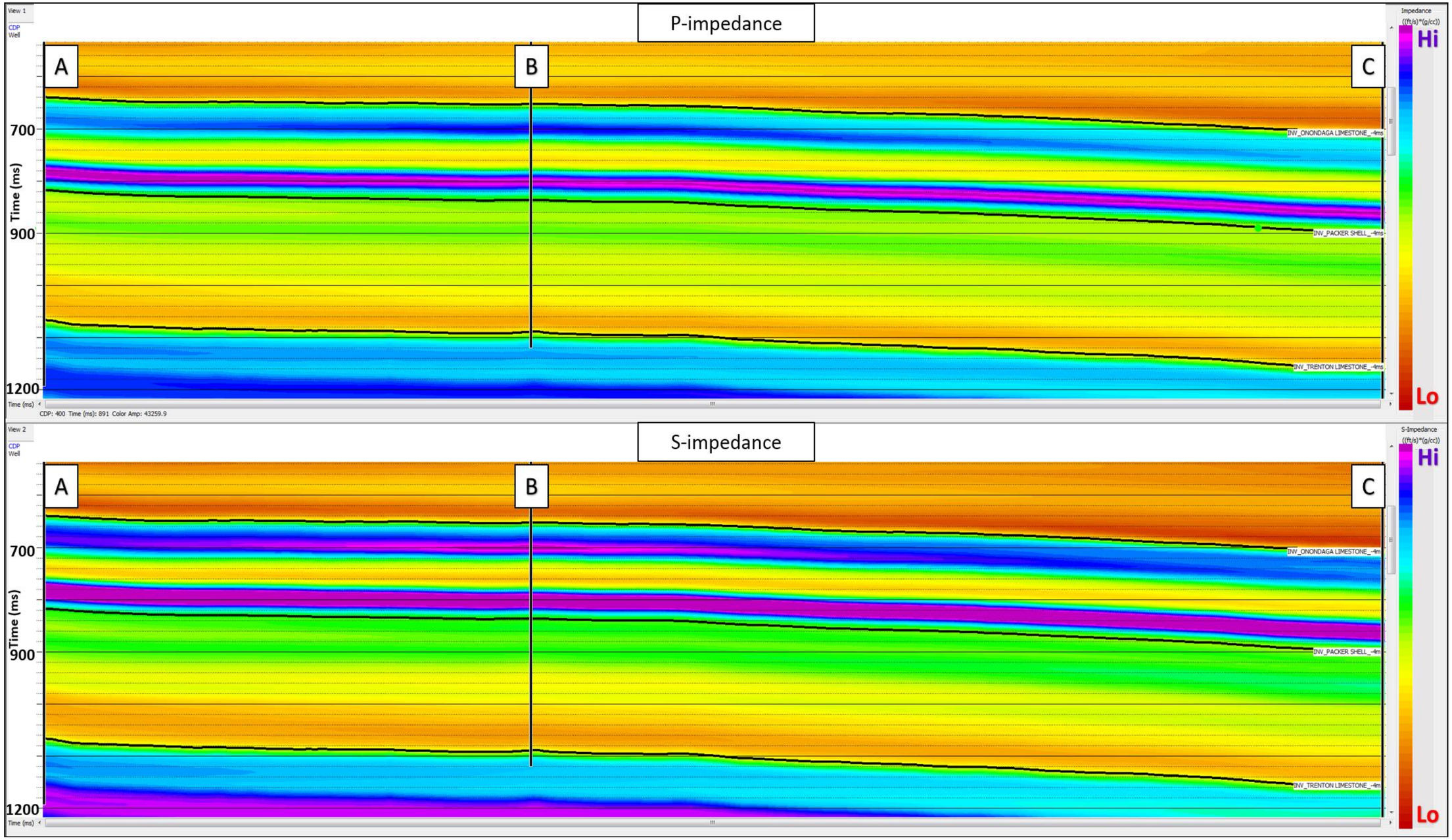

Figure 3.2.8 Cross-section of the P and S impedance low-frequency model through the study area.

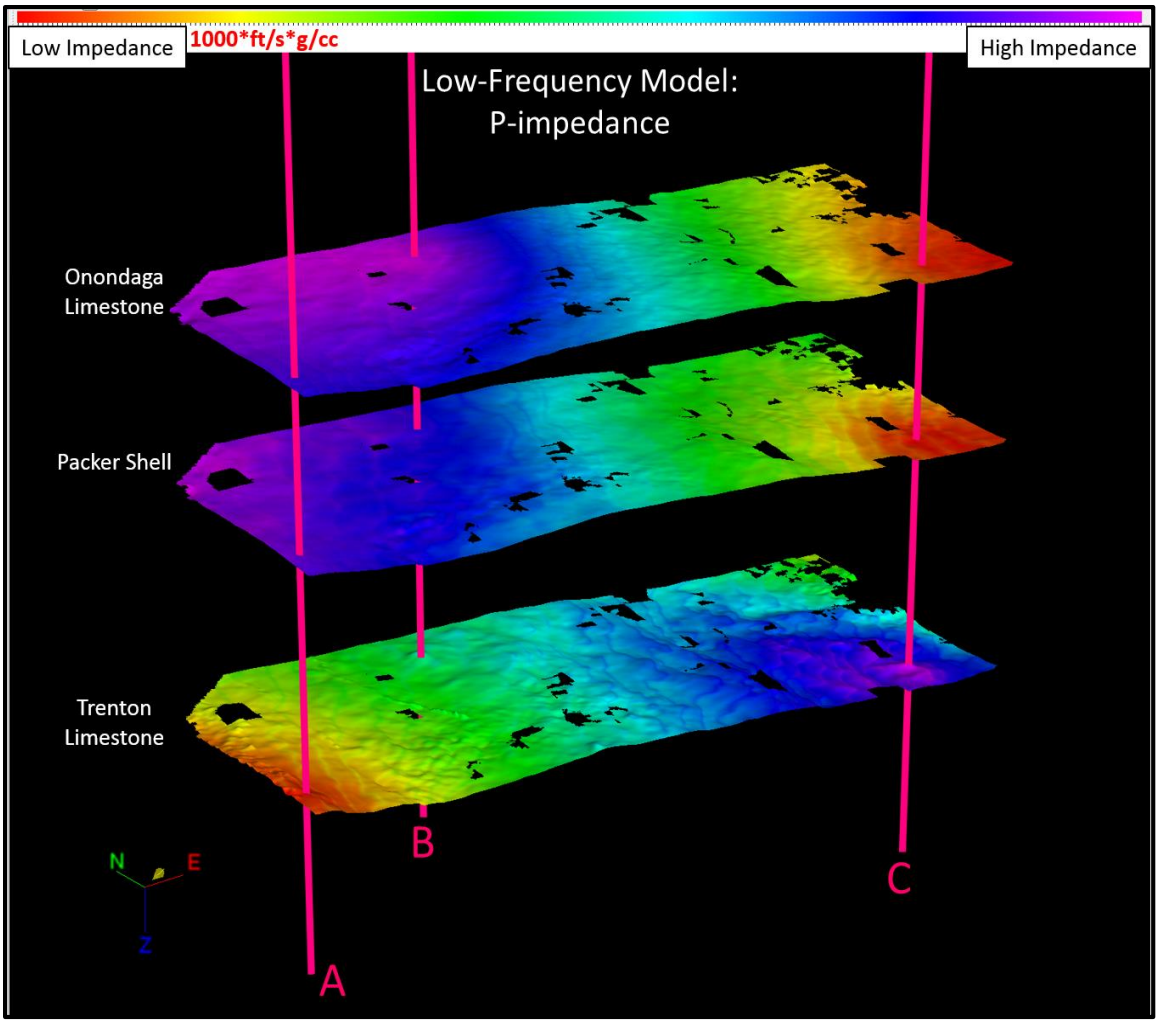

Figure 3.2.6 P-impedance low-frequency model on horizon slices within study area. Impedance increases from east to west for the Onondaga Limestone and the Packer Shell due to thickening to the west. Impedance increases from west to east for the Trenton Limestone due to thickening to the east.

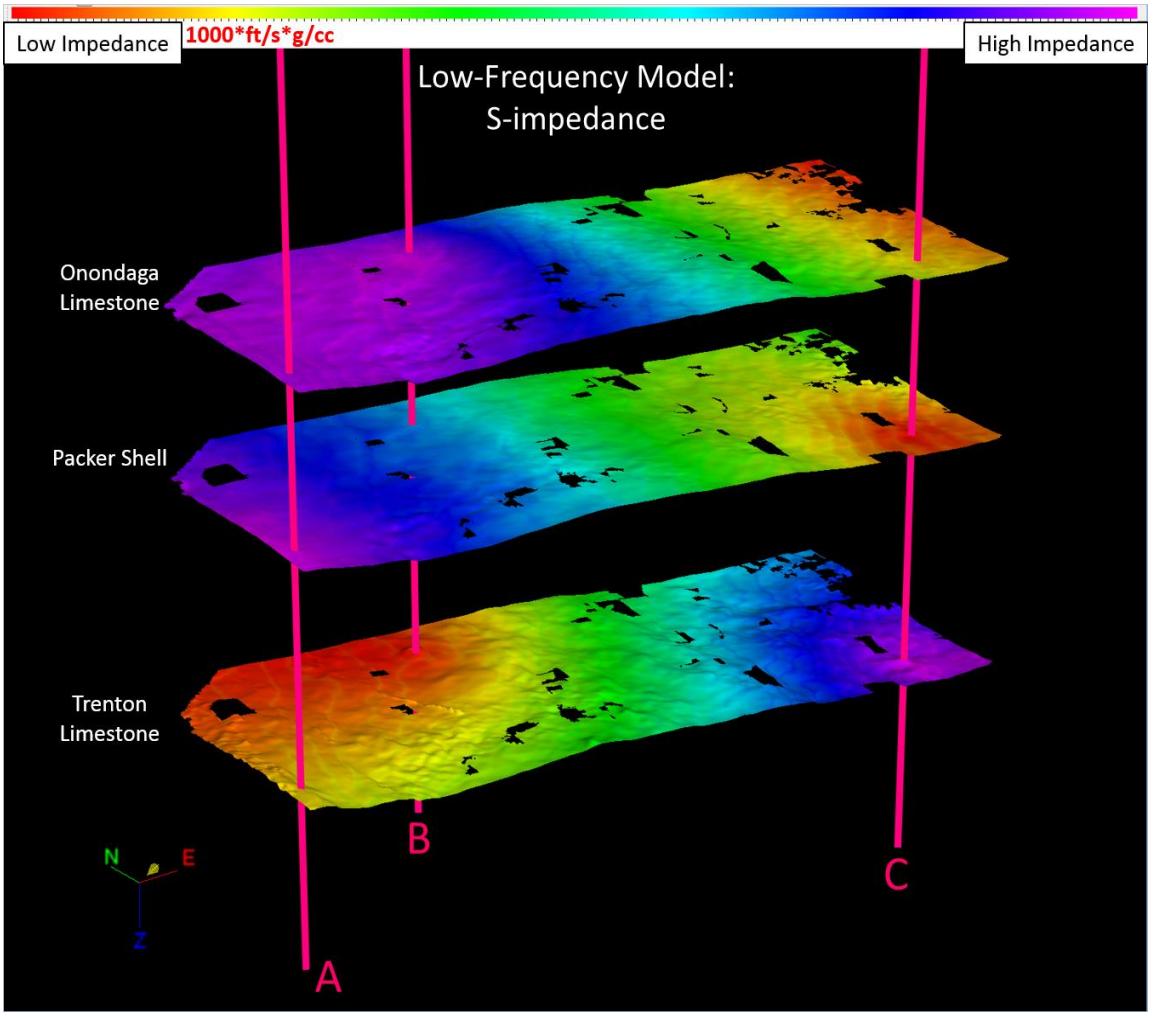

Figure 3.2.7 S-impedance low-frequency model on horizon slices. Impedance increases from east to west for the Onondaga Limestone and the Packer Shell due to thickening to the west. Impedance increases from west to east for the Trenton Limestone due to thickening to the east.

Using the low-frequency model, angle gathers and their associated group wavelet, the inversion analysis can be run as seen in Figures 3.2.9, 3.2.10, and 3.2.11. In the inversion analysis, well log response, low-frequency model response and inversion results are compared at each well prior to applying it to the volume. The time window used for the inversion analysis ranges between the Trenton Limestone and -50 ms above the Packer Shell. An angle range of 0-35 degrees was chosen since the events in the far angles potentially contain multiples as seen by the angle gather track which eliminates generation of a

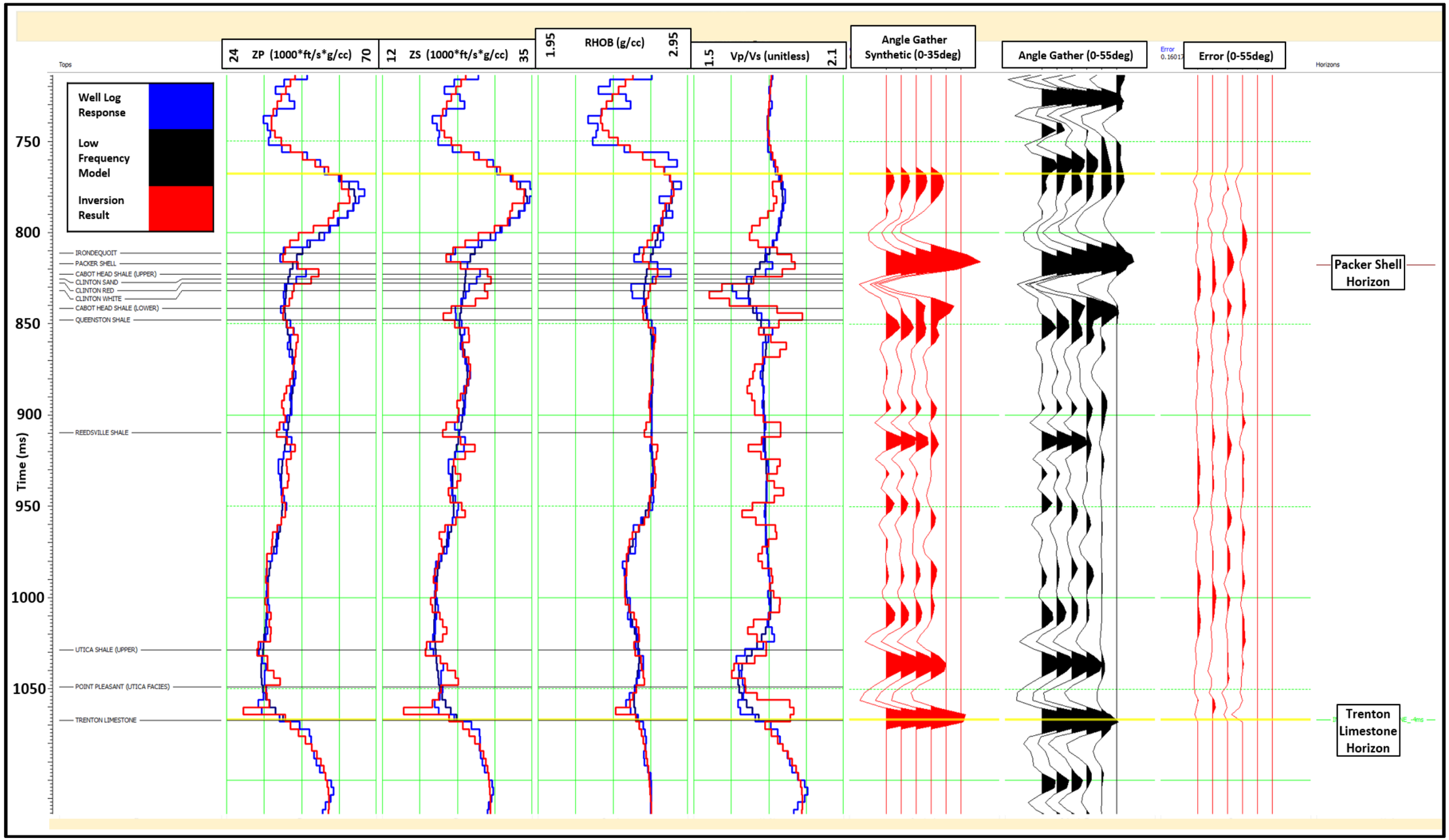

Figure 3.2.9 Inversion analysis at well A showing inversion result at well location.

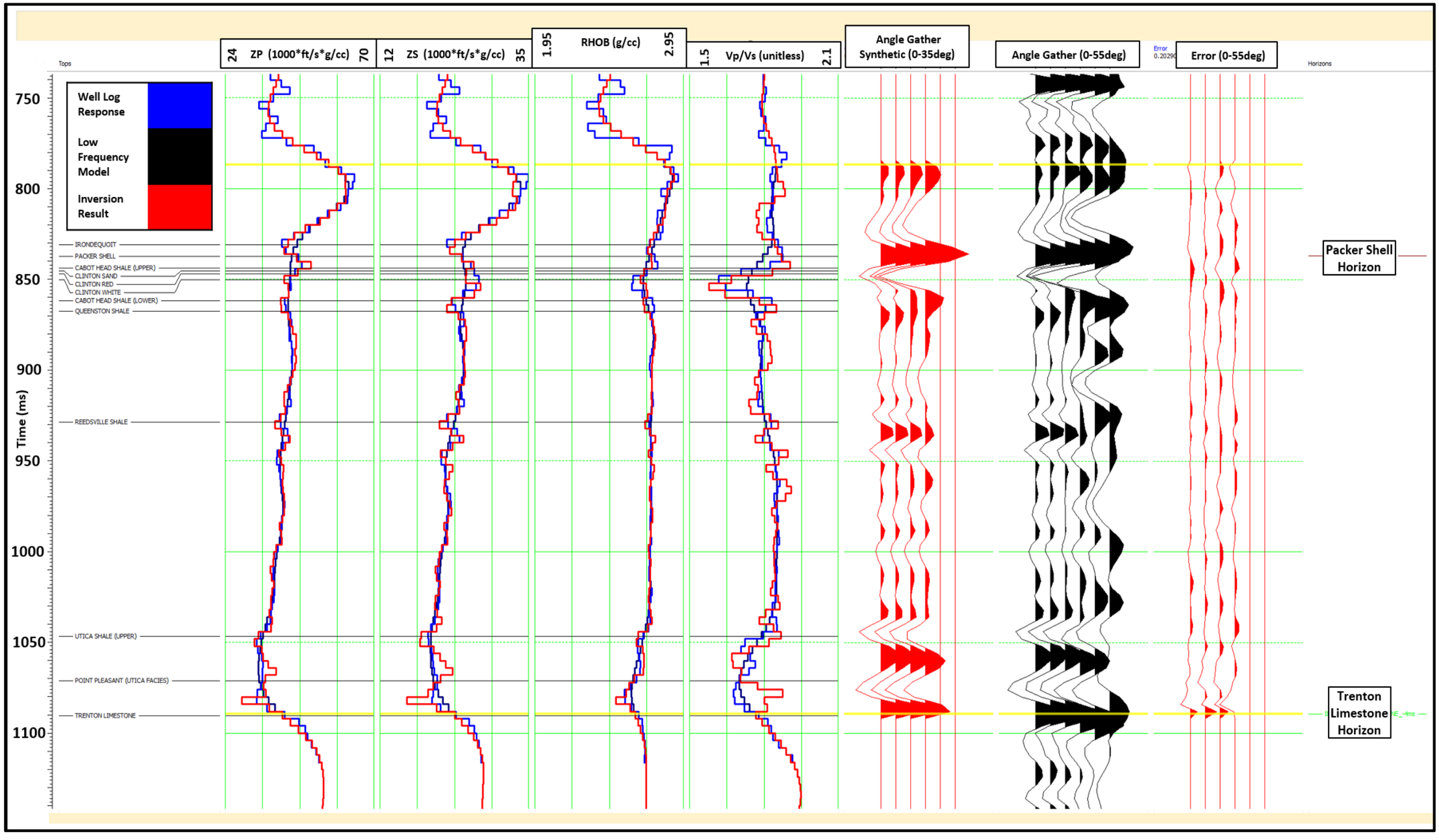

Figure 3.2.10 Inversion analysis at well B showing inversion result at well location.

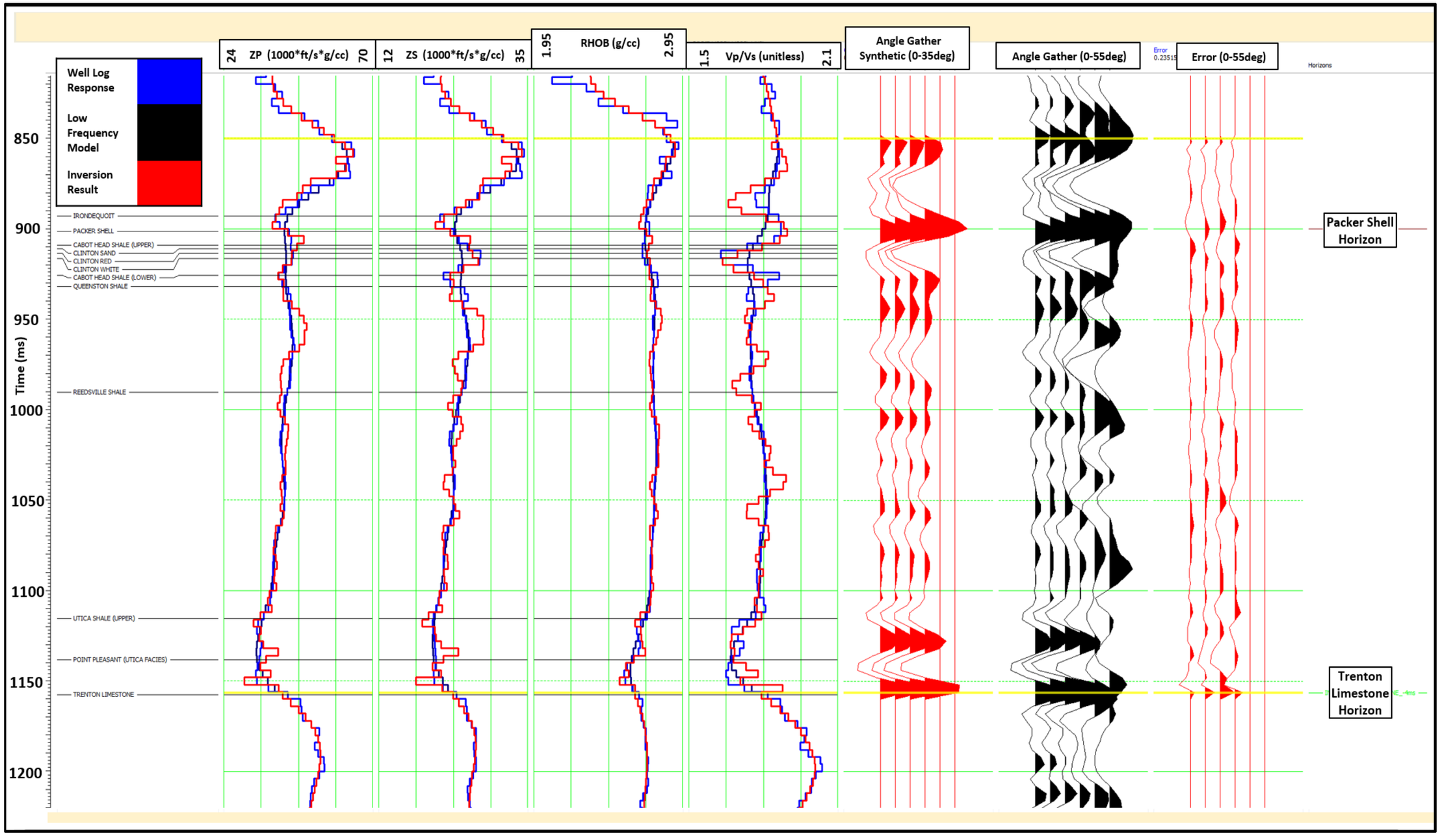

Figure 3.2.11 Inversion analysis at well C showing inversion result at well location.

reliable density volume. When viewing the Zp track, little variation can be seen in the target interval between the inversion result, and the well log response. Within the target interval, there is an increase in the Zs response for the inversion result. This relationship drives the large decrease in Vp/Vs seen within the Clinton interval seen in all of the wells. This anomaly is most profound within the Clinton White for wells A. From this, the inversion analysis was run for the entire volume to produce Zp, Zs, and Vp/Vs volumes. The Vp/Vs volume was then converted to Poisson's Ratio.

Chapter 4: Results and Conclusions

4.1 Geologic Mapping

Within the Clinton Sand interval, there are distinct variations amongst the Clinton Red and White targets. Both sand bodies vary with thickness and geometry leading to variations in depositional environments as well as reservoir within the ECOF. As previously described, the Clinton Sand is made up of eroded material from the Taconic Highlands that was transported from east to west and represents the last tectophase of the Taconic Orogeny (Ettensohn, 2008). Note: while the sufficient GR data allows for detailed mapping, the lack of porosity logs influences the spatial distribution of the pay values. The pay maps for all of the Clinton Sands lack the most data in the eastern portion of the maps as seen by the thin pay while the GR maps in this area generally show thicker sand.

The Clinton White was deposited in a both a tidal and wave influenced deltaic environment and is the thickest of the Clinton reservoirs. The delta fan geometry is clearly seen in the southern portion of the ECOF. Here, several deltaic lobes can be seen within the field along with channelized features. The Clinton White is thickest in the east and thins towards the paleo-geographic shoreline in the west. The lack of fan geometry in the western portion of the field is most likely to the presence of the paleo-shoreline re-working sands and creating sand bar

geometries (Figure 4.1.1). Similar geometry can be seen by the Clinton White pay map which can be interpreted as areas that have undergone the most geologic re-working and there for contain ideal reservoir. The thickest pay is found within the deltaic fan. The areas with channel like geometry and thin most likely represent mud filled channels implying higher GR values and small porosities (Figure 4.1.2). This figure highlights why the Clinton White is targeted due to its thick and widespread distribution within the field.

The Clinton Red was deposited in an active shore face environment. This can be seen by the sand bar features seen in the western edge of the ECOF which most likely represent the paleo-shoreline during deposition (Figure 4.1.3). In the ECOF, the Clinton Red was deposited on the shoreline as it was transported further west over the previously deposited deltaic fan and sandbars. The Clinton Red represents the maximum regressive surface prior to the sea-level rise which eventually deposited the Upper Cabot Head Shale and the Packer Shell. The Clinton Red pay map shows the thin nature of the reservoir at this interval with the thickest being found in the western portion of the ECOF (Figure 4.1.4).

When combined, the net sand map for the Clinton Interval shows a primarily shallow marine and deltaic depositional environment (Figure 4.1.5 and 4.1.6). Deltaic features are more prominent in the eastern portion of the field while an active shore line was present in the west. The target interval of the Clinton White was controlled by a prolonged period of deltaic deposition and is the primary control on the ECOF Clinton reservoirs as seem by both GR and pay mapping. This environment is significant in that it allowed for the accumulation of clean, porous sand with low-clay content to be deposited within the field. Net pay mapping shows that within the 3D boundaries, the best reservoir is south of well B within the field boundaries.

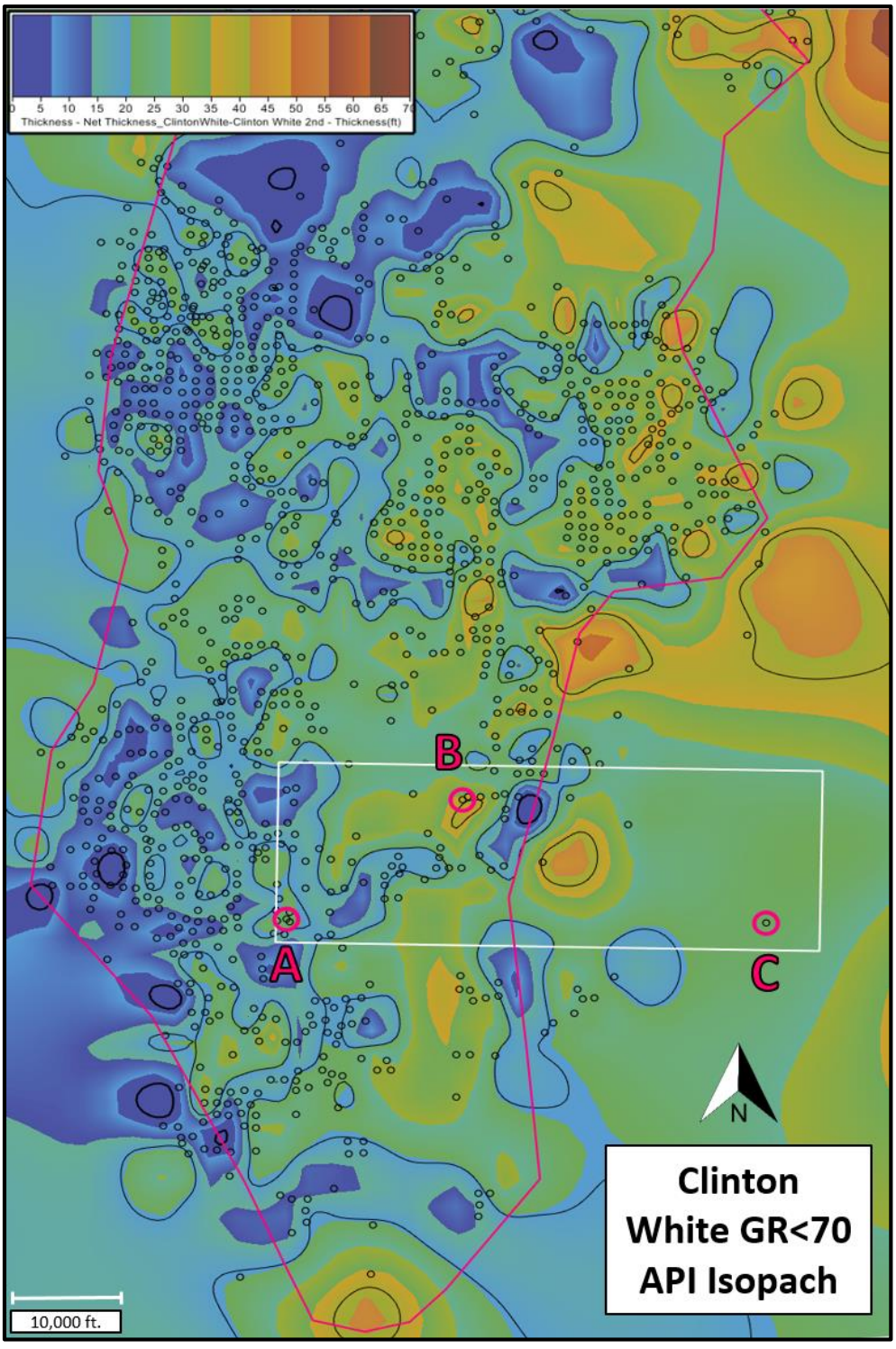

Figure 4.1.1 GR cutoff isopach map of the Clinton White with 20 ft contour within the ECOF (pink outline) showing a deltaic depositional environment. Seismic outline shown by white box with inversion wells as pink circles. GR wells annotated by black dots. Thickness color bar in upper left.

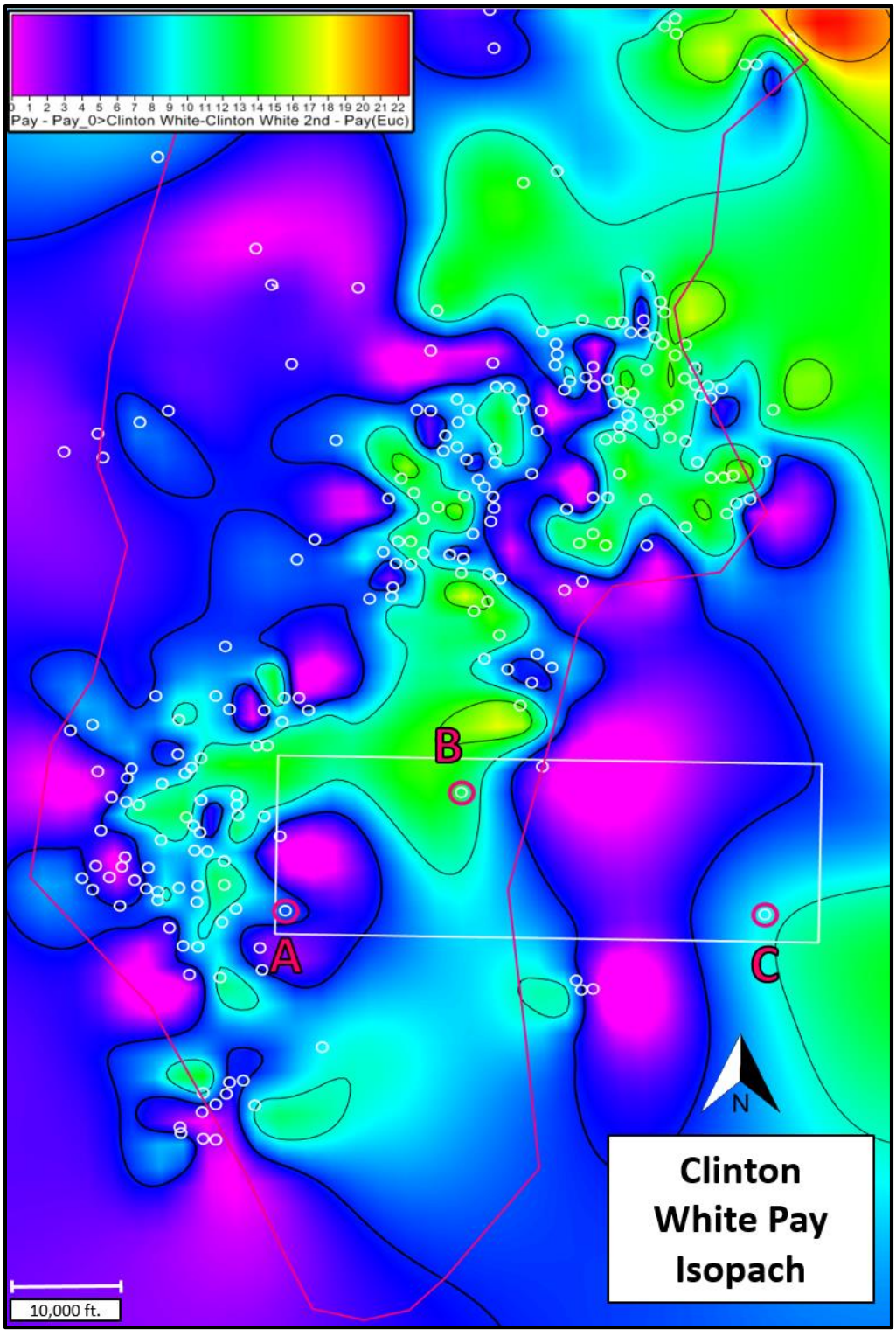

Figure 4.1.2 Pay isopach map of the Clinton White with 5 ft contour within the ECOF (pink outline) showing reservoir geometry. Seismic outline shown by white box with inversion wells as pink circles. Pay wells annotated by white dots. Thickness color bar in upper left.

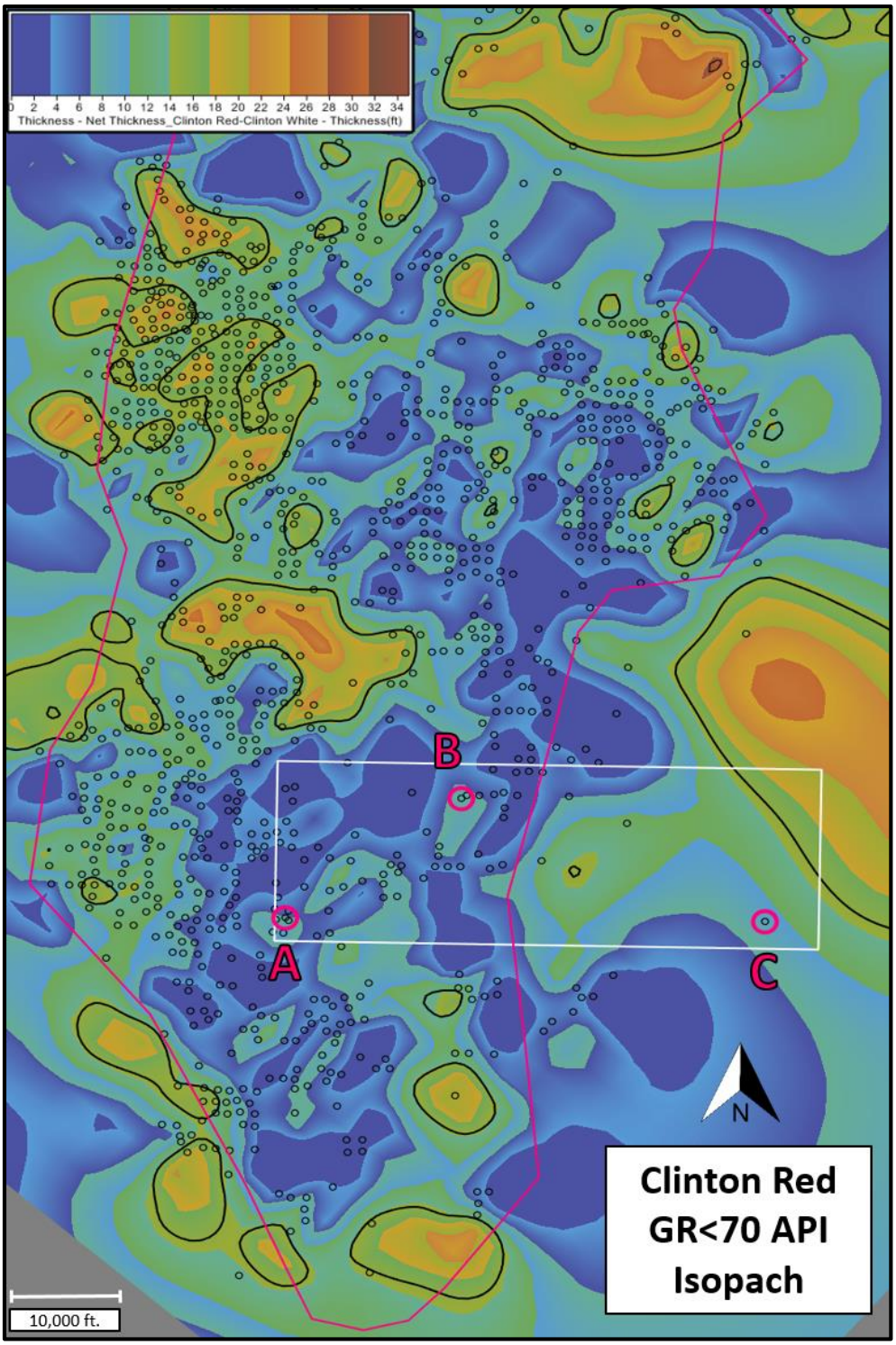

Figure 4.1.3 GR cutoff isopach map of the Clinton Red with 15 ft contour within the ECOF (pink outline) showing a shore face depositional environment. Seismic outline shown by white box with inversion wells as pink circles. GR wells annotated by black dots. Thickness color bar in upper left.

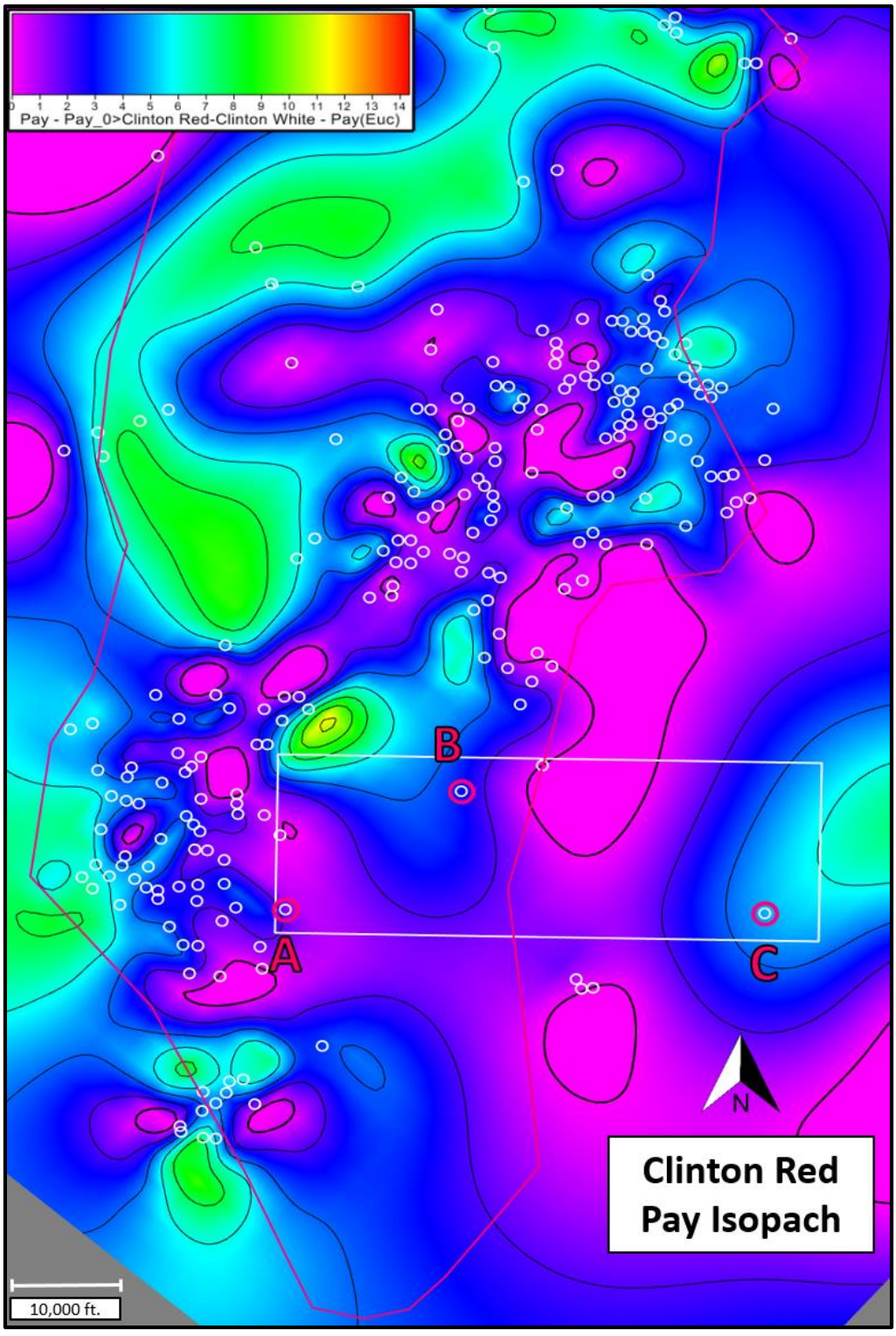

Figure 4.1.4 Pay isopach map of the Clinton Red with 2 ft contour within the ECOF (pink outline) showing reservoir geometry. Seismic outline shown by white box with inversion wells as pink circles. Pay wells annotated by white dots. Thickness color bar in upper left.

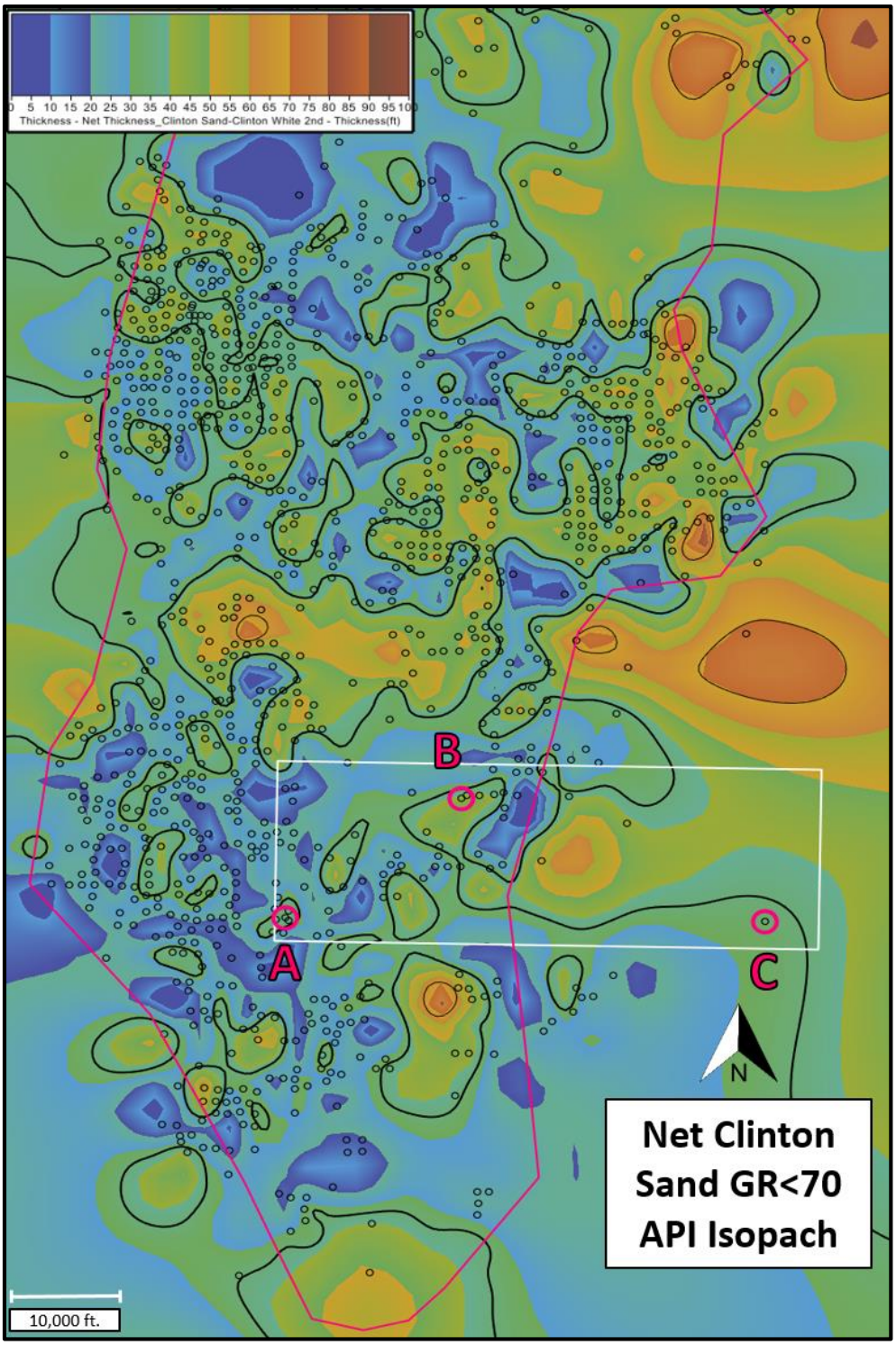

Figure 4.1.5 GR cutoff isopach map of the Net Clinton Sand with 35 ft contour within the ECOF (pink outline). Seismic outline shown by white box with inversion wells as pink circles. GR wells annotated by black dots. Thickness color bar in upper left.

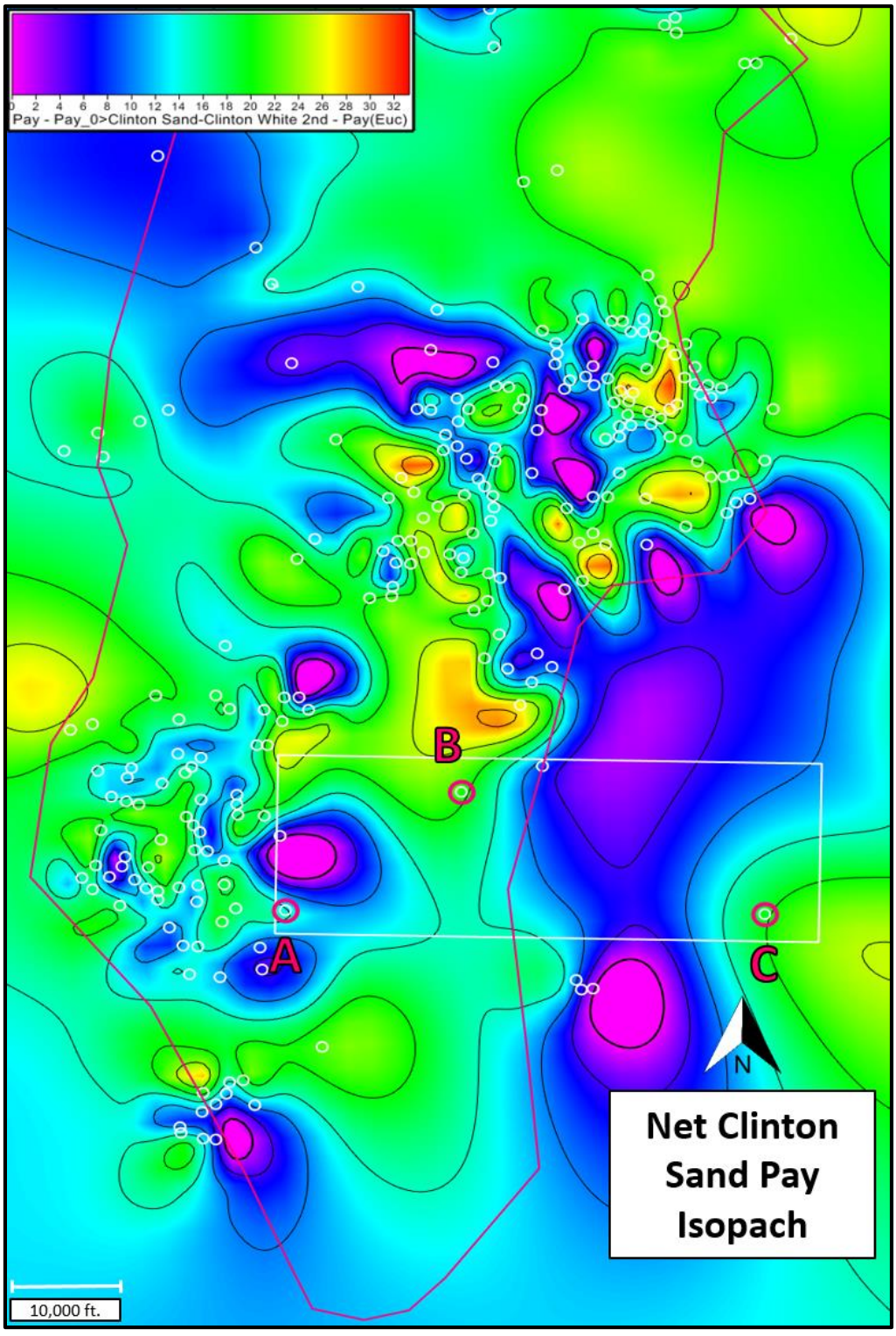

Figure 4.1.6 Pay isopach map of the net Clinton Sand with 5 ft contour within the ECOF (pink outline) showing reservoir geometry. Seismic outline shown by white box with inversion wells as pink circles. Pay wells annotated by white dots. Thickness color bar in upper left.

4.2 Reservoir Characterization

Wells B and C contain measured S-wave curves through the Clinton Interval. In order to model potential AVO anomalies in the Clinton Sand, AVO synthetic models were generated at wells B and C using the Aki-Richards AVO equation. Figures 4.2.1 and 4.2.2, show the AVO synthetic for well B and C. In Figure 4.2.1 at the top of the Clinton White in track 3, a large increase in S-wave (DTS) velocity can be seen. This sonic response is further represented by a large decrease in Poisson's ratio at the top of the Clinton White. At the base of the Clinton White there is a small decrease in in P-wave (DT) velocity which is represented by a small trough in the near angles of the synthetic. As the angle increases at the base of sand, the seismic character goes from a small trough to a large peak indicating the presence of an AVO anomaly. At well C in Figure 4.2.2, a similar but less profound AVO response can be seen.

In offshore reservoirs the presence of AVO anomalies can act as direct hydrocarbon indicators but, due to the tight sand reservoir nature of the Clinton sand, this anomalous response is most likely an indicator of well-developed sand. Well-developed sand represents sands that have undergone long periods of geologic reworking and thus contain ideal porosities and low Poisson's ratio. From this, the differences in AVO responses of wells B and C can likely be attributed to well C being outside of the ECOF boundaries in an area of poorer sand quality. Figure 4.2.3 summarizes the Clinton Sand AVO response. From this relationship, the base of the Clinton sand can be mapped using the Poisson's Ratio volume generated from the pre-stack inversion.

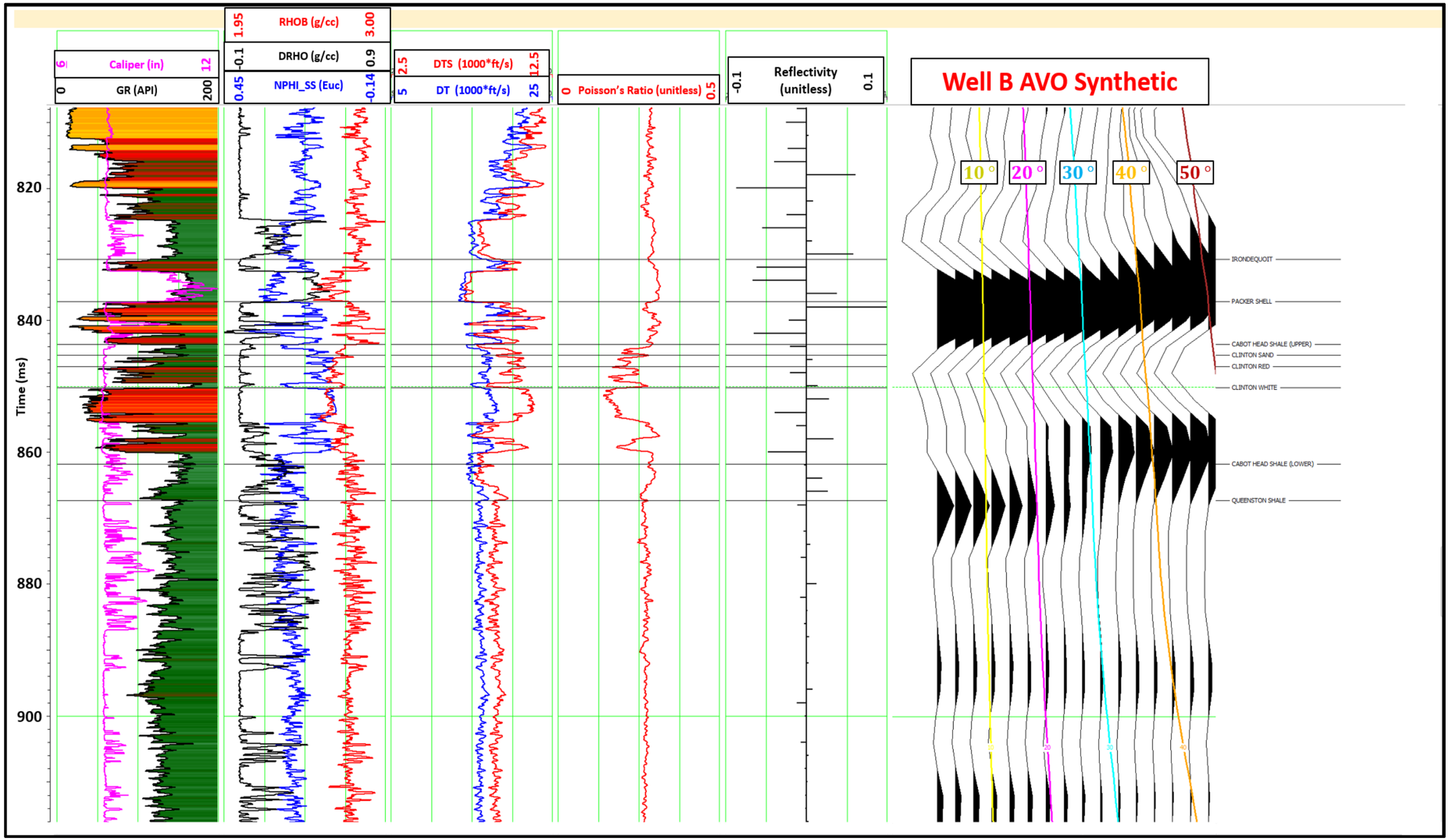

Figure 4.2.1 AVO synthetic at well B from 0-50 deg.

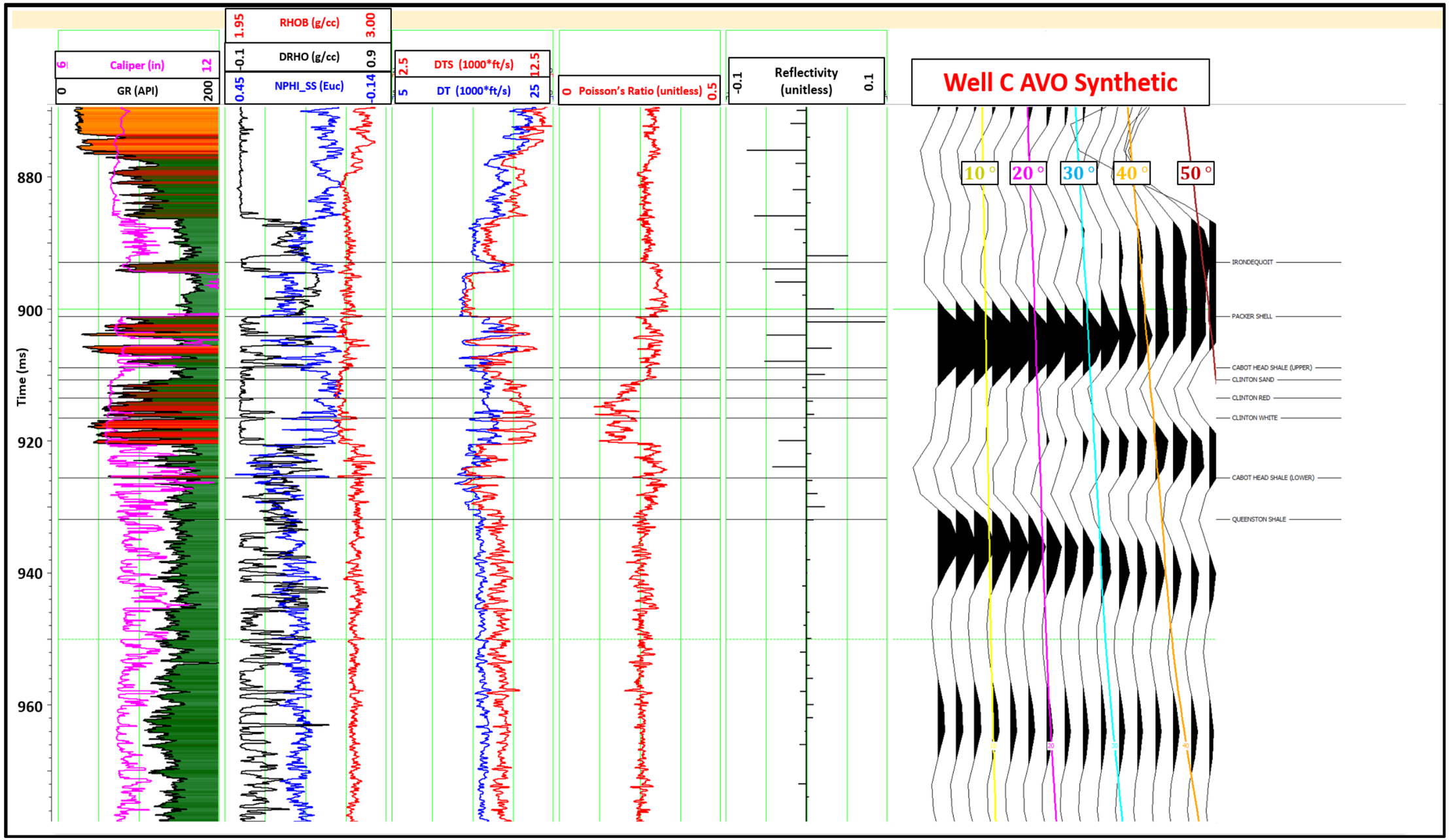

Figure 4.2.2 AVO synthetic at well C from 0-50 deg.

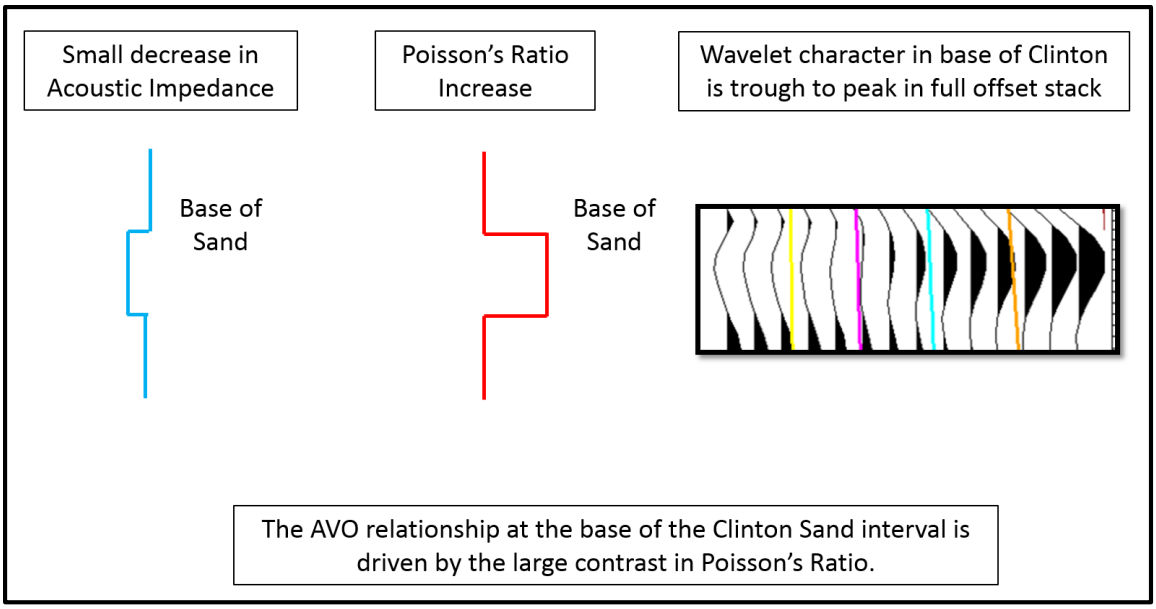

Figure 4.2.3 Summary of Clinton Sand AVO anomaly

In order to visualize changes in the Clinton reservoir, horizon slices and cross-sections were generated for the inverted volumes. Figure 4.2.4 shows a cross section through wells A, B, and C in both the Zp and Zs volumes. The Zp volume shows large impedance values for the Packer Shell. Within the Clinton Interval there is little change in impedance as was seen in the 0-offset synthetics. While the top of the Clinton is unresolvable, the Zp does separate out the Packer Shell and the Clinton White as seen by the impedance contrast. The Clinton White is best resolved in the Zs volume. The base of the Clinton White is clearly delineated from the Lower Cabot Head Shale. This contrast is largely driven by the strong shear wave anomaly previously discussed.

When interpreting the Poisson's Ratio volume, the Clinton White is clearly distinguished by a bright reflector above the Lower Cabot Head Shale with values of 0.25 and lower. These values are representative of consolidated sandstones with a high quartz content (Ikelle et al., 2005). This anomaly is thus an indicator of clean reservoir quality sand. Figure 4.2.5 and 4.2.6 shows the Poisson's Ratio extracted on the Clinton White (base of sand) horizon with a 10 ms window centered on the horizon pick. This clearly delineates the ECOF boundaries due to the

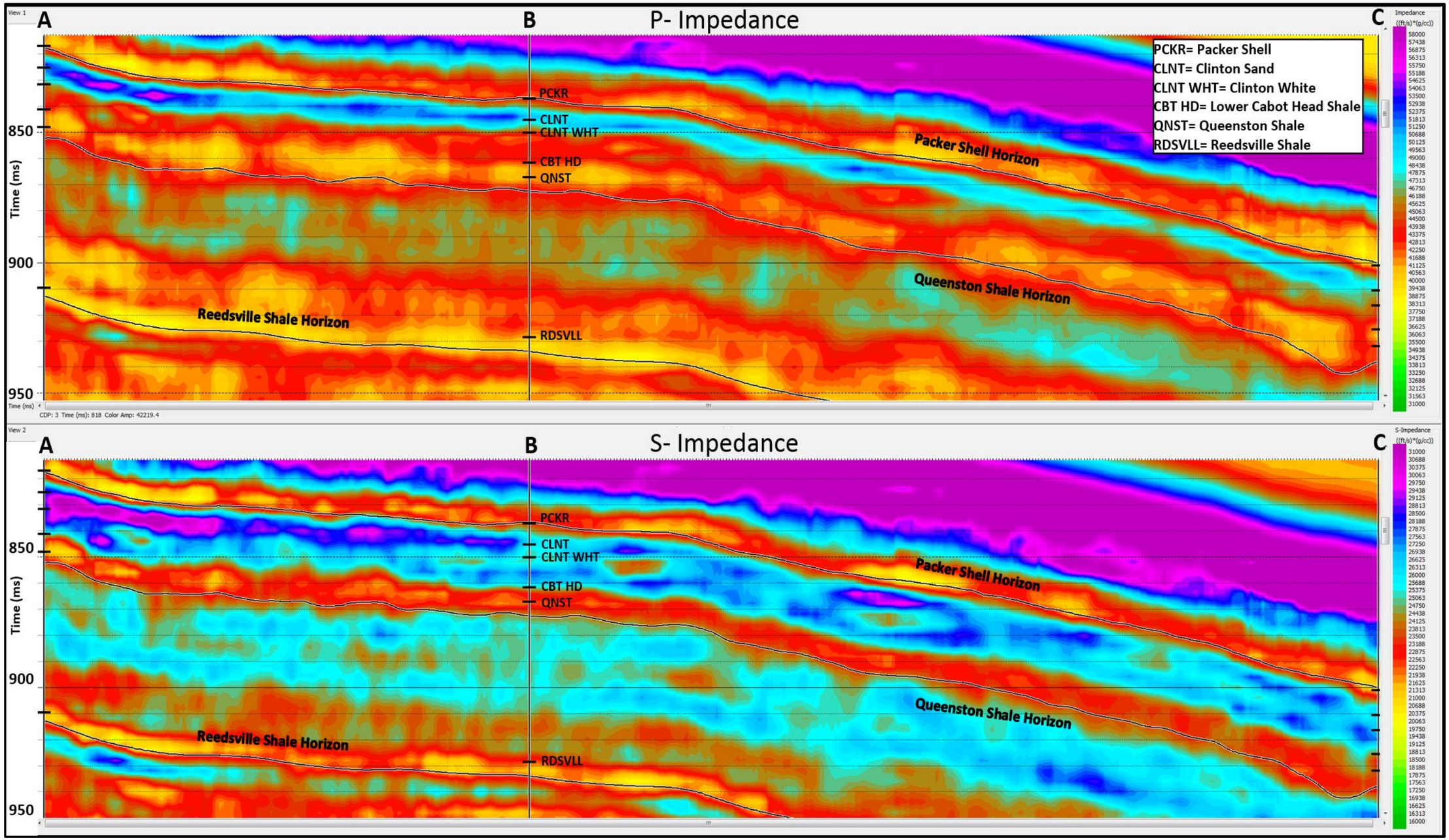

Figure 4.2.4 Cross-section through Zp & Zs volumes. Formation top acronyms are posted along well bore.

lowest values being within the field boundaries of known production and increases as you move outside of the field. The presence of this anomaly can be attributed to several factors. Due to the large impedance contrast between the Packer Shell and the Clinton Interval, the top of the Clinton Sand is not resolvable due to the contrast in reflection coefficients as well as the thinner deposition of the Clinton Red and Stray. Since the Clinton White's reflectivity is not influenced by the Packer Shell's, the Clinton White can be resolved. This combined with shear wave anomaly and thicker strata seen in the Clinton White allows for it to be mapped. In addition, the lowest values exist within the field boundaries which occur in areas that underwent the most geologic re-working of sediment due to the presence of the active deltaic/shore face environment.

Figure 4.2.7 in the back of the manuscript shows a cross-section through the Poisson's Ratio and seismic volume used for the well ties. In the Poisson's volume, the Clinton White anomaly is clearly seen and consistently falls within the formation top boundaries. When comparing the Poisson's Ratio and seismic volume, it is evident that the Clinton Interval is not resolvable due to the impedance contrast from the Packer Shell. At best, the base of the sand shows up as a very weak through as seen beneath the Clinton White formation top at well B. This figure highlights the advantages of mapping heterogeneous tight sand reservoirs using Poisson's ratio when the target cannot be resolved in the stacked data.

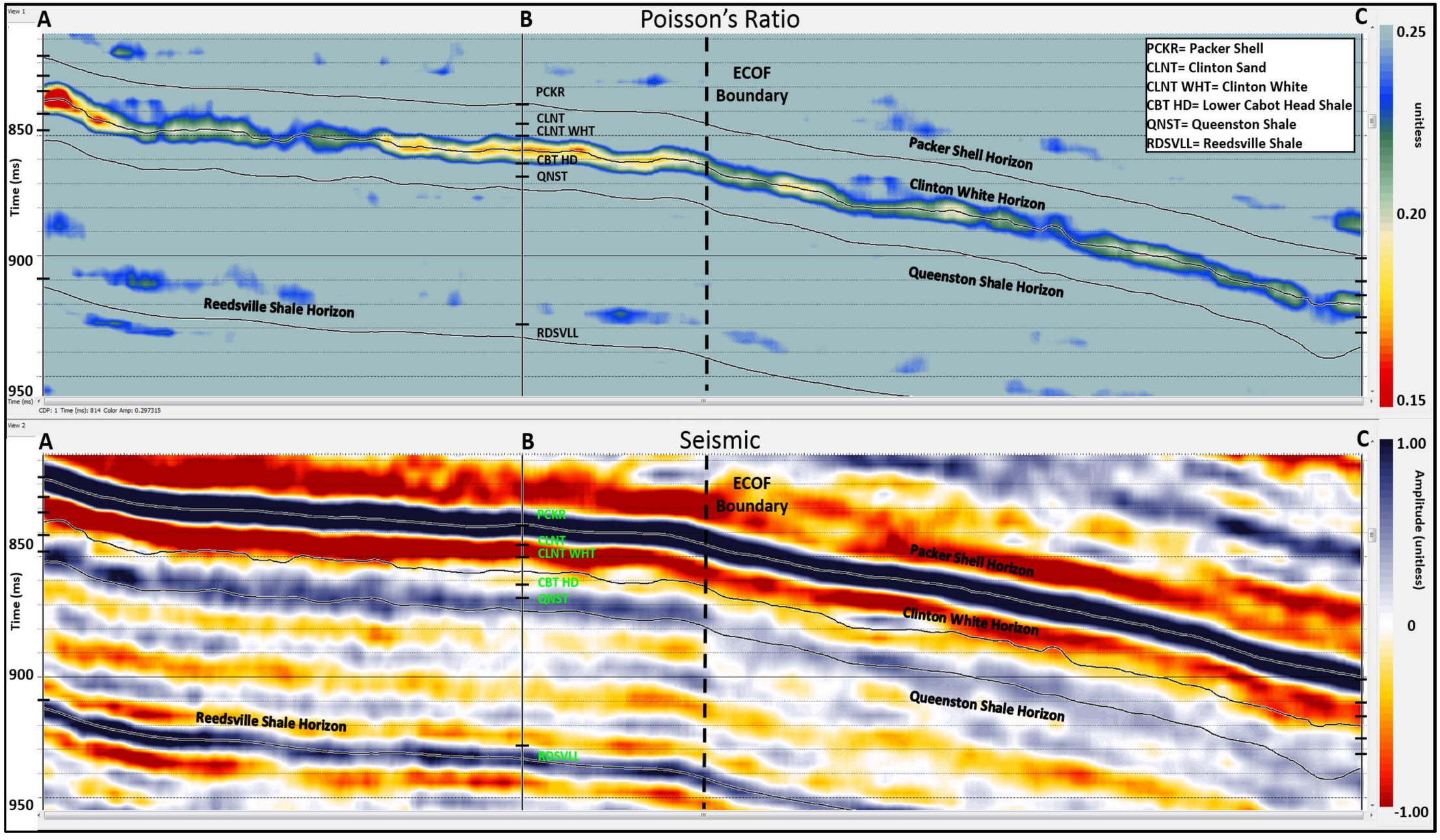

Figure 4.2.7 Cross-section through Seismic and PR volumes. Formation top acronyms are posted along well bore.

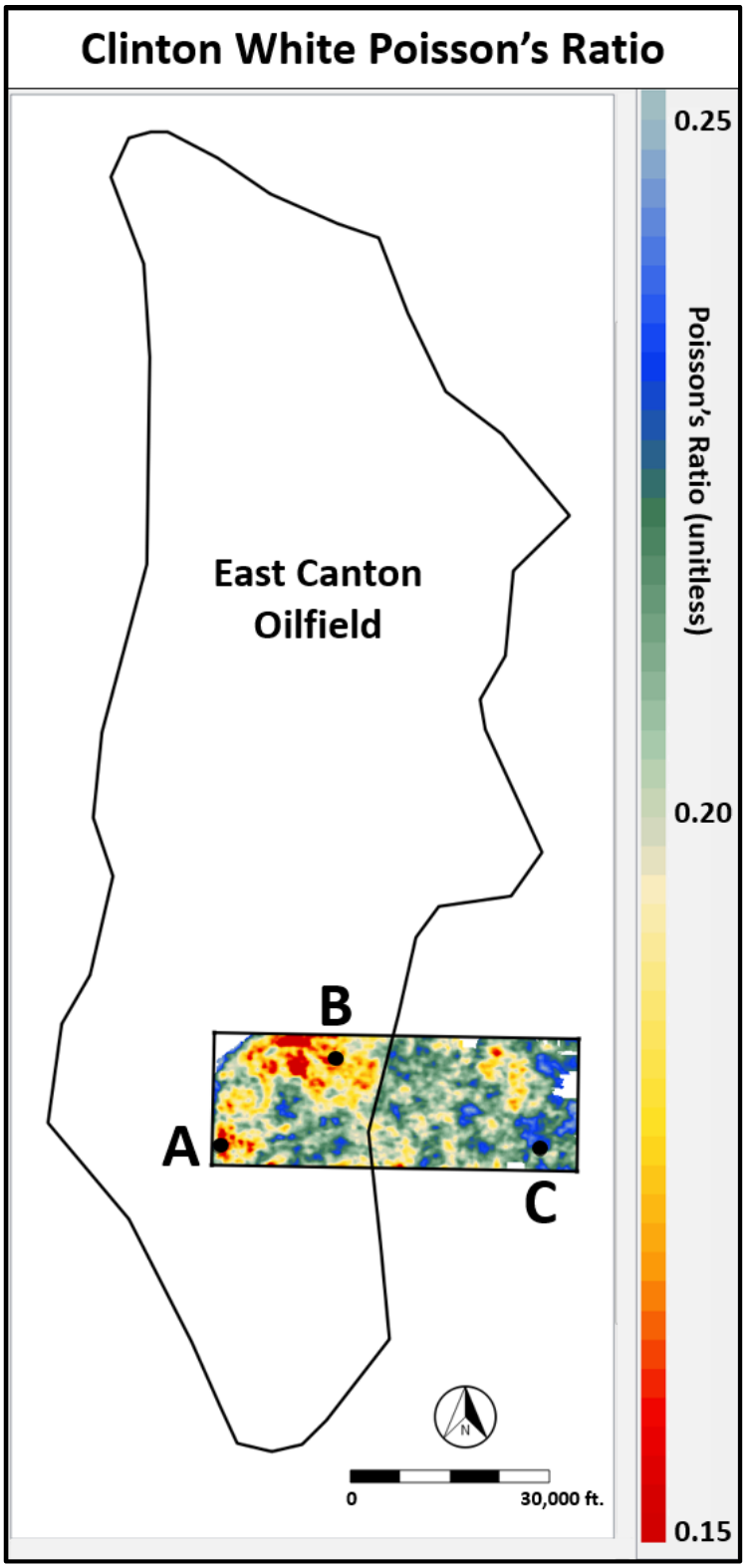

Figure 4.2.5 Poisson's Ratio horizon slice with 10 ms window on the Clinton White showing delineation of the ECOF.

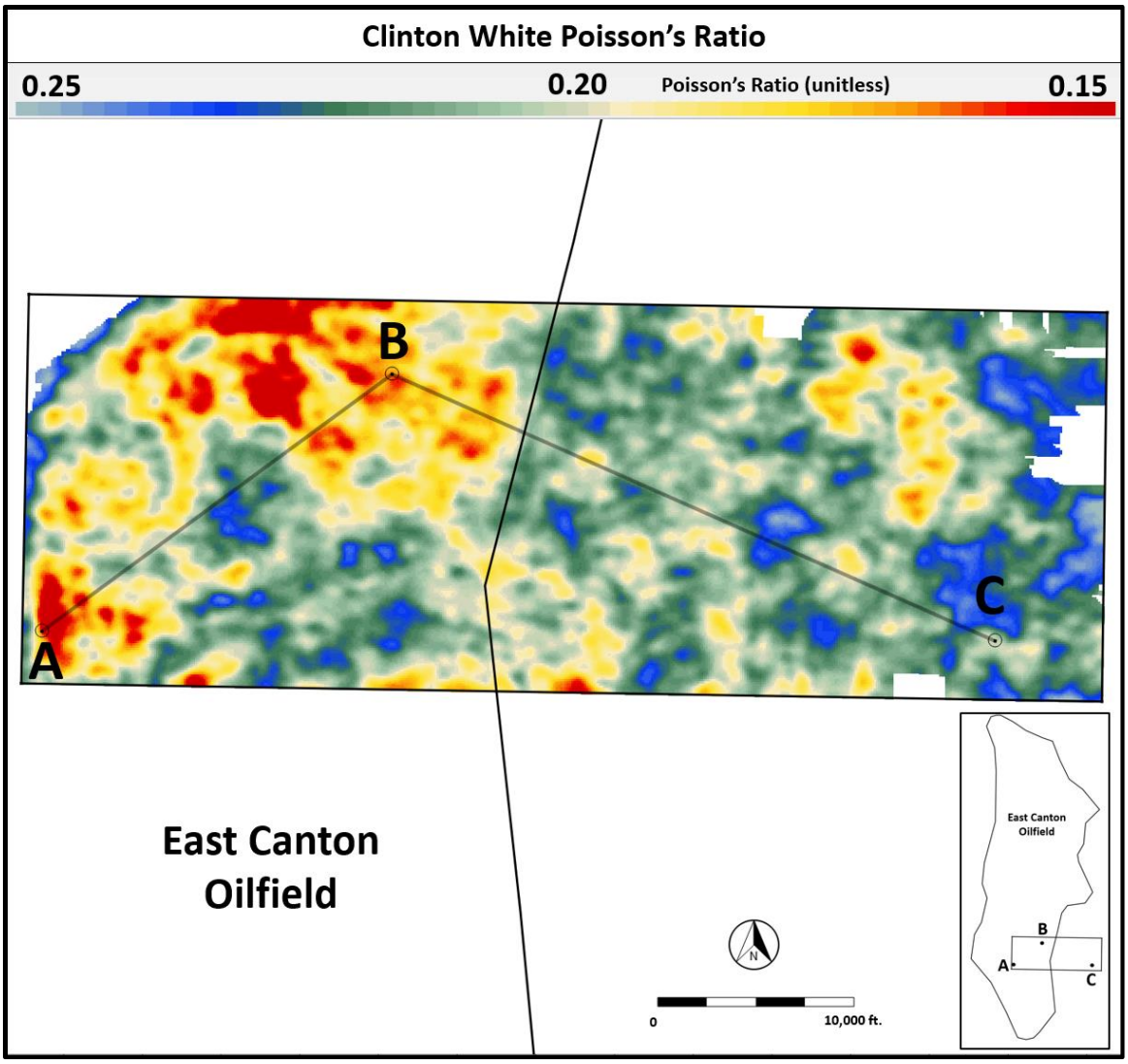

Figure 4.2.6 Zoomed in view of Poisson's Ratio horizon slice with 10 ms window on the Clinton White showing delineation of the ECOF. The Poisson's values show reservoir quality increasing from east to west.

4.3 LithoSI

With the pre-stack inversion results delineating the ECOF boundaries, the inversion wells and volumes were run through LithoSI in Hampson-Russell in order to assign lithological classes to the inversion volumes and reduce uncertainty through generation of probability volumes. In addition, the LithoSI work flow allows for the p-impedance volume to be integrated into the reservoir characterization. Using wells B and C, a p-impedance (x axis) vs. Poisson's ratio (y-

axis) well log cross plot was generated using log data between the Packer Shell and Queenston Shale. Well A was omitted since it doesn't contain a measured DTS curve. Carbonate and shale data points within the Clinton interval are included to establish background lithology. Figure 4.3.1 shows a P-impedance vs. Poisson's Ratio well log cross plot to separate out lithologies as well as to identify reservoir quality sands. Using a sandstone reference matrix, the amount of DPHI and NPHI separation is used to color the data points. Less porous data points are seen by the browns and yellows/red data points represent porous data points

Due to the data point separation caused by varying lithologies, facies classes can be assigned to the cross plot (Figure 4.3.2). High PR and ZP values below 47 impedance units are used to delineate carbonates from shales. Shales such as the Lower/Upper Cabot head as well as those interbedded within the Packer Shell fall within the brown box in the upper left portion of the cross plot. Carbonates such as the Packer Shell are defined by high ZP and PR values fall within the blue box in the upper right portion of the plot. Clinton Sands have a ZP between 50-38 impedance units and a Poisson's Ratio range of 0.25-0.10 While in conventional settings, this range of Poisson's could delineate gas vs. oil bearing sands, the range illustrates more clay prone vs. less clay prone sand in this tight reservoir. With the majority of the high porosity (large separation) data points plotting below a PR of 0.20, this can be defined as porous sand while data points between a PR of 0.25-0.20 are used to define dirty sand.

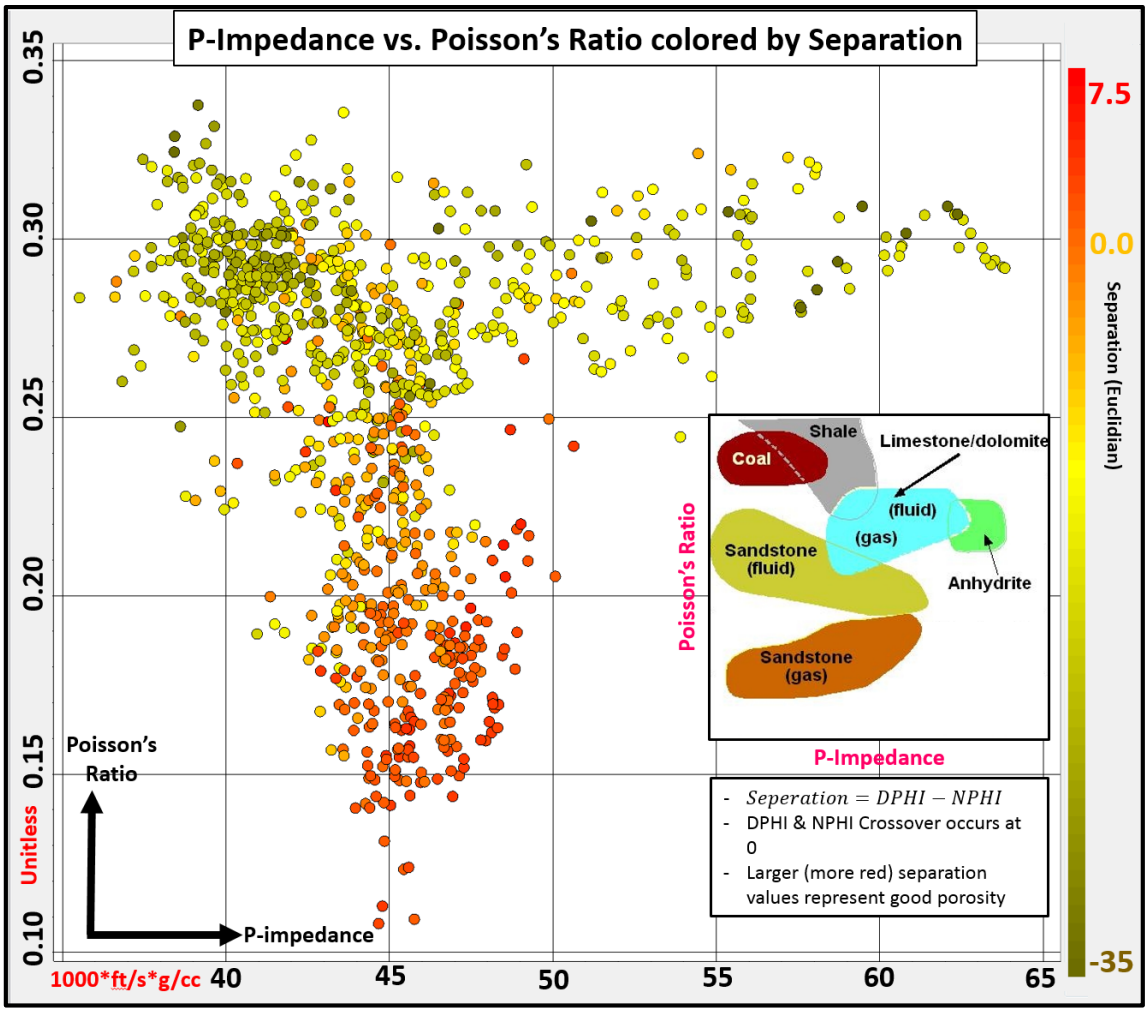

Figure 4.3.1 P-impedance vs. Poisson's Ratio cross plot showing the separation of the various lithologies between the Packer Shell and Queenston Shale. Data points are colored by porosity separation. P-impedance separates out the carbonates on the right while siliclastic rocks plot on the left. Sands and shales are discriminated based on Poisson's Ratio. High values represent shales while lower ones represent sands. Inset figure modified from Ikelle et al., 2005.

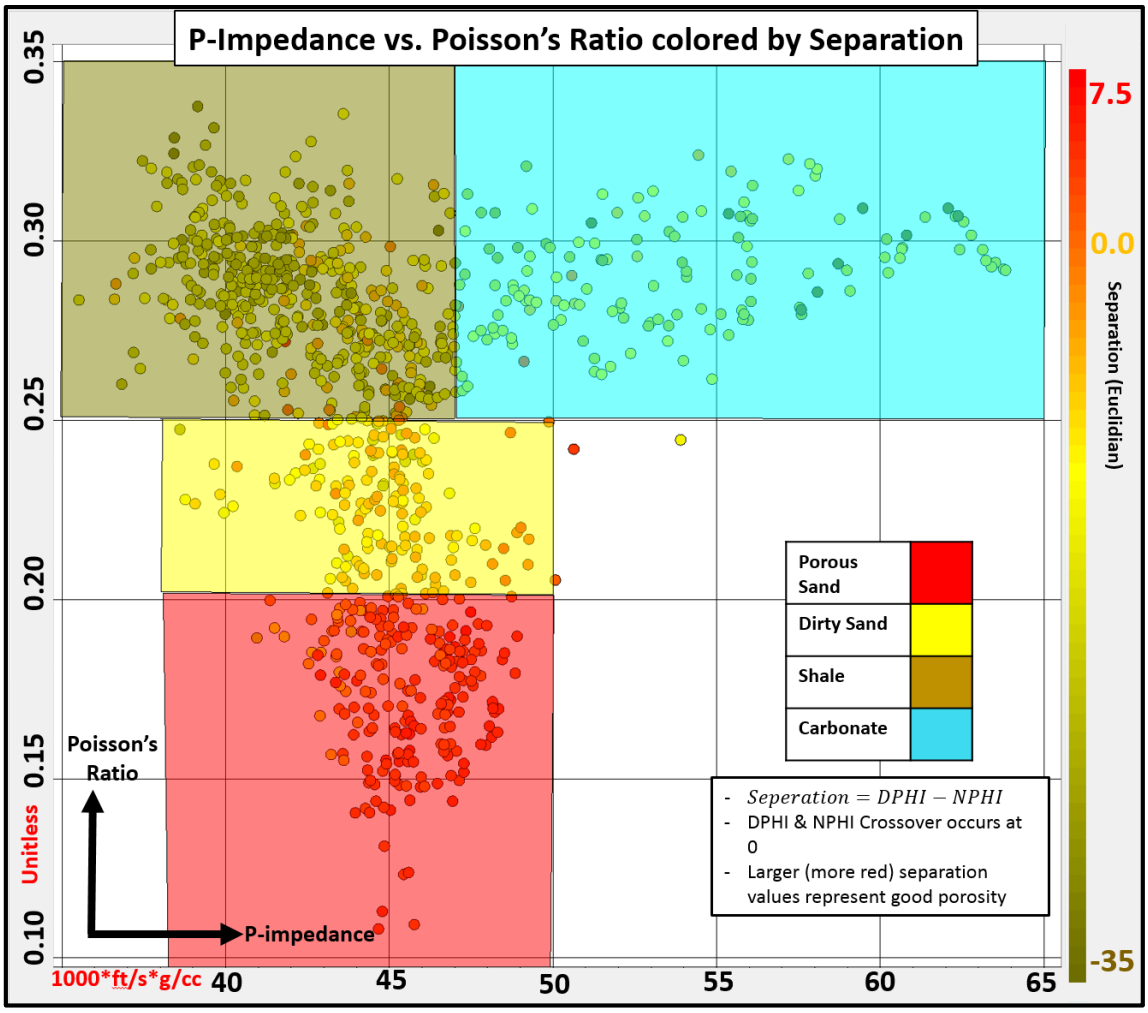

Figure 4.3.2 P-impedance vs. Poisson's Ratio cross plot showing the separation of the various lithologies between the Packer Shell and Queenston Shale along with their lithofacies. Lithofacies used to train inversion data. Data points are colored by porosity separation.

In order to QC the defined facies with other log curve properties, well log displays were generated for wells B and C with the lithofacies flagged on the ZP and PR log curves. Note well C does not have resistivity log curves. Figures 4.3.3 and 4.3.4 show the lithofacies in well log space flattened on the Packer Shell formation top for wells B and C. Analyzing wells B and C, it is clear that areas with 70 API sand correlate to areas with close to or complete crossover as illustrated by the orange/red on the separation curve. Since modern completion methods are now used on Clinton reservoirs, areas with not complete crossover as seen by the orange separation colors, can still be considered quality sands. This is seen in the

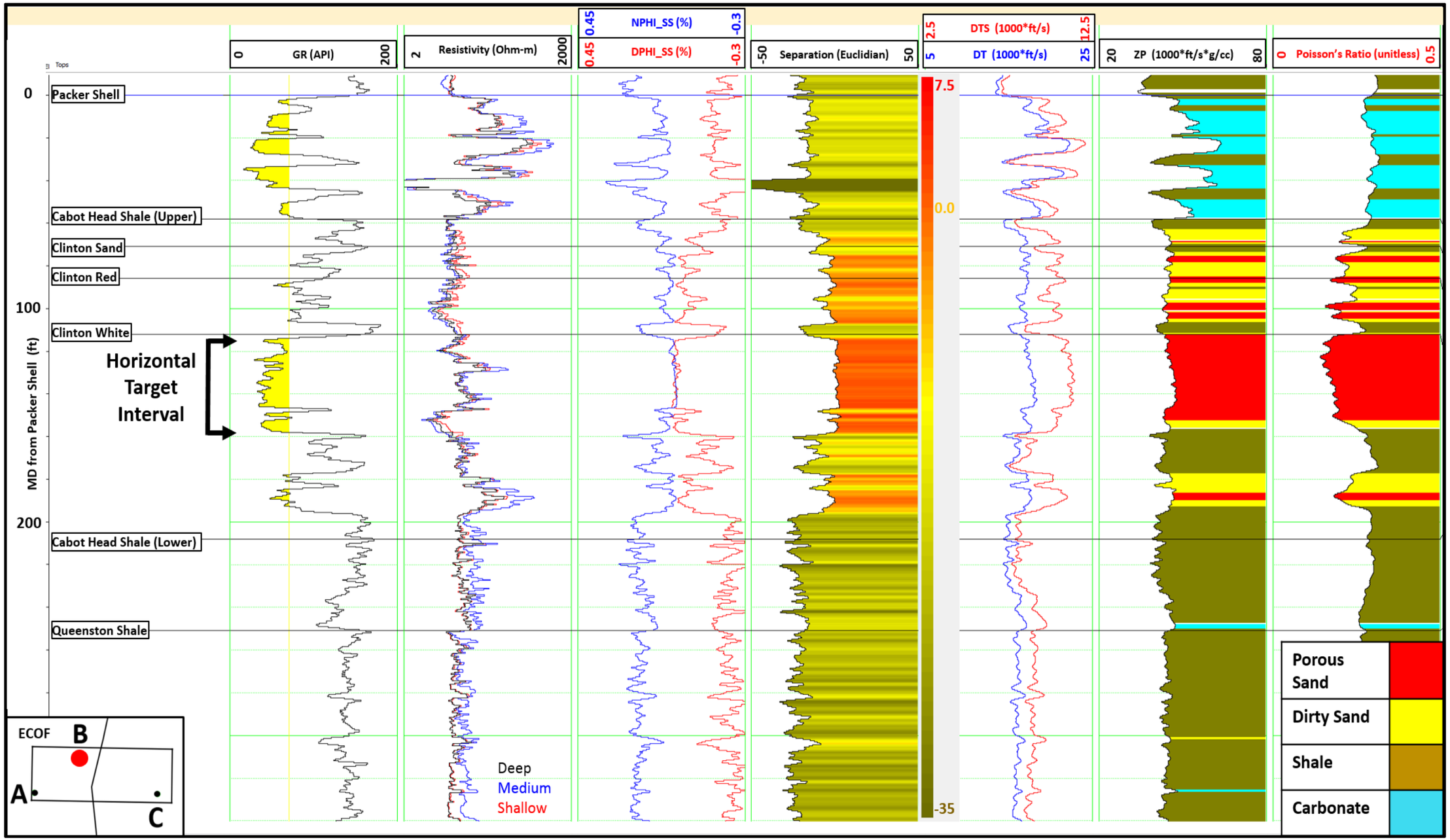

Figure 4.3.3 Well B log display showing lithofacies classes. 70 API shaded on GR log.

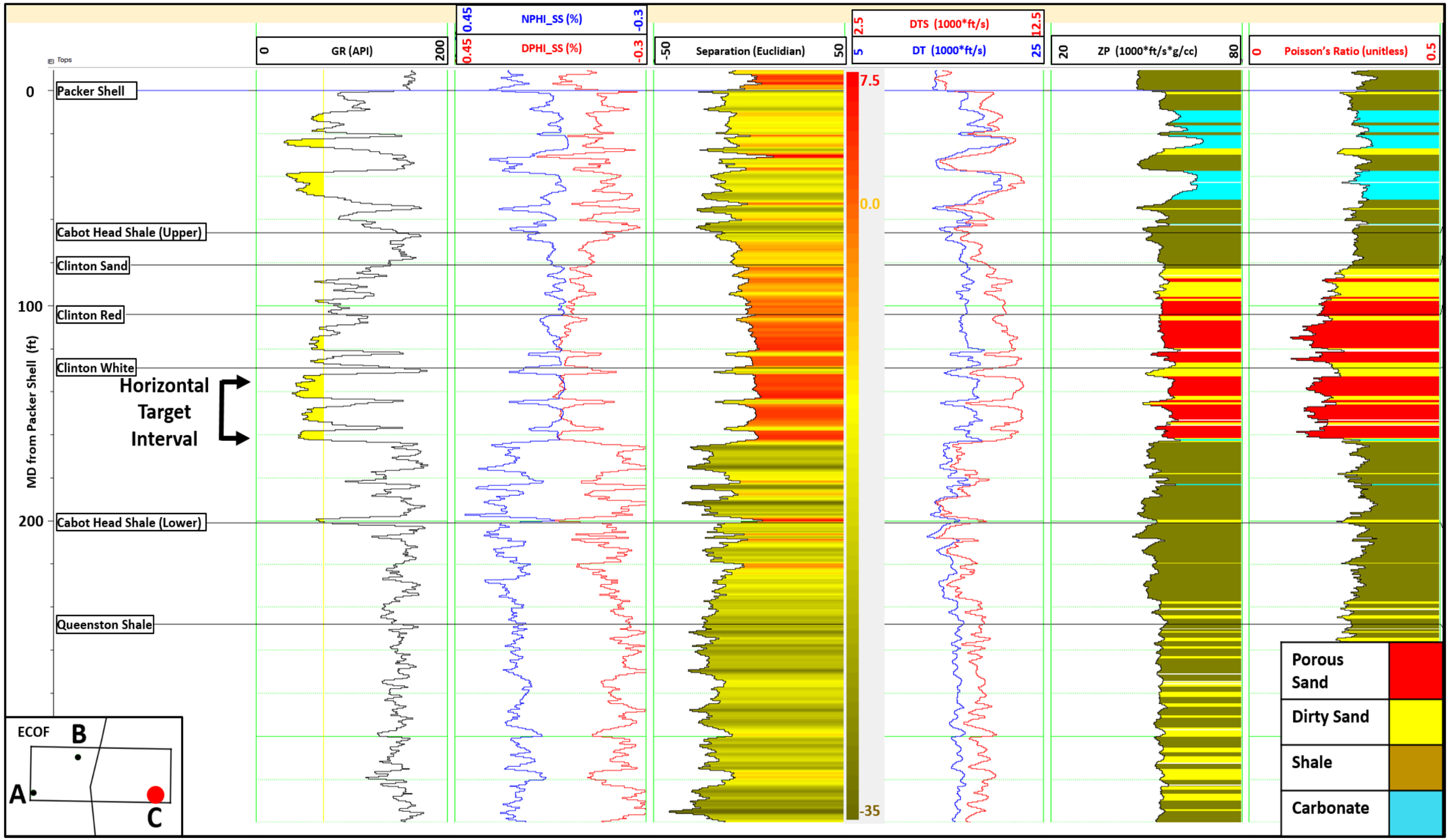

Figure 4.3.4 Well C log display showing lithofacies classes. 70 API shaded on GR log.

Clinton Red as well as thin Clinton White sand stringers are often seen directly above the Lower Cabot Head Shale. Comparing the 70 API sand and separation curves to the Poisson's Ratio, there is a clear correlation between these mechanical properties. Areas on the Poisson's Ratio curve flagged as dirty or porous sand line up well with areas containing GR values indicative of sand as well as areas of moderate to good separation. The porous sand lithofacies successfully flags ideal reservoir that occurs in the Clinton White with excellent separation and clean sand. While the target reservoir in well B (Figure 4.3.3) is located within a thick deltaic lobe, the previously described relationships hold up in areas with sporadic Clinton White deposition seen in well C (Figure 4.3.4). The Poisson's Ratio tracks the anastomosing in the Clinton White GR and separation log curves indicating that the Poisson's is respecting the complex deposition of the target reservoir.

The assigned lithofacies from the well data are used to train the ZP and PR inversion volumes in order to locate the defined facies within the inversion volumes. Prior to the process being run, probability density functions are applied to the ZP and PR cross plot with concentric circles representing the probability of encountering the defined lithofacies. Figure 4.3.5 shows the probability density functions in cross plot space for wells B and C. Viewing the ZP histograms on the x axis, it is difficult to discriminate the difference between the carbonates and sands. It is for this reason the Clinton cannot be resolved in the stacked data due to a lack in impedance contrast. The Poisson's Ratio histograms on the y axis are clearly able to separate out the porous sand from the carbonates and dirty sand lithologies. This separation offers confidence that the facies are being defined properly and that meaningful statistics can be applied to the inversion volumes.

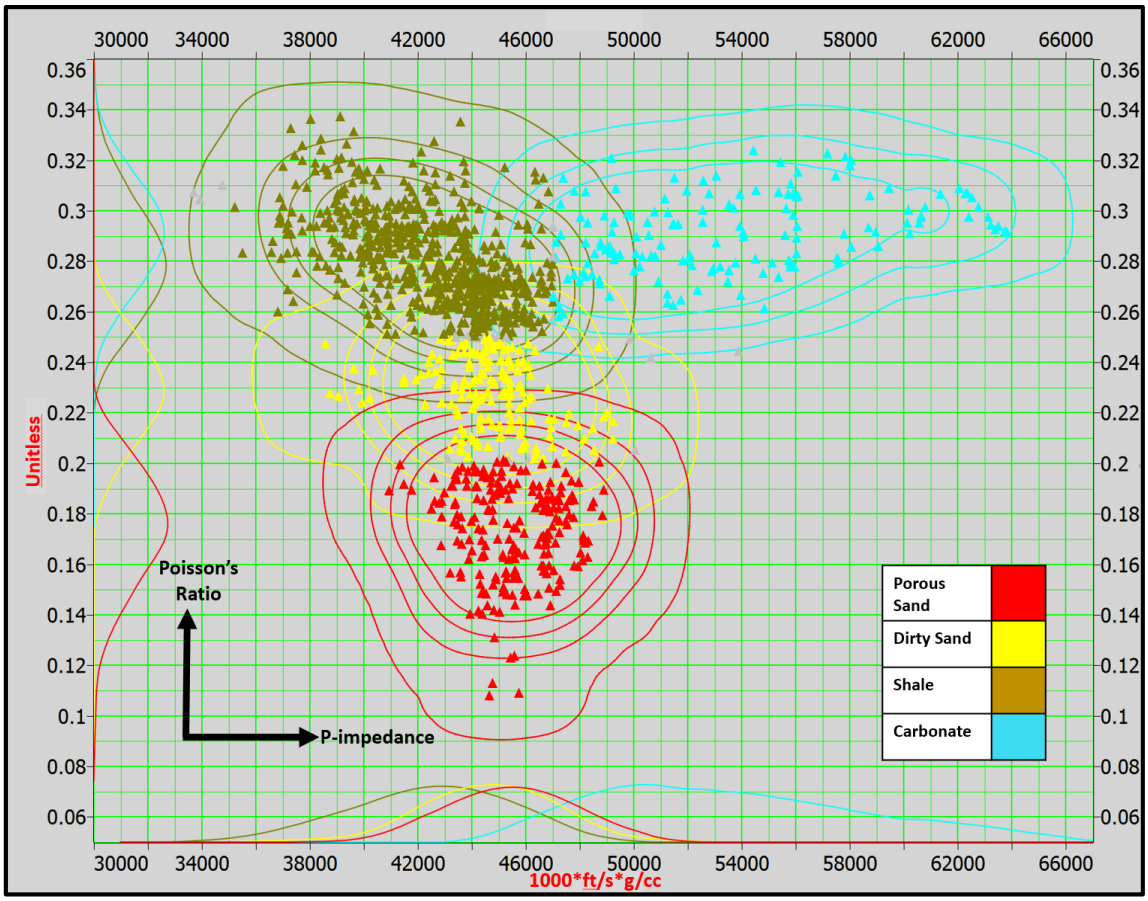

Figure 4.3.5 P-impedance vs. Poisson's Ratio cross plot with probability display functions applied for wells B and C between the Packer Shell and Queenston Shale horizons. Concentric circles are in 25% increments and percentage of finding the lithofacies decreases as you move away from the data cloud. Histograms for the corresponding lithofacies are plotted on the axis.

With lithofacies classes defined and probability functions assigned, the lithofacies class volumes can be generated. Figure 4.3.6 shows the Clinton White horizon slice on the porous sand probability volume. This figure is identical to the Poisson's Ratio Clinton White slice and is useful in that it provides statistical reasoning to high grade the reservoir. Similar to the Poisson's slice, the ECOF boundaries are clearly defined with the best sand occurring in the most active depositional environments. To further visualize the Clinton lithofacies, a cross-section through the dirty and porous sand probability volumes can be found in the back of the manuscript (Figure 4.3.7). With the Poisson's Ratio driving the probability volumes, the dirty sand cross-section shows that there is sand within and outside of the ECOF. Areas with the dirtiest sand lack porous

sand. This is explicitly seen outside of the ECOF boundaries. The porous sand cross-section shows the field delineation with ideal reservoir occurring within the field boundaries. The area within the field that has the highest probability of porous sand is most likely part of a thick seismically resolvable deltaic lobe.

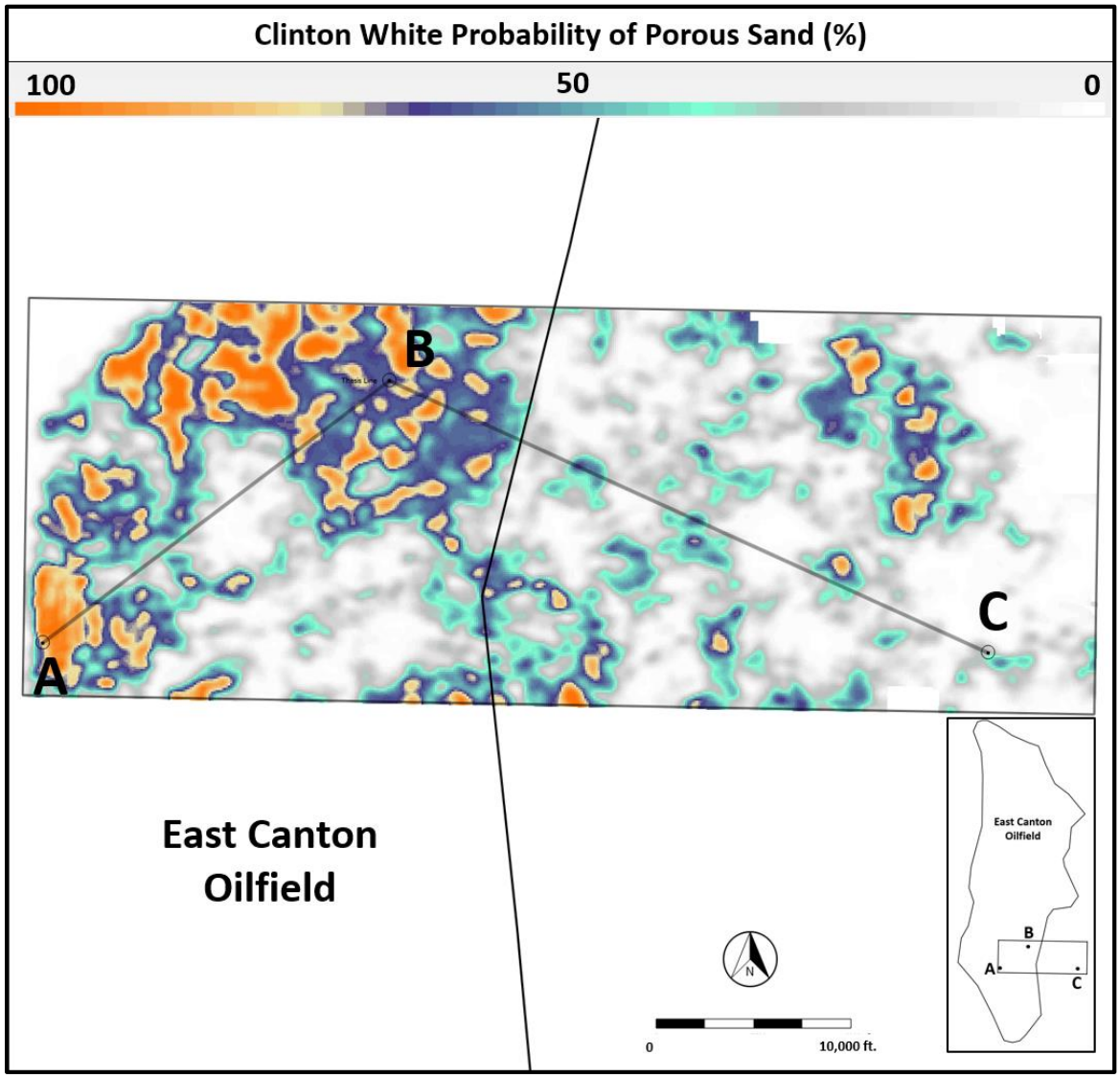

Figure 4.3.6 Zoomed in view of the probability of porous sand horizon slice with 10 ms window on the Clinton White showing delineation of the ECOF

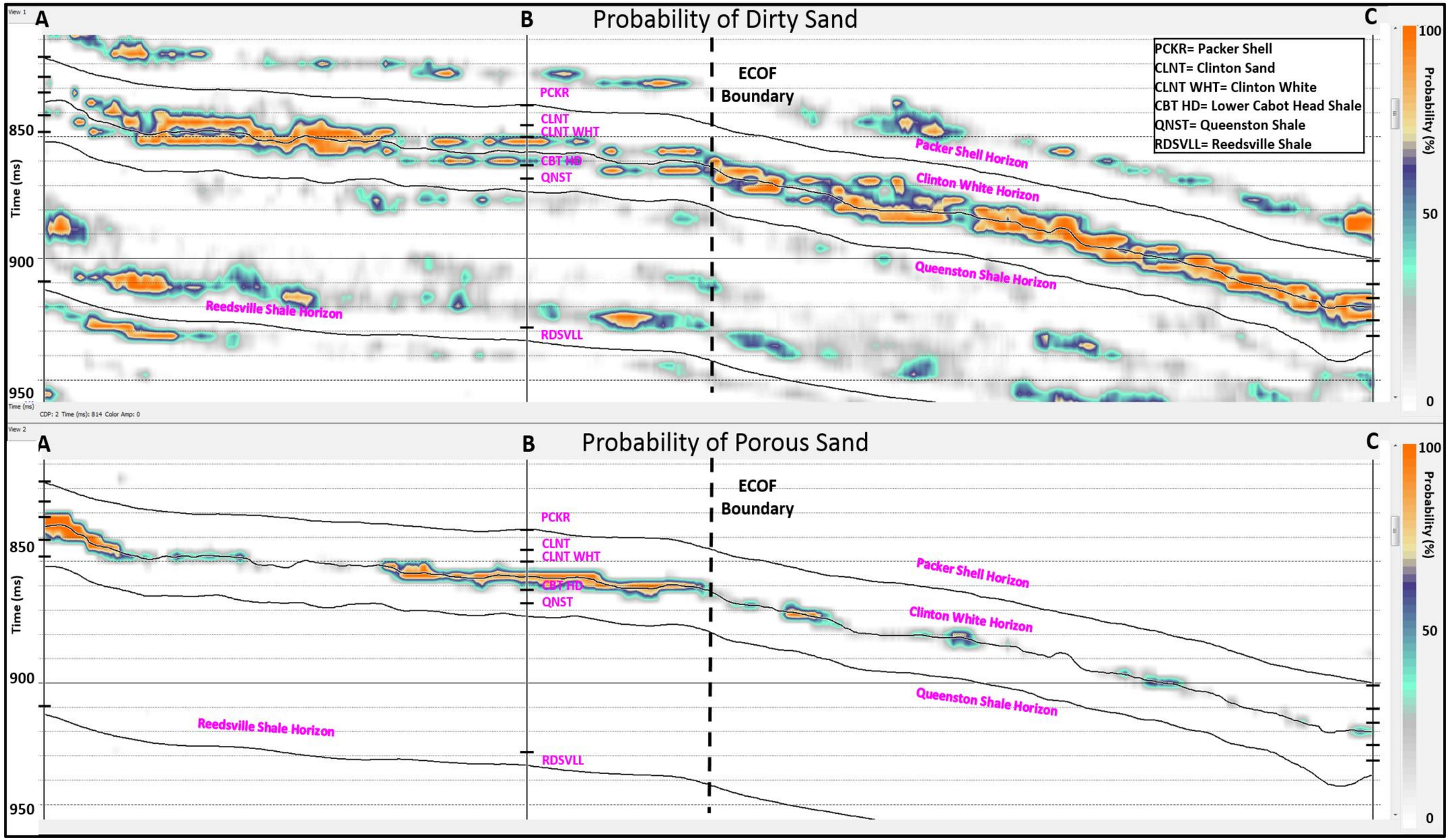

Figure 4.3.7 Cross-section through dirty and porous sand probability volumes. Formation top acronyms posted along well bore.

4.4 Summary

Comparing the PR response in the well logs for wells B and C with the PR horizon slice, there is a relationship between the sand thickness and the PR response. Viewing the GR and PR curves in Figures 4.3.3 (well B) and 4.3.4 (well C) it is evident of two different settings. Based on the GR at the top of the Clinton White in well B, this is part of a deltaic lobe based on its blocky signature and thickness of around 25 ft The PR curve also has a similar response as a blocky sand package based on the litho typing. This can also be confirmed by Figure 4.1.1 showing well B within a deltaic lobe. The GR log curve in well C show the Clinton White was most likely part of an anastomosing channel due to the three thin (2-5 ft) sand bodies separated by thin shale intervals. While a shale lithofacies isn't defined at the shale intervals seen on the GR, the PR log curve does show dirty sand occurring at the shale breaks. From these observations, it can be inferred that clean, thick Clinton White sand bodies of around 25 ft can be resolved from the PR volume. Figure 4.2.6 shows well B within low PR values indicating clean sand that is seismically resolvable while well C is located in thinner sand. While the well log response for well C indicates reservoir quality sand, the combination of thin sand lenses with interbedded shales cannot be seismically resolved. While porosity log well control is an issue as previously stated in the geologic mapping section, Figure 4.1.2 shows the thickest pay occurs around well B which has the best quality sand based on the PR mapping. To provide more understanding about the relationship between the PR and porosity, porosity was plotted against PR in Figure 4.4.1. An explicit linear relationship between porosity and PR is seen which indicates that the inversion result is mapping porous sand.

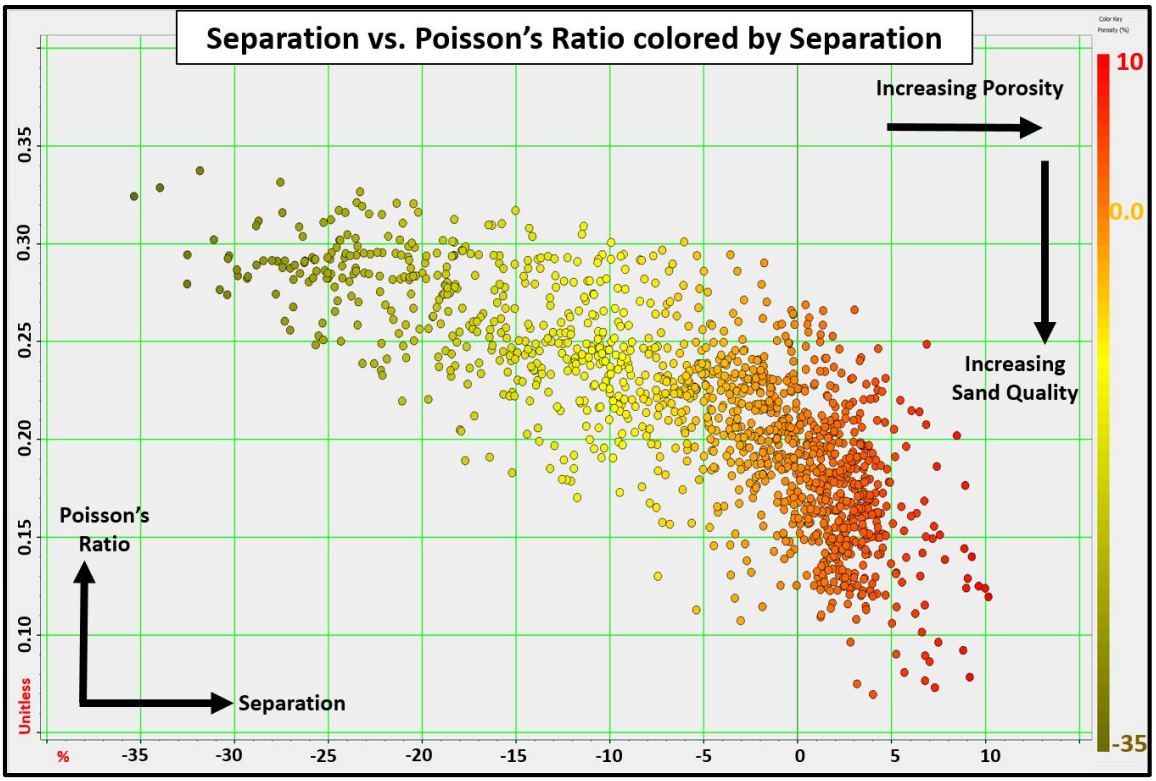

Figure 4.4.1 Separation (porosity) vs. Poisson's Ratio log curve cross plot colored by separation. Data range is between the Clinton Sand and the Lower Cabot Head Shale formation tops.

As discussed in the petroleum geology section, the ECOF is dominantly controlled by stratigraphic trapping but residual structure mapping of the Packer Shell shows a strong correlation to the largest one year production GOR map (Figure 1.2.3A and Figure 1.2.3B). Gas is shown to sit along structural highs while oil sits in the lows which suggests a structural element influencing the ECOF. The Clinton White horizon slice time structure map in Figure 4.4.2 shows that the study area is an east dipping monocline with no resolvable faulting. To further understand the production potential and hydrocarbon type within the study area, a production bubble map was generated with gas on top of oil. Cumulative data was used from 1984 to 2016 since prior to 1984 it was not required to maintain records. Figure 4.4.3 shows that the most gas can be found in the western margins of the field while the most oil is found in the central and eastern portions of the field. Based on the production and time structure mapping it can be suggested that the study

area falls within the oil window of the ECOF. Additionally, the Clinton White PR horizon slice potentially shows the conventional boundaries of the field since the low PR values are found within the ECOF boundaries. These low values represent thick intervals of clean sand while the thinner intervals (less seismically resolved) thought to be outside of the field could still be prospective horizontal targets as seen by the log response of well C.

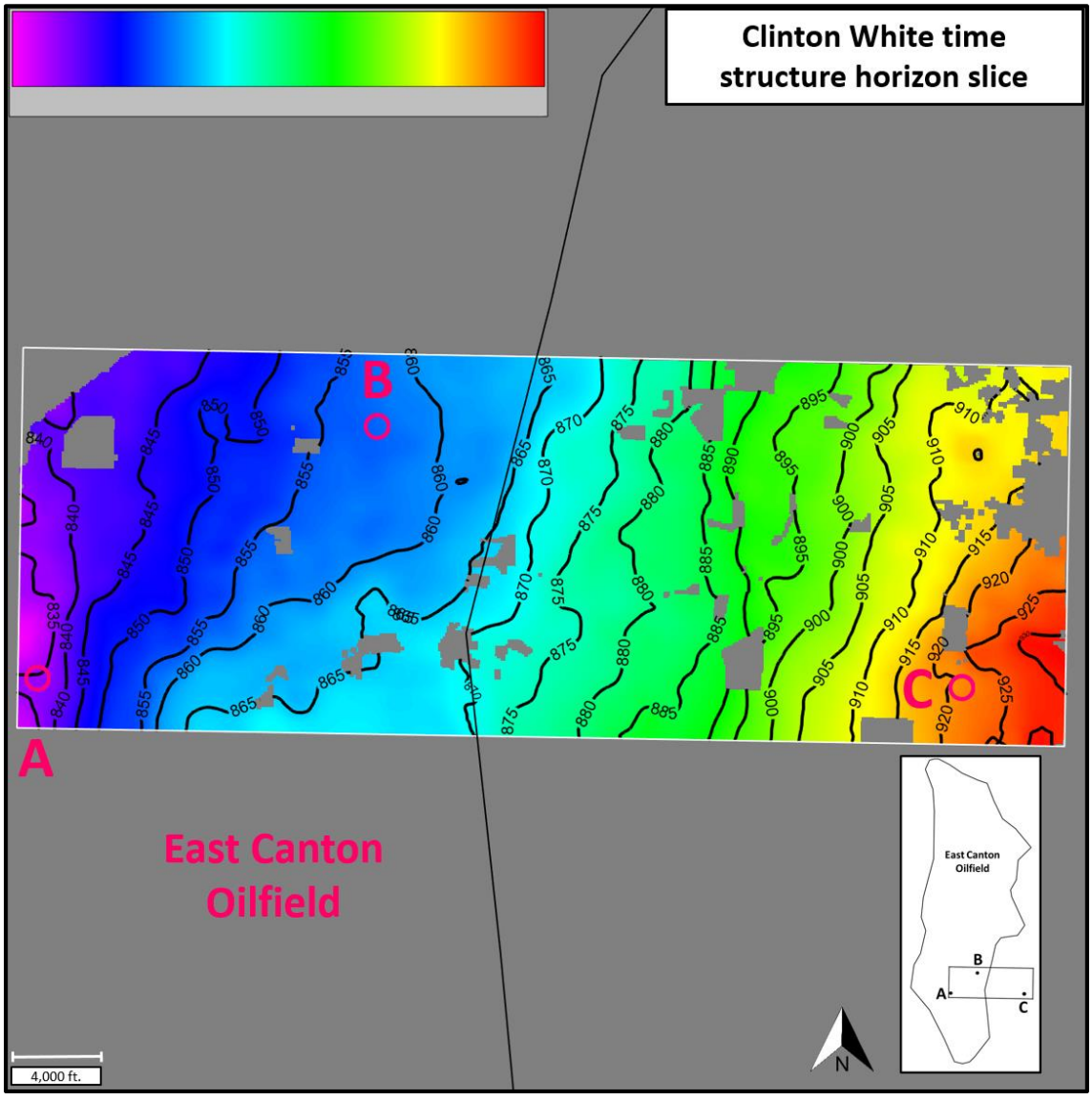

Figure 4.4.2 Horizon slice time structure map on the Clinton White with 5 ms contours. The Clinton White deepens to the east with increasing contour values. Inversion wells are annotated. Slice shows the east dipping monocline structural setting of the study area.

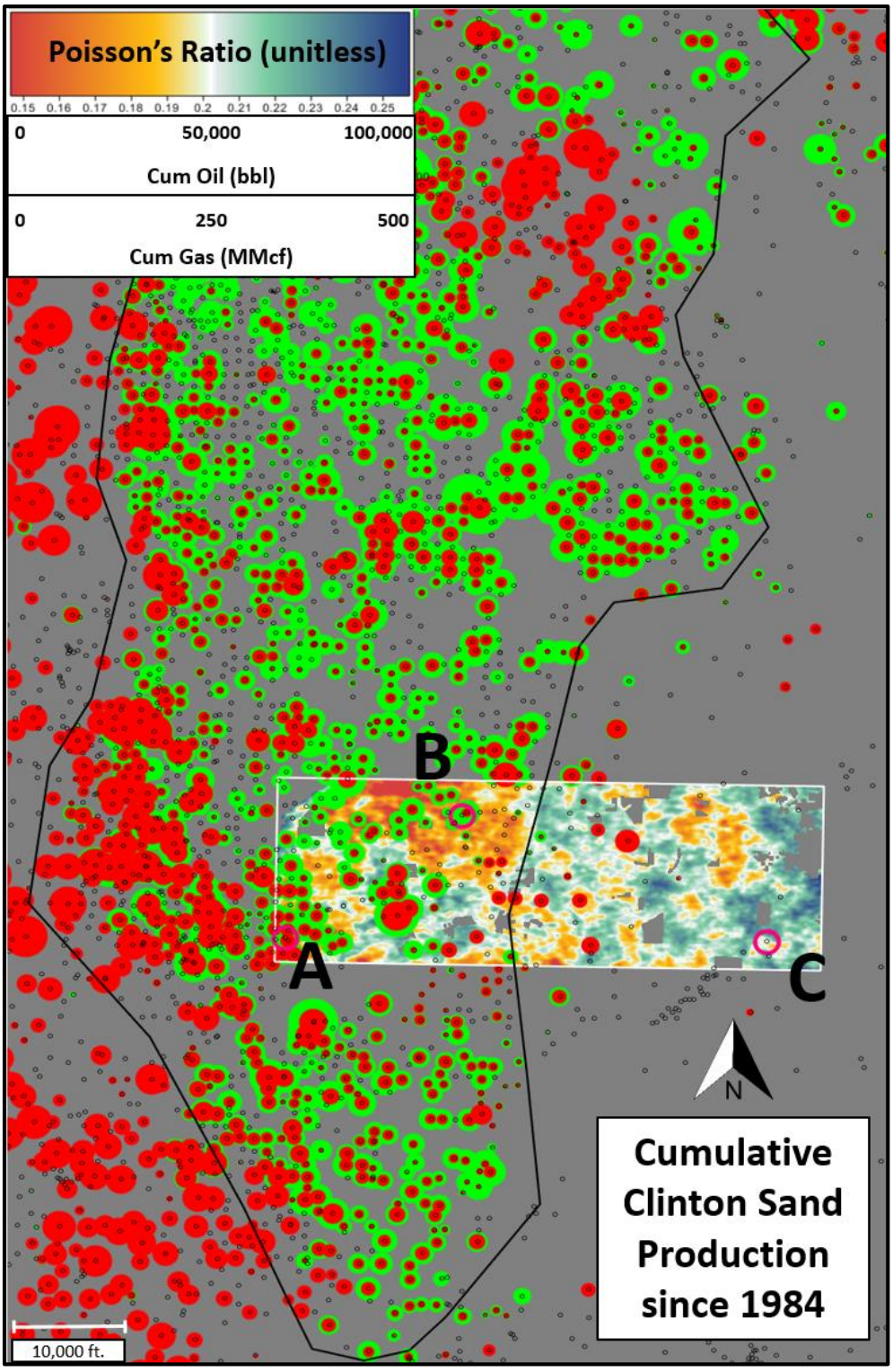

Figure 4.4.3 Cumulative Clinton Sand production since 1984. Gas in the red is plotted on top of oil in the green to show stratigraphic influence on the study area. PR Clinton White 10 ms horizon slice with values less than 0.20 in orange and greater in blue. Seismic outline shown by white outline.

Within the study area when all of the maps are considered, it is evident that the Clinton White is most prospective within the deltaic lobe adjacent to well B. The GR, pay, PR and probability of sand maps show that the probability of encountering clean and porous sand is the greatest in this area. While legacy GR mapping delineates the main facies boundaries, Pay mapping using DPHI and NHPI curves high grades the most prospective areas. Structure and production mapping have shown that the study area most likely falls within a more oil prone area of the ECOF since the largest accumulation of the gas is found on its western edges implying a stratigraphic trap. The Clinton White is effectively transparent in stacked seismic volumes but has a low PR anomaly that can be imaged through seismic inversion allowing for reservoir delineation in areas with scarce-well control. While the elastic properties anomalies found are mostly influenced by lithology and not fluids, they are fundamental to delineate the better quality reservoir extents but not sufficient to predict fluid properties. This research has shown that inverting for PR can be a useful tool in mapping tight, discontinuous onshore sand reservoirs when integrated with geological and production information.

References

Blakey, R. "North American paleogeographic maps." (2007). http://jan.ucc.nau.edu/rcb7/nam.html

Carter, K. M., Kostelnik, J., Laughrey, C., Harper, J. A., Barnes, D. A., Harrison III, W. B., ... & Perry, C. J. Characterization of geologic sequestration opportunities in the MRCSP region: Middle Devonian-Middle Silurian formations: MRCSP Phase II Topical Report under DOE Cooperative Agreement No. MRCSP Phase II Topical Report under DOE Cooperative Agreement No. DE-FC26-05NT42589. (2010)

Cole, G. A., Drozd, R. J., Sedivy, R. A., & Halpern, H. I. Organic geochemistry and oil-source correlations, Paleozoic of Ohio. AAPG Bulletin, 71(7), (1987): 788-809.

Dewan, John T. Essentials of modern open-Hole log interpretation. Pennwell, (1983)

Dykstra, John CF, and Mark W. Longman. "Gas reservoir potential of the Lower Ordovician Beekmantown Group, Quebec Lowlands, Canada." AAPG bulletin 79.4 (1995): 513-530.

Ettensohn, Frank R. "The Appalachian foreland basin in eastern United States." Sedimentary Basins of the World (2008): 105-179.

Ikelle, Luc T., and Lasse Amundsen. Introduction to petroleum seismology. Tulsa, OK: Society of Exploration Geophysicists, (2005): 45-46.

Knight, William V. "Historical and economic geology of Lower Silurian Clinton Sandstone of northeastern Ohio." AAPG Bulletin 53.7 (1969): 1421-1452.

McCormac, M. P., Mychkovsky, G. O., Opritza, S. T., Riley, R. A., Wolfe, M. E., Larsen, G. E., & Baranoski, M. T. (1996). Play Scm: Lower Silurian Cataract/Medina Group ("Clinton") sandstone play. The atlas of major Appalachian gas plays: West Virginia Geological and Economic Survey Publication, 25, 156-163. Patchen, Douglas G., et al. "Creating a Geologic Play Book for Trenton-Black River Appalachian Basin Exploration." West Virginia University Research Corporation Semi-Annual Report April–September 51 (2005).

Patchen, Douglas G., ed. A geologic play book for Utica Shale Appalachian Basin exploration. Utica Shale Appalachian Basin Exploration Consortium, (2015).

Riley, Ronald A. "Oil and Gas Exploration in the Rose Run Sandstone." Ohio Geology (1994)

Riley, Ronald, John Wicks, and Christopher Perry. Silurian" Clinton" Sandstone Reservoir Characterization for Evaluation of CO2-EOR Potential in the East Canton Oil Field, Ohio. Baard Energy, (2009).

Ryder, Robert T., and William A. Zagorski. "Nature, origin, and production characteristics of the Lower Silurian regional oil and gas accumulation, central Appalachian basin, United States." AAPG bulletin 87.5 (2003): 847-872.

Ryder, Robert T. Assessment of Appalachian Basin oil and gas resources: Utica-Lower Paleozoic total petroleum system. US Department of the Interior, US Geological Survey, (2008).

Smith Jr, Langhorne B. "Origin and reservoir characteristics of Upper Ordovician Trenton–Black River hydrothermal dolomite reservoirs in New York." AAPG bulletin 90.11 (2006): 1691-1718.

Thompson, Part II, Stratigraphy and Sedimentary Tectonics, Chapter 5: Ordovician, in C.H. Shultz ed, The Geology of Pennsylvania: Pennsylvania Bureau of topographic and Geologic Survey Special Publication 1, p 74-89, A.M. Thompson, (1999): 74-89

Wickstrom, Larence H., Eric R. Venteris, John A. Harper, James McDonald, Ernie R. Slucher, Kristin M. Carter, Stephen F. Greb, Joseph G. Wells, William B. Harrison III, Brandon C. Nuttall, Ronald A. Riley, James A. Drahovzal, John A. Rupp, Katharine L. Avary, Sacha Lanham, David A. Barnes, Neeraj Gupta, Mark A. Baranoski, Premkrishnan Radhakkrishnan, Michael P. Solis, Gerald R. Baum, Donovan Powers, Michael E. Hohn, Martin P. Parris, Karen McCoy, G. Michael Grammer, Susan Pool, Catherine Luckhardt, and Patrick Kish. Characterization of Geologic Sequestration Opportunities in the MRCSP Region: Phase I Task Report . Technical paper. January 1, (2005). https://geosurvey.ohiodnr.gov/portals/geosurvey/PDFs/OpenFileReports/OFR_2005-1.pdf.

Wickstrom, Larry, Chris Perry, Ron Riley, and Matthew Erenpreiss. The Utica-Point Pleasant Shale Play of Ohio. Issue brief. March 13, (2012). http://geosurvey.ohiodnr.gov/portals/geosurvey/energy/Utica-PointPleasant_presentation.pdf.

Yilmaz, Ozdogan. Seismic data analysis: processing, inversion, and interpretation of seismic data. Edited by Stephen M. Doherty, vol. 1, Society of Exploration Geophysicists, (2001).